The Henryk Niewodniczański
INSTITUTE OF NUCLEAR PHYSICS
Polish Academy of Sciences
ul. Radzikowskiego, 31-342 Kraków, Poland

www.ifj.edu.pl/publ/reports/2007/

Kraków, February 2007

Report No. 1994/AP

Finite element model of thermo-mechanical-metallurgical processes

Jacek Ronda, Graeme John Oliver

Contents

List of Figures

Chapter 1

Introduction

The simulation of thermo-mechanical-metallurgical (TMM) processes in metals requires the modelling of a number of subsequent phenomena occurring during heating and cooling periods of metal heat treatment. The problem is solved for the three state variables: temperature, displacement and metallurgical volume phase fraction, controlling the thermo-mechanical metallurgical process. The interaction between the three processes is taken into account in a consistent way.

The solution of the balance laws governing these processes, with respect to these state variables, are determined using the finite element method (FEM). Differential equations describing equilibrium of the metallurgical volume phase fraction are thus obtained to be used in the finite element method. We also seek to formulate the solution of the phase transformation fraction as a state variable rather than an internal variable. Past work in this field have generally treated the phase transformation evolution as an internal variable for the stress solutions. We describe a governing differential equation for the solution of the volume phase fraction in addition formulating the evolution equations (the time dependent differential equations) for phase transformations. Both descriptions allow for the addition of a vector of possible volume phase fractions to be added to the global vector of state variables in the finite element model of TMM process.

The constitutive laws, which govern the displacement solution and the couplings with the other state variables, take into account both transformation plasticity and transformation induced plasticity. They are obtained by extending the conventional thermo-plastic constitutive equations. The simultaneous finite element solution in terms of the three state variables is further found using tangent moduli consistent with this solution algorithm. This is what is meant by a consistent fully coupled thermo-mechano-metallurgical

(CTMM) model.

A difficulty encountered when formulating the incremental TMM problem is that the equations used in material science describing the evolution of solid phases are mostly given in the form of algebraic equations while the evolution equations which we need should be expressed in the form of differential equations because those are more suitable for the incremental numerical analysis of thermo-mechanical problems where balance equations, the heat conduction equation for non-rigid body, and constitutive equations are given in terms of derivatives. Thus the basic postulates and notions for various phase transformation laws are studied and their final forms of ordinary differential equations, called evolution equations, are derived. These equations show the relation between a phase fraction rate $\dot{y}_i$ and rates of quantities controlling phase transformation expressed in terms of constitutive variables $\dot{\mathbf{L}}$, $\mathbf{S}$, θ, and time t. Various types of phase growth laws reviewed here have got a heuristic or phenomenological nature. The following phase evolution equations have been derived in this report on the basis of works by Authors:

evolution law	fraction	related to
Johnson-Avrami-Mehl [39] [57] for diffusional transformations	ferrite or pearlite	rate of internal stress rate of temperature, time
extended Koistinen-Marburger [37] for diffusionless transformation modified by stress and pressure	martensite	rate of equivalent stress, rate of temperature
three-dimensional generalization of thermo-dynamical-statistical [54]	martensite	rate of strain energy, rate of temperature

All evolution laws are derived from the basis assumption of the proportionality of a daughter phase increment to the decrement of a generalized transformation driving "force". Evolution laws reviewed here can be evaluated accordingly to the cost of identification of material parameters and functions associated with transformation kinetics.

The coupled and mathematically consistent thermo -mechano -metallurgical (CTMM) problem is formulated as a variational problem and solved by the Galerkin type FE technique. The metal heat treatment model formulated here as a CTMM problem can be seen as being more general than the one proposed by Leblond et al. [43], [44] and the metallurgical transformation model developed by the Laboratoire de Science et Génie des Matériaux Métalliques de Nancy (LSG2M) and proposed by Fernandes et al. [21], [22].

The real microstructure is not projected into FE structure and thus the concept of hybrid isobaric finite elements is used to follow the idea of dispersed particles. In hybrid elements the phase composition of welded material is represented at material points which in FEM solution is generally taken to

be the Gauss integration points. The solution of the metallurgical volume phase fraction is thus also found at the Gauss integration or material points simultaneously with the displacement and temperature solution.

Consistent tangent moduli (CTM) have been evaluated here for the CTMM model. Such derivation meets significant complications as five constitutive equations are involved in the formulation of CTMM problem. Derivations of tangent moduli appropriate for CTMM are based on own previous work for example [67].

Chapter 2

Evolution Differential Equations for Metallurgical Phase Transformation

We apply a uniform mathematical approach to all reviewed kinetic laws which can be derived from the fundamental assumption of proportionality of a daughter phase increment and variation of a transformation driving "force", which is expressed by variables controlling transformation. The transformation driving "force" should be called more correctly as the transformation driving power. The following quantities: time, temperature, internal stress, chemical energy, and a potency of material structural defects, are considered here as variables controlling phase transitions. The growth laws for phase fraction are expressed usually in the form of algebraic parabolic laws or ordinary differential equations, also called evolution equations. Evolution laws reveal a rate type nature of interactions between constitutive variables and a transformation products.

2.1 Gibbs Free Energy and Nucleation of the New Phase

The Gibbs free energy is driving metallurgical reactions in solids and hence, in this section we are reviewing the expressions for the this energy both for diffusional and diffusionless transformations.

Transformation Type	Parent Phase	Daughter Phase
diffusional	austenite	ferrite, pearlite
diffusional/diffusionless	austenite	bainite
diffusionless	austenite	martensite

Gibbs Energy for Diffusional Transformation

Diffusional transformations, ferritic and pearlitic, are associated with heterogeneous nucleation. Hence, the change of Gibbs free energy driving such reactions is related to heterogeneous nucleation and has the following four contributions:

symbol	energy name	caused by
$V_i^{nuc}\Delta G_{ch_i}$	volume free energy reduction (chemical energy)	creation of volume V_i^{nuc} of the new phase at θ where this phase is stable
$A_i^{nuc}\gamma_i$	free energy increase	the creation of A_i^{nuc} of an interface of the parent and daughter phase
$V_i^{nuc}\Delta G_{\sigma_i}$	strain energy	dissipation of mechanical energy proportional to a volume of the new phase inclusion
ΔG_{d_i}	free energy	destruction of a defect and reducing the activation energy barrier due to the creation of the new phase nucleus

The free energy change can be expressed as

$$\Delta G_i^{nuc} = -V_i^{nuc}(\Delta G_{ch_i} - \Delta G_{\sigma_i}) + A_i^{nuc}\gamma_i - \Delta G_{d_i}, \tag{2.1}$$

where V_i^{nuc} is the nucleus volume, γ_i is the interfacial free energy per unit area and it is also the work that must be done at constant temperature θ to create a unit area of phases interface. The subscript i assumes here two values: $i = 2$ for ferritic transformation, and $i = 3$ for pearlitic reaction. Units of ΔG_i^{nuc} are joules per nucleus. Ignoring the variation of γ_i with interface orientation and assuming the spherical shape of the new phase nucleus, Eq.(2.1) becomes

$$\Delta G_i^{nuc} = -\frac{4}{3}\pi r^3(\Delta G_{ch_i} - \Delta G_{\sigma_i}) + 4\pi r^2\gamma_i - \Delta G_{d_i}, \tag{2.2}$$

where r is the radius of the spherical nucleus. The rate of homogeneous

nucleation [57] is given by

$$N_i = \omega_i C_{1_i} \exp\left(-\frac{\Delta G_{m_i}}{k_B \theta}\right) \exp\left(-\frac{\Delta {G_i}^*}{k_B \theta}\right), \tag{2.3}$$

where ω_i is the factor that includes the vibration frequency and the area of the critical nucleus, $C_{1_i} = \frac{1}{\Omega}$ is a concentration of nucleation centres, Ω is the atomic volume, ΔG_{m_i} is the activation energy for atomic migration per atom, $\Delta {G_i}^*$ is a change of Gibbs free energy for the critical nucleus diameter r_i^*, k_B is the Boltzmann constant. The critical value of r can be evaluated from

$$r^* = \frac{2\gamma_i}{\Delta G_{ch_i} - \Delta G_{\sigma_i}}; \qquad \Delta G_i^* = \frac{16\pi\gamma_i^3}{3(\Delta G_{ch_i} - \Delta G_{\sigma_i})^2}, \tag{2.4}$$

where ΔG_i^* is the critical value of the free energy ΔG_i^{nuc}.

The same equation can be written for the case of heterogeneous nucleation when

$$(\Delta G_i^*)^{hetero} = (\Delta G_i^*)^{homo}\, \varpi(\theta), \tag{2.5}$$

with a factor $\varpi(\theta)$ related to the interfacial energies.

The Boltzmann constant is given by $k_B = R/N_a$, where N_a is the Avogadro number equal to $6.023 \times 10^{+23}$ and R is the universal gas constant. The rate of nucleation gives the number of nuclei per cubic meter and per second, and the unit of N_i is [nuclei $m^{-3}s^{-1}$].

Gibbs Energy for Diffusionless Transformations

Two phases are produced due to diffusionless transformations: bainite or more precisely bainitic ferrite, and martensite. Bainite is marked with subscript $k = 4$, and quantities related to martensite are labelled by subscript $k = 5$.

The Gibbs free energy associated with the formation of one coherent inclusion, which appears due to diffusionless transformation, see [57], [40], is expressed as:

$$\Delta G_k^{nuc} = A_k^{nuc}\gamma_k + V_k^{nuc}(\Delta G_{\sigma_k} - \Delta G_{ch_k}), \tag{2.6}$$

where $A_k^{nuc}\gamma_k$ is the elastic coherency interfacial energy, γ_k is the austenite-daughter phase interfacial free energy, ΔG_{σ_k} is the strain energy, ΔG_{ch_k} is

the volume free energy release, V_k^{nuc} is the nucleus volume, and A_k^{nuc} is the nucleus surface. The strain energy of the coherent nucleus is more important than the surface energy because of high shear strain producing relatively large strains in the austenitic matrix. Moreover, twinning of the nucleus is also evaluated by shear strain.

A martensitic or bainitic ferrite nucleus is considered as a thin ellipsoidal disk, with radius a and thickness $2c$.

The free energy Eq.(2.6) for the coherent nucleus generated by a simple shear strain, s, can be written

$$\Delta G_k^{nuc} = 2\pi a^2 \gamma_k + \frac{4}{3}\pi(\frac{s^2}{\mu} ac^2 - a^2 c\ \Delta G_{ch_k}), \tag{2.7}$$

where γ_k is the coherent interfacial energy, μ is the elastic shear modulus of austenite. The critical nucleus dimensions a^* and c^* can be found from

$$c^* = 2\gamma_k \ / \ \Delta G_{ch_k}; \qquad a^* = 4\gamma_k \mu s^2 \ / \ (\Delta G_{ch_k})^2. \tag{2.8}$$

Substituting the above into Eq.(2.7) yields the expression for the maximum value of ΔG_k^{nuc}

$$\Delta G_k^* = \frac{32}{3} \frac{\gamma_k^3}{(\Delta G_{ch_k})^4} \frac{s^4}{\mu^2} \pi. \tag{2.9}$$

The nucleation barrier to form coherent nuclei can be reduced by the elastic strain field of dislocation which interacts with the strain field of the martensite nucleus and results in the reduction of the total energy of nucleation. Such interaction modifies the total free energy Eq.(2.6) which, following [72], can be written by

$$\Delta G_k^{nuc} = A_k^{nuc} \gamma_k - \Delta G_d + V_k^{nuc} (\Delta G_{\sigma_k} - \Delta G_{ch_k}), \tag{2.10}$$

where ΔG_d is the energy of dislocation interaction reducing the nucleation energy barrier. Assuming that a complete loop of dislocation is interacting with the nucleus, the interaction energy is expressed by

$$\Delta G_d = 2\pi ac\ \mu\ b, \tag{2.11}$$

where b represents a length of the Burgers vector of dislocation. Subtracting Eq.(2.11) from the RHS of Eq.(2.7) results in the expression of the total energy of a martensite nucleus

$$\Delta G_k^{nuc} = 2\pi a^2 \gamma_k + \frac{4}{3}\pi(ac^2 \mu\ s^2 - a^2 c\ \Delta G_{ch_k}) - 2\pi ac\ \mu\ b. \tag{2.12}$$

The energy ΔG_k^{nuc} is related to diameter a and thickness c of the ellipsoidal disk, the simple shear strain s, and the strain field generated by dislocation.

2.2 Kinetics of Diffusional Transformation

The diffusional transformations are nucleation and growth controlled transformations with a velocity of growth rate defined by

$$v \cong \nu_D b \exp\left(-\frac{\Delta G_{m_i}}{k_B\theta}\right)\frac{\Delta G_{ch_i}\ \Omega}{k_B\theta}, \tag{2.13}$$

with Debye's frequency ν_D and an atomic spanning b.

The rate of a volume fraction growth of i-th phase is

$$\dot{y_i} = \beta\ v = \beta_0 \exp\left(-\frac{\Delta G_{m_i}}{k_B\theta}\right)\frac{\Delta G_{ch_i}\ \Omega}{k_B\theta}, \tag{2.14}$$

where β and β_0 are empirical parameters of phase transformation.

Evolution Law for Diffusional Transformations

The kinetic equation for two diffusional transformations, ferritic, and pearlitic, has the form of the parabolic growth law known as the Johnson-Avrami-Mehl equation [39], [57]

$$y_i = 1 - \exp(-b_i\ \ t^{n_i}), \tag{2.15}$$

where y_i is the volume fraction of i-th phase in the considered microregion V^{mic}, n_i and b_i are empirical parameters related to cooling rate and the nucleation rate, t is time equal to zero at the end of the nucleation period. This equation can be derived from the basic assumption that the daughter phase increment dy_i is proportional to the decrement of transformation driving force measured by the differential of the Gibbs free energy, $d\Delta G_i^{mic}$ where $i = 2$ or 3 for ferritic and pearlitic reactions. Therefore, the Johnson-Avrami-Mehl equation can be expressed in one of the incremental forms shown in Table(2.1). Identifying the rate of the Gibbs free energy variation, $\dot{\mathcal{G}}$, as an explicit function of time

$$\dot{\mathcal{G}} = n_i\ b_i\ t^{n_i - 1}, \tag{2.16}$$

$\frac{dy_i}{d\mathcal{G}} = 1 - y_i$	$\frac{dy_i}{1-y_i} = d\mathcal{G}$	$\frac{\dot{y}_i}{1-y_i} = \dot{\mathcal{G}}$
where $d\mathcal{G} = d\Delta G_i^{mic}$		

Table 2.1: Forms of the Johnson-Avrami-Mehl equation.

and substituting to Table(2.1) yields the expression

$$\frac{dy_i}{1-y_i} = n_i\, b_i\, t^{n_i-1}\, dt. \tag{2.17}$$

The parabolic growth law Eq.(2.15) for ferritic and pearlitic transformations can be obtained by integrating Eq.(2.17)

$$\ln(1-y_i) = -b_i\, t^{n_i}, \tag{2.18}$$

and expressing that in the exponential form

$$1 - y_i = \exp(-b_i\, t^{n_i}). \tag{2.19}$$

Eq.(2.15) was originally proposed for the case when the cells of the new phase were continuously nucleated throughout the transformation at a constant rate. Example values of parameters n_3 and b_3 are given in [29] for austenite-pearlite transformation for 1080 steel. The exponent n_i is not related directly to temperature as long as the nucleation mechanism does not change during cooling. The growth parameter b_i for nucleation as well as growth controlled transformation is temperature dependent [57] and related to both the rate of homogeneous nucleation $N_i(\theta)$, defined by Eq.(2.3), and the cell growth rate $\nu_i(\theta)$. This is defined by

$$b_i(\theta) = \tfrac{1}{3}\pi N_i(\theta){\nu_i}^3(\theta), \tag{2.20}$$

and is valid until the saturation when growing particles collide. The phase growth law expressed by Eq.(2.15) assumes the complete transformation of austenite into the new phase. Such reaction does not proceed instantaneously and therefore the growth law appropriate for the partial transformation during a continuous cooling process is defined by introducing the fictitious fraction [28], [30]

$$y_i^{\phi} \equiv y_i\, \frac{y_{i_{max}}}{y_\gamma} = 1 - \exp[-b_i(\theta)\ \ t^{n_i}], \tag{2.21}$$

where $y_{i_{max}}$ is the final fraction of phase i, and y_γ is the fraction of austenite at the beginning of transformation i.

Expressing Eq.(2.21) in the logarithmic form

$$\ln(1 - y_i^\phi) = -b_i(\theta)\ t^{n_i}, \tag{2.22}$$

and differentiating this with respect to time t, yields to the following evolution equation

$$\dot{y}_i^\phi - (1 - y_i^\phi) t^{n_i} \left[\frac{db_i}{d\theta}\ \dot{\theta} + \frac{b_i(\theta) n_i}{t} \right] = 0. \tag{2.23}$$

Modified Kinetics of Diffusional Transformation

The kinetics of isothermal decomposition of austenite is influenced by hydrostatic pressure and stress [2], [15], [20]. The effect of hydrostatic pressure is observed as a decrease of the temperature A_3 of $\gamma \rightarrow \beta$ iron transformation, a reduction of the eutectoid temperature A_1 of the $Fe - C$ diagram, and shifting the eutectoid transformation point toward lower carbon composition [25], [32], [48]. Following these modifications of specific temperatures and the eutectoid point relocation, the TTT and CCT diagrams show a displacement of curves towards longer transformation times and lower temperatures. Tensile or compressive stresses have the opposite effect on the pearlitic transformation as they accelerate the transformation and result in displacing of the TTT and CCT curves towards shorter times of transformation [50].

The nucleation and growth rate of pearlite is influenced by the stress [17], [50], and such effect is modelled by relating material parameter b_3 of the Johnson-Avrami-Mehl model with the nucleation rate N_3. The situation with the exponent n_3 is vague because it is either decreasing [50] or increasing [17] respectively to internal stresses. The influence of internal stress on kinetics of the pearlitic transformation has been presented in [17]. This concept consists of shifting of TTT diagrams either towards shorter times for tensile and compressive stresses or towards longer times for hydrostatic pressure. The shift D of the TTT diagram is postulated as a function of the second invariant J_2' of the Piola Kirchoff stress deviator $\mathbf{S}$, the spherical part of stress i.e. hydrostatic pressure, and the second invariant I_E of plastic Green-Lagrange strain $\mathbf{E}^{pl}$. This relation can be written as

$$D = \mathcal{F}_D(J_2', p, I_E), \tag{2.24}$$

where $J_2' = [\frac{1}{2}\mathbf{S}{:}\mathbf{S}]^{\frac{1}{2}}$, $I_E = [\frac{2}{3}\mathbf{E}^{pl}{:}\mathbf{E}^{pl}]^{\frac{1}{2}}$, $p = \frac{1}{3}\ S_{KK}$, and ":" means the full contraction of the second order tensor. The simple example of $\mathcal{F}_D$, shown in [17], is given by the linear function of J_2', such that,

$$D = C\ J_2', \tag{2.25}$$

where $C = 8.5 \times 10^{-3}\ \ [MPa]^{-1}$ for the isothermal transformation at temperature $\theta = 663°C$.

Postulating the relation between the growth parameter b_i and the shift D in the form

$$b_{D_i} = \frac{b_i}{(1-D)^{n_i}}, \tag{2.26}$$

and substituting this into Eq.(2.21), the modified growth law for the partial transformation becomes

$$y_i^{\phi} \equiv y_i\ \frac{y_{i_{max}}}{y_\gamma} = 1 - \exp(-b_{D_i}\ \ t^{n_i}). \tag{2.27}$$

The plastic deformation of austenite grains during the pearlitic transformation, called the transformation induced plasticity, TRIP, acts almost similarly as tensile and compressive stresses, and results in shifting of the TTT and CCT curves towards shorter times. The TRIP effect accelerates the phase transformation [15], [45], [50], [69], [78] by increasing the rate of heterogeneous nucleation N_i.

The evolution equation for Eq.(2.27) with Eq.(2.26) and Eq.(2.25) can be expressed in the following form

$$\dot{y}_i^{\phi} - \frac{(1-y_i^{\phi})t^{n_i}}{(1-CJ_2')^{n_i}}\left[\frac{db_i}{d\theta}\dot{\theta} + \frac{b_i(\theta)n_iC}{1-CJ_2'}\ \frac{dJ_2'}{d\mathbf{S}}\ \dot{\mathbf{S}} + \frac{b_i(\theta)n_i}{t}\right] = 0, \tag{2.28}$$

where the relation between rates of the phase fraction, temperature and stress is written explicitly.

2.3 Kinetics of Diffusional-Diffusionless Bainitic Transformation

The kinetic equation for the bainitic transformation proposed in [5], [61] is based on the assumption of the linear relation between an increment of the

bainitic volume fraction dy_4 and volume increment of nucleus dN_4. This can be written as

$$dy_4 = (1 - y_4)V^{mic}\langle dN_4\rangle; \tag{2.29}$$

where y_4 is a volume fraction of bainite, V^{mic} is the volume of a microregion, dN_4 is an increment of nucleation per unit volume, and angular brackets $\langle\rangle$ mean the volume average. Division of both sides of Eq.(2.29) by time increment dt leads to the rate type form of the bainitic transformation kinetic law

$$\frac{\dot{y}_4}{1 - y_4} = V^{mic}\langle\dot{N}_4\rangle. \tag{2.30}$$

Nucleation of bainite sub-unit starts below the Widmanstatten temperature W_s. The nucleation rate $\dot{N}_4$ is related to quantities measured on two graphs: the first is a free energy diagram, which consists of free energy curves for ferrite and austenite versus a carbon content, and the second is the universal curve representing the minimum free energy change, which is necessary for displacive nucleation of ferrite at temperature W_s.

The change of maximum nucleation free energy, $\Delta G_{4_{max}}$, is determined from the free energy diagram following a procedure described in [11], [31]. This method consists of the estimation of the free energy change as a distance between two parallel straight lines which are tangents respectively to ferrite and austenite energy curves. Knowing the content of carbon at a nucleus, a locus on the austenite free energy curve, and the corresponding tangent direction can be found. When such direction is known, the parallel line, which is tangent to the second curve, can be drawn. The location of a common point of a curve and a tangent line determines carbon content at the bainitic ferrite.

The magnitude of $\Delta G_{4_{max}}$ exceeds value G_N measured on the universal curve of minimum energy at temperature W_s. The nucleation rate is expressed in terms of $\Delta G_{4_{max}}$, its initial value $\Delta G^0_{4_{max}}$, and value G_N. This can be written in the form

$$\Delta G_{4_{max}} = \Delta G^0_{4_{max}} - y_{4_{max}}\left(\Delta G^0_{4_{max}} - G_N\right). \tag{2.31}$$

The nucleation rate of bainite is defined in [61] by the following expression:

$$\langle\dot{N}_4\rangle = K_1\ \exp\left[-\frac{K_2}{R\,\theta}\left(1 + \frac{\langle\Delta G_{4_{max}}\rangle}{r}\right)\right], \tag{2.32}$$

where K_1 is a linear function of austenite grain size as has been postulated in [61], K_2 is constant, R is the gas constant, and r is the positive constant which appears in approximation of G_N given by

$$G_N = p\ \mathrm{W}_s - r, \tag{2.33}$$

with $p = 3.6375$, and $r = 2540\ [J\ mol^{-1}]$.

Substituting Eq.(2.32) to Eq.(2.30), the evolution equation for bainitic transformation can be expressed as

$$\dot{y}_4 - (1 - y_4) V^{mic} K_1 \exp\left[-\frac{K_2}{R\,\theta}\left(1 - \frac{\langle \Delta G_{4_{max}} \rangle}{r}\right)\right] = 0. \tag{2.34}$$

Accounting for the effect of auto-catalysis, when the increase of the bainitic ferrite fraction is accompanied by the increase in number density of nucleation sites, the denominator $(1 - y_4)$ in Eq.(2.34) should be replaced by $(1 - \beta y_4)$, where β is the auto-catalysis factor.

2.4 Kinetics of Martensitic Transformation

Kinetic equations for martensitic transformation can be classified in one of the following three types:

heuristic laws
relations derived from thermodynamics and statistics
equations derived from thermodynamics of continua

Heuristic Laws

Heuristic laws are represented by the Koistinen-Marburger law [41] and its modifications proposed in [37], [38] and [75], and issued from identification techniques to achieve the best coincidence of a transformation model with experiment. The Koistinen-Marburger law is based on the assumption of the linear relation between the martensitic fraction increase dy_5 and temperature decrease $d\theta$ below the temperature M_s, where martensitic transformation starts. This can be expressed by

$$\frac{dy_5}{d\theta} = \alpha\ (1 - y_5), \tag{2.35}$$

where for most steels the constant coefficient $\alpha = 1.1 \times 10^{-2} [K^{-1}]$.

The Koistinen-Marburger law can be derived following the procedure:

take all terms of Eq.(2.35) with y_5 to the left $\frac{dy_5}{1-y_5} = \alpha\, d\theta \quad \text{for} \quad \alpha > 0$
introduce the new variable $z = 1 - y_5$
integrate $\int_1^z \frac{1}{\xi} d\xi = \alpha \int_{M_s}^{\theta} d\vartheta$
write the result in the form $\ln \xi \,\big|_1^z = \alpha(\theta - M_s) \quad \Rightarrow \quad \ln(1 - y_5) = -\alpha(M_s - \theta)$

The last relation reveals the exponential nature of martensitic transformation kinetics, i.e.

$$y_5 = 1 - \exp[-\alpha(M_s - \theta)]. \tag{2.36}$$

The simple evolution equation for the martensitic fraction can be obtained from Eq.(2.35) assuming α constant, and $y_5(t)$, $\theta(t)$ being functions of time

$$\dot{y}_5 - (1 - y_5)\alpha\dot{\theta} = 0, \tag{2.37}$$

with the initial condition $y_5(0) = 0$ for $\theta(0) \leq M_s$. However, parameter α depends on composition of the alloy, crystallography of the martensite habit planes, cooling rate, internal stress state, and is somehow related to the transformation driving force ΔG_5^{mic}.

The improved Koistinen-Marburger law which accounts for the effect of pressure and stress on transformation temperature has been proposed in [37], [38]. The modification of M_s is a linear function of hydrostatic pressure and the equivalent stress

$$\Delta M_s = A\, p \;\; + \;\; B\, \hat{S}, \tag{2.38}$$

where A and B are material parameters, and $\hat{S} = (J_2')^{\frac{1}{2}}$. Substituting Eq.(2.38) in Eq.(2.36) results in the extended Koistinen-Marburger law

$$y_5 = 1 - \exp[-\alpha(M_s - \theta + Ap + B\hat{S})]. \tag{2.39}$$

Differentiation of the logarithmic form of Eq.(2.39) in respect of time yields the evolution equation corresponding to the extended Koistinen-Marburger law

$$\dot{y}_5 - (1 - y_5)\alpha(A\dot{p} + B\frac{\partial \hat{\mathbf{S}}}{\partial \mathbf{S}}\dot{\mathbf{S}} - \dot{\theta}) = 0, \tag{2.40}$$

with the initial condition $y_5(0) = 0$ for $\theta(0) \leq M_s$, $p(0) = 0$, and $\hat{S}(0) = 0$.

The other proposition of the modified Koistinen-Marburger law is given in [23], [75] and has the form

$$y_5 = \{1 - \exp[-\alpha_G(M_s - \theta) - \mathcal{E} : \mathcal{S}]\}, \tag{2.41}$$

with

$$\alpha_G = k_M V^{mic} \langle \frac{\partial \Delta G_5^{mic}}{\partial \theta} \rangle; \qquad \mathcal{E} = k_M V^{mic} \mathbf{E}_c^*$$

where

global stress tensor corresponding to the macroscopic strain tensor $\mathbf{E}$	$\mathcal{S}$
difference of the free energy per unit volume of the microregion	ΔG_5^{mic}
average of $\frac{\partial \Delta G_5^{mic}}{\partial \theta}$ over the mesodomain	$\langle \cdot \rangle$
critical value of the macroscopic strain reached when entire microregion transforms to martensite	$\mathbf{E}_c^*$
microregion volume	V^{mic}
proportionality factor defined by Magee [46]	$k_M = \frac{dn}{dG}$ $dG = \langle d\Delta G_5^{mic} \rangle$
number of microregions transforming to martensite per unit volume of the parent phase	n

Martensitic Transformation Law Derived from Thermodynamics and Statistics

The growth law proposed in [54] is an example of the kinetic equation issued from thermodynamics and statistical analysis. This kinetic law for martensitic transformation is based on the identification of the fraction y_5 with the probability ρ_{prob} and written in the form

$$y_5 \equiv \rho_{prob} = 1 - \exp[-V^{mic} N_V], \tag{2.42}$$

where ρ_{prob} measures the probability [14] that at least one nucleation site is contained in V^{mic}, and N_V is a cumulative structural defect potency. Five different transformation laws are proposed as shown in Tables (2.2) - (2.6) according to the the structural defect potency.

The cumulative structural defect potency N_V is modified by the change of mechanical energy on habit planes. The mechanical contribution of ΔG_5^{mic} is

1-st thermodynamical-statistical martensitic transformation law	
$y_5 = 1 - \exp[-V^{mic} N_V(n)]$	
$N_V(n) = N_V^0 \ \exp(-\alpha\ n)$ $n = 2\ \gamma_5 / \Delta G_5^{mic}\ d_5$ $\Delta G_5^{mic} = A_5^{mic}\gamma_5 - \Delta G_{ch_5}^{mic} + \Delta G_\sigma^{mic} + \Delta G_F^{mic}$	
N_V^0	total number density of defects of all potencies
α	constant shape factor
d_5	close packed interplanar spacing
γ_5	nucleus specific interfacial energy
ΔG_5^{mic}	the total volume free-energy change
ΔG_σ^{mic}	strain energy
ΔG_F^{mic}	frictional work of interfacial motion

Table 2.2: Transformation law with the cumulative structural defect potency related to the defect size parameter n

2-nd thermodynamical-statistical martensitic transformation law	
$y_5 = 1 - \exp[-V^{mic} N_V(\mathcal{G}_\sigma)]$	
$N_V(\mathcal{G}_\sigma) = \int_{\mathcal{G}_\sigma}^{\mathcal{G}_\sigma^{max}} M(\mathcal{G}) \exp[-\alpha n(\mathcal{G})] d\mathcal{G}$ $\mathcal{G}_\sigma = \Delta G_\sigma^{mic}$ $\mathcal{G}_\sigma^{max} = \Delta G_\sigma^{max}$ $\Delta G_\sigma^{mic} = \frac{A^{hab}}{V^{mic}} (\Delta G_{\tau\sigma}^{mic} + \Delta G_{\sigma\sigma}^{mic})$ $\Delta G_{\tau\sigma}^{mic} = \sum_{h=1}^{H} \left(\vec{\tau}^h \cdot \vec{\gamma}^h\right) = \frac{1}{2} \sum_{h=1}^{H} \left(\tau_i^h m_{ij}^h \gamma_j^h\right)$ $\Delta G_{\sigma\sigma}^{mic} = \sum_{h=1}^{H} \left(\vec{\sigma}^h \cdot \vec{\epsilon}^h\right) = \frac{1}{2} \sum_{h=1}^{H} \sigma_i^h \epsilon_i^h$ $m_{ij}^h = cos\zeta_{ij}^h$	
$M(\mathcal{G})$	linear function of $\frac{dN_V^0(\mathcal{G})}{d\mathcal{G}}$
ΔG_σ^{max}	maximal change of mechanical energy on habit planes
$\cdot$	scalar product
ϵ_i^h	the normal displacement
γ_i^h	the tangent displacement (shear)
m_{ij}^h	directional tensor
ζ_{ij}^h	angle between the transformation tangent displacement $\vec{\gamma}^h$ and $\vec{\tau}^h$ direction
$\vec{\sigma}^h$	normal component of true stress vector $\vec{\mathbf{t}}$ on habit plane h
$\vec{\tau}^h$	tangent component of true stress vector $\vec{\mathbf{t}}$ on habit plane h

Table 2.3: Transformation law with the cumulative structural defect potency modified by the change of mechanical energy on habit planes.

orientation dependent and requires a decomposition of the true stress vector in microregion $\vec{\mathbf{t}}$ into its normal $\vec{\sigma}^h$ and tangential $\vec{\tau}^h$ components on each habit plane h. The total number of habit planes H is the sum of habit planes of b.c.c. austenitic crystals in a microregion. Habit planes have the same area A^{hab}. The true stress vector corresponding to the Kirchoff stress tensor t_{ij} on a habit plane is defined by

$$t_i^h = \frac{\rho}{\rho_0} t_{ij}\, n_j^h = \frac{\rho}{\rho_0} t_{ij}\, cos2\vartheta_i^h \tag{2.43}$$

where initial and actual density is ρ_0 and ρ, directional vectors, which define the orientation of the h-th habit plane normal, are $\mathbf{n}^h$, and ϑ_i^h is the angle between stress axis and the normal to the habit plane, where the daughter phase appears.

When deformation is controlled by stress coupled with phase transformation, experimental results available for a one-dimensional test [12] show the linear relation between the martensite fraction y_5 and the resulting plastic strain $\bar{E}^p$. This originally has been used in [54] to propose a kinetic equation suitable for one-dimensional microregion. Following this proposition we are postulating a 3-D generalization of this 1-D evolution law. That can be obtained by using the expression for n in Table 2.2 in the equation for $N_V(\mathcal{G}_\sigma)$ of Table 2.3 and substituting the resultant relation to Eq.(2.42). This generalized kinetic equation is written in the form:

$$y_5 = \frac{\bar{E}^p}{\bar{E}_1} = 1 - \exp[-V^{mic} N_V(\mathcal{G}_\sigma)], \tag{2.44}$$

where $\bar{E}^p = (\frac{4}{3} I_{E^p})^{\frac{1}{2}}$ is the effective plastic strain, and $\bar{E}_1 = (\frac{4}{3} I_E)^{\frac{1}{2}}$ is the effective total strain for the fully martensitic structure of a microregion when $y_5 = 1$.

Assuming $\mathcal{G}_\sigma = \mathcal{G}_\sigma^{min}$ and splitting the integral $\int_{\mathcal{G}_\sigma}^{\mathcal{G}_\sigma^{max}} M(\mathcal{G}) \exp[-\alpha n(\mathcal{G})] d\mathcal{G}$ in Table 2.3 into two terms: $\int_{\mathcal{G}_\sigma^{min}}^{\mathcal{G}_\sigma^{max}} ... d\mathcal{G} = \int_0^{\mathcal{G}_\sigma^{max}} ... d\mathcal{G} - \int_0^{\mathcal{G}_\sigma^{min}} ... d\mathcal{G}$, the third expression for the nucleation-site potency N_V is obtained. The corresponding martensitic transformation law and formulas can be seen in Table 2.4.

A simpler transformation model is obtained by postulating the structural defect potency as a function of $\mathcal{G}_\sigma$ and G that has been shown in Table 2.5.

The next form of the martensitic transformation law is obtained assuming

$$N_V = \mathcal{N}(\mathcal{G}_\sigma, \theta) = N_V^0 \ \exp\left(-\frac{2\alpha\gamma_5}{\Delta G_5^{mic}\, d_5}\right), \tag{2.45}$$

3-rd thermodynamical-statistical martensitic transformation law	
$y_5 = 1 - \exp[-V^{mic}(\mathcal{I}_{max} - \mathcal{I}_{min})]$	
$N_V = \mathcal{I}_{max} - \mathcal{I}_{min}$ $\mathcal{I}_{min}(\mathcal{G}_\sigma^{min}) = \int_0^{\mathcal{G}_\sigma^{min}} M(\mathcal{G}) \exp\left(\frac{L}{D_1}\right) d\mathcal{G}$ $\mathcal{I}_{max}(\mathcal{G}_\sigma^{max}) = \int_0^{\mathcal{G}_\sigma^{max}} M(\mathcal{G}) \exp\left(\frac{L}{D_2}\right) d\mathcal{G}$ $D_1 = (A_5^{mic}\gamma_5 - \Delta G_{ch_5}^{mic} + \Delta G_F^{mic}) d_5$ $D_2 = D_1 + \mathcal{G}_\sigma d_5$ $L = 2\ \alpha\ \gamma_5$ $\mathcal{G}_\sigma^{min} = \Delta G_\sigma^{min}; \quad \mathcal{G}_\sigma^{max} = \Delta G_\sigma^{max}$ $d\mathcal{G} = d(\Delta G_\sigma^{mic})$	
α	0.84
N_V^0	$2.0E+17[m^{-3}]$
γ_5	$0.15\ [J/m^2]$
$A_5^{mic}\gamma_5 + \Delta G_F^{mic}$	$6.1E+7\ [J/m^3]$
above values can be found in [14] and [54]	

Table 2.4: Transformation law with the cumulative structural defect potency expressed by $N_V = \mathcal{I}_{max} - \mathcal{I}_{min}$.

4-th thermodynamical-statistical martensitic transformation law
$y_5 = 1 - \exp\left[-V^{mic} N_V^0(\mathcal{G}_\sigma)\ \exp(G)\right]$
$N_V = N_V^0(\mathcal{G}_\sigma)\ \exp(G)$ $G = \frac{2\alpha\gamma_5}{d_5\left(A_5^{mic}\gamma_5 - \Delta G_{ch_5}^{mic} + \mathcal{G}_\sigma^{max} + \Delta G_F^{mic}\right)}$

Table 2.5: Transformation law with the cumulative structural defect potency expressed by $N_V = N_V^0(\mathcal{G}_\sigma)\ \exp(G)$.

5-th thermodynamical-statistical martensitic transformation law
$y_5 = 1 - \exp[-V^{mic}\ N_V(\mathcal{G}_\sigma, \theta)]$
$N_V(\mathcal{G}_\sigma, \theta) = N_V^0\ \exp\left(-\frac{2\alpha\gamma_5}{\Delta G_5^{mic}\ d_5}\right)$ $\mathcal{G}_\sigma = \Delta G_\sigma^{mic}$ $\mathcal{G}_{ch} = \Delta G_{ch_5}^{mic}$ $\Delta G_5^{mic} = A_5^{mic}\gamma_5 + \Delta G_F^{mic} - \mathcal{G}_{ch} + \mathcal{G}_\sigma$

Table 2.6: Transformation law with the cumulative structural defect potency expressed by $N_V = \mathcal{N}(\mathcal{G}_\sigma, \theta)$

and the corresponding relations are shown in Table 2.6.

The evolution equation that is the most general for all five propositions of the thermodynamical-statistical martensitic transformation law corresponds to Table 2.6 and is obtained after the complex differentiation with respect to time that leads to

$$\dot{y}_5 - (1-y_5)V^{mic}\, N_V^0\, \exp(-M)\, \frac{M}{\Delta G_5^{mic}} \left(\dot{\mathcal{G}}_\sigma - \frac{\partial \mathcal{G}_{ch}}{\partial \theta}\dot{\theta} \right) = 0, \tag{2.46}$$

with $M = \frac{2\alpha\gamma_5}{\Delta G_5^{mic}\, d_5}$.

Martensitic Transformation Laws Derived from Thermodynamics

Growth laws developed on the basis of thermodynamics of continua and micromechanics have been presented in [51] and [74]. Both of them are based on the following observations:

- a volume average of the differential of the Gibbs free energy, $\langle d\Delta G_5^{mic} \rangle$, together with temperature θ controls the martensitic transformation,
- the macroscopic increment of the daughter phase dy_5 is proportional to the increment of the total driving force.

These notions are used to express the fraction y_5 as a function of temperature θ and external loading stress $\mathcal{S}$, such as $y_5 = \mathcal{Y}_1[\tilde{\mathbf{S}}(\mathcal{S}), \theta] = \mathcal{Y}_2(\mathcal{S}, \theta)$.

In this section a kinetic law, originally shown in [51] for the case, when the growth of martensitic fraction is the only reaction, is slightly generalized to be used for a description of transformation occurring in the presence of products of diffusional transformations y_2, y_3, y_4 and y_5.

The proportional relation between a phase fraction and the driving force is expressed here in terms of dy_5 and $d\mathcal{G}$, and is written in the form:

$$\frac{dy_5}{\langle d\mathcal{G} \rangle} = -k_F V^{mic}(1-y_5); \qquad \mathcal{G} \equiv \mathcal{G}(\tilde{\mathbf{S}}, \theta) = \Delta G_5^{mic}(\tilde{\mathbf{S}}, \theta), \tag{2.47}$$

where $\tilde{\mathbf{S}}$ is the total stress related linearly to $\mathcal{S}$, V^{mic} is the microregion volume average, and k_F is a constant given for steel in [51] as $k_F V^{mic} = 0.0206\ m^2/N$.

Eq.(2.47), as all previously reviewed kinetic equations, is subjected to another assumption about the exponential form of the function $y_5 = \mathcal{Y}_1(\tilde{\mathbf{S}}, \theta)$. This becomes obvious due to the following transformations:

- move all terms with y_5 to the left

$$\frac{dy_5}{1-y_5} = -k_F V^{mic} \langle d\mathcal{G} \rangle, \tag{2.48}$$

- integrate

$$\ln(1-y_5) = k_F V^{mic} \langle \mathcal{G} \rangle + \mathcal{C}, \tag{2.49}$$

- express Eq.(2.49) in exponential form

$$y_5 \equiv \mathcal{Y}_1(\tilde{\mathbf{S}}, \theta) = 1 - \exp\left[k_F V^{mic} \langle \mathcal{G}(\tilde{\mathbf{S}}, \theta) \rangle + \mathcal{C}\right], \tag{2.50}$$

  with the integration constant $\mathcal{C}$,

- assume $\mathcal{C}$ equal to zero.

Eq.(2.50) reveals the interaction between the martensitic transformation product y_5, the total stress $\tilde{\mathbf{S}}$, and temperature θ.

The required function $y_5 = \mathcal{Y}_2(\mathcal{S}, \theta)$ is derived by considering chemical and mechanical components of the total Gibbs free energy. The total driving force can be represented by a difference of mechanical and chemical components of the total Gibbs free energy:

$$\Delta G_5^{mic} = \Delta G_\sigma^{mic} - \Delta G_{ch}^{mic} \tag{2.51}$$

when neglecting frictional effects on habit planes ΔG_F^{mic} and the elastic coherency interfacial energy $A_5^{mic}\gamma_5$ in the expression for ΔG_5^{mic} in Table(2.2). The strain energy is given by

$$\Delta G_\sigma^{mic} = \tilde{\mathbf{S}} : \mathbf{E}^*, \tag{2.52}$$

where $\mathbf{E}^*$ is the microscopic transformation strain measured in the stress free state as a difference of strains before and after phase transformation. The chemical free energy is derived using Eqs.(2.6), (2.7), and is defined by

$$\Delta G_{ch}^{mic} = \sum_{l=1}^{\mathcal{N}(t)} V_l^{nuc} \Delta G_{ch_5} = \sum_{l=1}^{\mathcal{N}(t)} a_l^2 c_l \Delta G_{ch_5}, \tag{2.53}$$

with the time related number of nuclei in a microregion $\mathcal{N}(t)$.

The total stress $\tilde{\mathbf{S}}$ in Eq.(2.52) is a sum

$$\tilde{\mathbf{S}} = \tilde{\mathbf{S}}_{eq}^{act} + \tilde{\mathbf{S}}_{eq}^{fur} + \mathcal{S}, \tag{2.54}$$

of the following components:

$\tilde{\mathbf{S}}_{eq}^{act}$	actually self-equilibrating stress
$\tilde{\mathbf{S}}_{eq}^{fur}$	further generated self-equilibrating stress
$\mathcal{S}$	loading external stress assumed to be homogeneous in the mesodomain

The actually self-equilibrating stress reveals the interaction of all actually transformed microregions with the microregion under consideration. The further self-equilibrating stress is generated by the interaction of the microregion which undergoes transformation and the surrounding mesodomain. The load stress is assumed to be homogeneous in the mesodomain.

Substituting Eq.(2.54) in Eq.(2.52) results in

$$\Delta G_{\sigma}^{mic}(\mathbf{S}) \equiv \Delta G_{\sigma}^{mic}(\mathcal{S}, \tilde{\mathbf{S}}_{eq}^{act}, \tilde{\mathbf{S}}_{eq}^{fur}) = \tilde{\mathbf{S}}_{eq}^{act} : \mathbf{E}^* + \tilde{\mathbf{S}}_{eq}^{fur} : \mathbf{E}^* + \mathcal{S} : \mathbf{E}^*. \tag{2.55}$$

The total differential of $\Delta G_{\sigma}^{mic}(\mathcal{S}, \tilde{\mathbf{S}}_{eq}^{act}, \tilde{\mathbf{S}}_{eq}^{fur})$ with respect of $\tilde{\mathbf{S}}$ components is given as

$$d\Delta G_{\sigma}^{mic} = d\tilde{\mathbf{S}}_{eq}^{act} : \mathbf{E}^* + d\tilde{\mathbf{S}}_{eq}^{fur} : \mathbf{E}^* + d\mathcal{S} : \mathbf{E}^*. \tag{2.56}$$

Substituting Eq.(2.56) in the differential form of Eq.(2.51) and averaging $d\Delta G_5^{mic}$ over volume gives

$$\langle d\mathcal{G} \rangle = \langle d\tilde{\mathbf{S}}_{eq}^{act} : \mathbf{E}^* \rangle + \langle d\tilde{\mathbf{S}}_{eq}^{fur} : \mathbf{E}^* \rangle + \langle d\mathcal{S} : \mathbf{E}^* \rangle - \langle d\Delta G_{ch}^{mic} \rangle. \tag{2.57}$$

The volume average of work done by the external stress $\mathcal{S}$ on the microscopic strain $\mathbf{E}^*$ is replaced by the contraction of $\mathcal{S}$ and the volume average of $\mathbf{E}^*$, that is expressed by

$$\langle d\mathcal{S} : \mathbf{E}^* \rangle = d\mathcal{S} : \langle \mathbf{E}^* \rangle. \tag{2.58}$$

This replacement can be done because at the start of transformation, $y_5 \ll 1$, the martensitic inclusions are oriented "optimally" in respect to $\mathcal{S}$ and when the transformation develops internal stress increases and martensitic microregions get less favourable orientation [51]. Substituting Eq.(2.57) and Eq.(2.58) in Eq.(2.48) and rearranging the resulting equation by shifting the

first two RHS terms evidently related to the progress of martensitic transformation to the LHS results in

$$\left[\frac{1}{1-y_5}+k_F V^{mic}\langle\frac{d\tilde{\mathbf{S}}^{fur}_{eq}}{dy_5}:\mathbf{E}^*\rangle+\ k_F V^{mic}\langle\frac{d\tilde{\mathbf{S}}^{act}_{eq}}{dy_5}:\mathbf{E}^*\rangle\right]dy_5$$

$$= \quad k_F V^{mic}\langle\frac{d\Delta G^{mic}_{ch}}{d\theta}\rangle d\theta - k_F V^{mic}\langle\mathbf{E}^*\rangle : d\mathcal{S}. \tag{2.59}$$

Considering y_5, temperature θ, and external stress $\mathcal{S}$ as time dependent functions, the above kinetic equation can be written as the evolution equation

$$\left[\frac{1}{1-y_5}+k_F V^{mic}\langle\frac{d\tilde{\mathbf{S}}^{fur}_{eq}}{dy_5}:\mathbf{E}^*\rangle+\ k_F V^{mic}\langle\frac{d\tilde{\mathbf{S}}^{act}_{eq}}{dy_5}:\mathbf{E}^*\rangle\right]\dot{y}_5$$

$$= \quad k_F V^{mic}\langle\frac{d\Delta G^{mic}_{ch}}{d\theta}\rangle \dot{\theta} - k_F V^{mic}\langle\mathbf{E}^*\rangle : \dot{\mathcal{S}}. \tag{2.60}$$

The simple form of this evolution equation is obtained due to the following operations and assumptions:

- The third term of LHS of Eq.(2.60) can be expressed by

$$\langle\frac{d\tilde{\mathbf{S}}^{act}_{eq}}{dy_5}:\mathbf{E}^*\rangle = -p\frac{d\mathcal{F}}{dy_5}\langle\mathbf{I}:\mathbf{E}^*\rangle = -2p\ y_5\ \mathrm{tr}\mathbf{E}^*, \tag{2.61}$$

  when the stress $\tilde{\mathbf{S}}^{act}_{eq}$ is substituted by $-(p\mathcal{F}(y_5)\mathbf{I})$, and the function $\mathcal{F}(y_5)$ is assumed to be the quadratic one i.e. $\mathcal{F}(y_5)=y_5^2$. The average final hydrostatic stress at $y_5=1$ is p, and $\mathbf{I}$ is the unit second order tensor.

- The second term of RHS of Eq.(2.60) can be replaced by

$$k_F V^{mic}\langle\mathbf{E}^*\rangle : \dot{\mathcal{S}} = k_F V^{mic} y_5^{\frac{1}{n}}\ \mathbf{E}^*_{cr} : \dot{\mathcal{S}}, \tag{2.62}$$

  with $\mathbf{E}^*_{cr}$ being $\mathbf{E}^*$ when $y_5=1$ and the entire microregion transforms to martensite, and the exponent $n>1$. This replacement reflects a decrease of deformation and $\frac{d\mathbf{E}^*}{dy_5}$ due to the internal stress increase during transformation.

- The term with $\tilde{\mathbf{S}}^{fur}_{eq}$ in Eq.(2.60) can be neglected because its influence is indirectly accounted for by evaluation of thermo-elastic stresses. This assumption follows the Eshelby concept presented in [19] and utilised previously in [74].

Therefore the simplified evolution equation for the martensitic transformation has the form

$$\begin{aligned} & \left(\frac{1}{1-y_5} - 2k_F V^{mic} p\ y_5\ \mathrm{tr}\mathbf{E}^*\right)\dot{y}_5 \\ = \quad & k_F V^{mic}\langle\frac{d\Delta G^{mic}_{ch}}{d\theta}\rangle\dot{\theta} - k_F V^{mic} y_5^{\frac{1}{n}}\ \mathbf{E}^*_{cr} : \dot{\mathcal{S}}. \end{aligned} \tag{2.63}$$

The solution of Eq.(2.60) and/or Eq.(2.63) is the function $\mathcal{Y}_2(\mathcal{S},\theta)$ which determines the martensitic volume fraction y_5 as a function of the external load stress $\mathcal{S}$ and temperature θ.

Parameters of evolution equation Eq.(2.63) have the following values given in [51]: $k_F V^{mic} = 0.0206\ m^2/N$, hydrostatic pressure $p \in [0, 50]\ MPa$, the first invariant of strain tensor $\frac{1}{3}\mathrm{tr}\mathbf{E}^* = 0.04$, $[k_F V^{mic}(\frac{d\Delta G^{mic}_c}{d\theta})] = 0.0484°C^{-1}$, and the magnitude of components of the microscopic transformation strain, $\mathbf{E}^*$, are in the range $[0.07, 0.29]$.

2.5 Governing Differential Equation for Phase Transformation

We have presented metallurgical phase transformation laws as differential equations. We now propose to write a governing differential equation for phase transformation leading ultimately to a variational form for the metallurgical volume phase fraction.

In this work we have adopted an averaging principle to describe the rate of transformation of a phase in a particular volume. We have used a phenomenological approach to arrive at evolution equations to describe phase transformation at a point. We have also identified two principle behaviours governing phase transformation that of diffusive mechanism and a displacive or mechanism in transforming the metallurgical structure.

In arriving at a governing differential equation for this description of metallurgical phase transformation we consider an elemental volume undergoing a phase transformation such as the one in Fig.2.1

We consider firstly the diffusive mechanism acting to produce such a transformation at a given rate. If we consider the surfaces of the elemental volume we have, as indicated by the arrows, a rate of diffusion which we can characterize

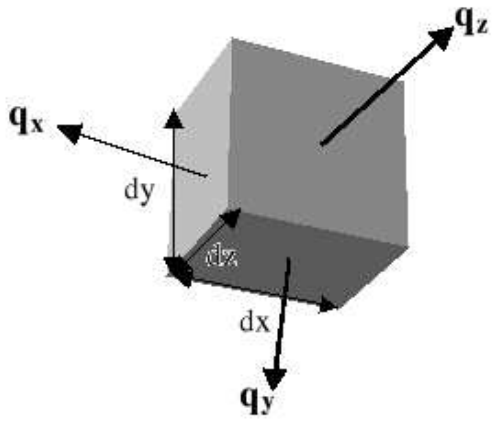

Figure 2.1: Phase transformation rates across and elemental volume

by Fick's first law [57] of diffusion in one dimension:

$$J_B = -D_B \frac{\partial C_B}{\partial x} \tag{2.64}$$

where J_B is the rate of diffusion , D_B is the intrinsic coefficient of diffusion of the solute, B and $\frac{\partial C_B}{\partial x}$ is the concentration gradient.

For a phase transformation dependent on a diffusional process only the rate of diffusion of solute into the elemental volume is equal to the rate of phase change occurring in the elemental volume. The particular part of the rate of phase change attributable to diffusion only we will represent by $\frac{\partial \underline{y}_p}{\partial t}$.

So that for a particular phase change of the set of possible phase changes, $\underline{y}$, produced by a rate of diffusion, q, we have

$$dx\ dy\ \frac{\partial q}{\partial z}\ dz + dx\ dz\ \frac{\partial q}{\partial y}\ dy + dy\ dz\ \frac{\partial q}{\partial x}\ dx = \frac{\partial \underline{y_p}}{\partial t}\ dV \tag{2.65}$$

From Fick's law we have

$$q = -D^p \frac{\partial \underline{y}}{\partial x} \tag{2.66}$$

with D^p describing the diffusivity of the transformation. Substituting into equation 2.65 we obtain:

$$\left[\frac{\partial}{\partial x}\left(-D^p \frac{\partial \underline{y}}{\partial x}\right) + \frac{\partial}{\partial y}\left(-D^p \frac{\partial \underline{y}}{\partial y}\right) + \frac{\partial}{\partial z}\left(-D^p \frac{\partial \underline{y}}{\partial z}\right)\right]\ dV = \frac{\partial \underline{y^p}}{\partial t}\ dV \tag{2.67}$$

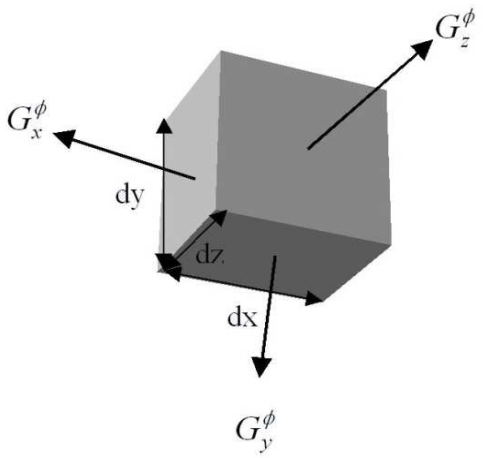

Figure 2.2: Rates of change of Gibbs free energy across and elemental volume

which for and arbitrary finite non-zero volume gives the governing equation for phase transformations resulting from a diffusive mechanism

$$\frac{\partial \underline{y}^p}{\partial t} + \nabla \cdot (\mathbf{D}^p \nabla \underline{y}) = 0 \tag{2.68}$$

where $\mathbf{D}^p = D_{ij}^p$ is a diagonal tensor describing the diffusivity of transformation in the three directions (x,y,z).

We now consider the elemental volume in Fig. 2.2 undergoing a phase change induced by a displacive rearranging of the crystal structure such as occurring in the martensitic transformation. It has been shown that the available Gibbs free energy for such a transformation is accounted for by the change in free energy of an austenitic structure compared to for example a martensitic structure and also by the Bain strain produced in rearranging the crystal structure from fcc to bct. This process is also affected by the applied stress. We represent the rate of phase change attributable to the displacive transformation as $\frac{\partial \underline{y}^m}{\partial t}$. Using the Gibbs free energy, as described in Eq. 2.50, we can write a general relation for such a displacive phase transformation. If we let $G^\phi = \dot{\mathcal{G}}$ be the rate of change of the Gibbs free energy, then we can write a relation for the volume fraction change within a volume as a result of changes in the Gibbs free energy happening across the volume. Referring to Fig. 2.2

$$dx\ dy\ \frac{\partial G^\phi}{\partial z}\ dz + dx\ dz\ \frac{\partial G^\phi}{\partial y}\ dy + dy\ dz\ \frac{\partial G^\phi}{\partial x}\ dx = -f_g \frac{\partial \underline{y}^m}{\partial t}\ dV \tag{2.69}$$

Which can be written simply as

$$\frac{\partial \underline{y}^m}{\partial t} = -f_g \nabla G^{\phi} \tag{2.70}$$

where f_g a proportionality factor which includes a factor reflecting the fact not all the of the available energy can be used for the transformation from the Second Law of Thermodynamics.

If we now consider such a volume and postulate that within it there exists a set of potential functions,$G_i^{\psi}(\theta, \mathbf{T})$ each corresponding to a particular metallurgical phase of the y_i phases, such that

$$G_i^{\phi} = D^m \left[\nabla G_i^{\psi}(\theta, \underline{y}, \mathbf{T}) \right] \tag{2.71}$$

which we can expand as

$$G_i^{\phi} = D^m \left[\frac{\partial G_i^{\psi}}{\partial \theta} \nabla \theta + \frac{\partial G_i^{\psi}}{\partial \mathbf{T}} \nabla \mathbf{T} \right] \tag{2.72}$$

where $\mathbf{T}$ is the second Piola-Kirchoff stress tensor. Substituting Eq.2.72 into Eq.2.70 we obtain

$$\frac{\partial \underline{y}^m}{\partial t} = -f_g \nabla \cdot \left(D^m \left[\frac{\partial G_i^{\psi}}{\partial \theta} \nabla \theta + \frac{\partial G_i^{\psi}}{\partial \mathbf{T}} \nabla \mathbf{T} \right] \right) \tag{2.73}$$

Since Eq.2.73 and Eq.2.68 each account for part of the vector of phase transformations occurring we can combine them to obtain a governing differential equation for phase transformation

$$\frac{\partial \underline{y}}{\partial t} + \nabla \cdot (\mathbf{D}^p \nabla \underline{y}) + f_g \nabla \cdot \left(D^m \left[\frac{\partial G_i^{\psi}}{\partial \theta} \nabla \theta + \frac{\partial G_i^{\psi}}{\partial \mathbf{T}} \nabla \mathbf{T} \right] \right) = 0 \tag{2.74}$$

Non-linear solution techniques, as used for the solution of the temperature and displacement equilibrium, will be necessary to solve for phase transformation equilibrium. The Galerkin Method can be applied directly to Eq. 2.74 to yield finite element equations for the solution of metallurgical volume phase fraction equilibrium for boundary value problems.

Chapter 3

Model of Thermo-Mechano-Metallurgical Process

The solution of the fully coupled thermo-mechanical-metallurgical heat treatment problem requires simultaneous solution for the following set of equations

1. heat equation for non-rigid conductor with singular surface and phase transformation,
2. evolution equations for material phase composition,
3. constitutive equations,
4. momentum balance law.

The result will provide the solution at the state of total equilibrium which is constructed on the basis of the following equilibriums:

1. displacement equilibrium in a mechanical analysis,
2. temperature equilibrium in a thermal analysis,
3. volume phase fraction equilibrium in a metallurgical phase and transformation analysis.

3.1 Lagrangian Description of Body Motion

The polycrystalline body is idealized by using the concept of a generalized material point representing a micro-region which is part of a grain deforming

due to phase transformations without the restraints of the neighboring parts of body.

The stress inside the micro-region is averaged, and the strain and displacement are measured only at one or more particular points of the bounding surfaces where continuity conditions must be fulfilled for neighboring regions. This concept allows one to treat the polycrystalline body motion as a continuum with internal local deformation of particles. It is also assumed that the shape of a micro-region does not vary significantly during the deformation process.

Lagrangian analysis is used with the initial position of the generalized particle $\mathbf{X}$ and the time t taken as independent variables. The variables (X_1^0, X_2^0, X_3^0) of $\mathbf{X}$ are global and called the Lagrangian or material variables. The internal deformation of the generalized particle is defined in terms of the local coordinate system. The local coordinate system can be transformed to the global one by using the orthogonal transformation matrix shown in [23].

The generalized particle is the smallest microstructural element of the alloy and can be imagined as the micro-region defined in [23] and [24] and seen to be like a point of the considered body. The definition of a micro-region and its deformation are developed from the concept of "free" deformation. This "free" deformation is defined with respect to phase transformation and means the deformation to the extent when neither the other micro-region nor the remaining part of the grain restrains the local deformation. For example, a micro-region for the martensitic transformation is a block of lathes or a plate dependent on the form of martensitic precipitation. A group of micro-regions form a mesodomain and will be represented in FE analysis by a finite element. The motion, which carries a fixed material element through various spatial

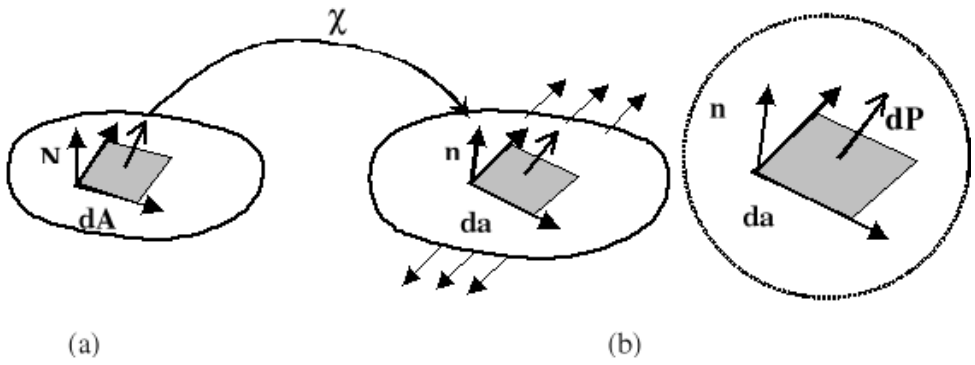

Figure 3.1: Differential surface traction in (a) reference and (b) deformed configurations

positions, can be expressed by the function of motion $\mathbf{x} = \chi(\mathbf{X}, t)$. This function, expressed in terms of Lagrangian variables, describes the variation of physical parameters for a given particle during its wandering through the space. The vector joining the point X and its actual position in the space $\mathbf{x} = (X_1^1, X_2^1, X_3^1)$ is the displacement vector given by $\mathbf{u} = \mathbf{X} - \mathbf{x}$. The constitutive variables, i.e. the stress and strain measures, used in the Lagrangian formulation are the second Piola-Kirchoff stress and the Green-Lagrange strain which are conjugate in terms of energy according to the Hill definition.

Referring to Fig. 3.1 the second Piola-Kirchoff or material stress tensor $\mathbf{T}$ is given by:

$$\mathbf{N} \cdot \mathbf{T} = \lim_{dA \to 0} \left(F^{-1} \frac{dP}{dA} \right) \tag{3.1}$$

where $\mathbf{F}^{-1}$ is the inverse of the deformation gradient defined as

$$\mathbf{F} = \frac{\partial \mathbf{x}}{\partial \mathbf{X}}; \;\; F_{iK} = x_{i,K} = \frac{\partial x_i}{\partial X_K}; \tag{3.2}$$

where $\mathbf{X}$ and $\mathbf{x} = \chi(\mathbf{X}, t)$ are the reference and current coordinates respectively.

The Green-Lagrange strain is conjugate to the second Piola-Kirchoff stress and is defined by

$$\tilde{\mathbf{L}} = \tfrac{1}{2} \left(u_{I,J} + u_{J,I} + u_{K,I} u_{K,J} \right) \tag{3.3}$$

where the displacement gradient is

$$u_{I,J} = \frac{\partial u_I}{\partial X_J} \tag{3.4}$$

The large indices I, J, K refer to the reference configuration. The "," is the usual abbreviated notation for differentiation with respect to coordinates.

Material parameters such as Young's modulus E, Poisson's ratio ν, yield limit, hardening parameters, thermal and others parameters of a mesodomain are evaluated by using a linear mixture rule that in vector form can be written as

$$\langle E \rangle = \underline{E} : \underline{y} \;, \;\; \langle \nu \rangle = \underline{\nu} : \underline{y} \tag{3.5}$$

where $\underline{y}$ is a vector of phase fractions y_i present at a mesodomain.

3.2 Balance Laws for TMM Process

The mathematical model of the TMM process consists of expressing thermal and mechanical equilibrium, i.e. the balance of internal energy and the balance of momentum as well as then governing differential equation for phase equilibrium. These principles have been derived to account for the coupling of thermal, mechanical and metallurgical effects for a thermo-inelastic body with solid phase transformations. The balance of momentum for a solid is given by the following equations:

$$\begin{array}{rl} \left(T_{KL}x_{i,L}\right)_{,K} + \ b_i = 0 & \text{for} \quad \mathbf{X} \in V \\ T_{KL}x_{i,L}N_K = T_i & \text{for} \quad \mathbf{X} \in \partial V \end{array} \tag{3.6}$$

where b_i is the body force, T_i is the nominal given stress vector and N_K is the surface normal vector. where b_i is the body force, T_i is the nominal stress vector.

The local balance of internal energy, neglecting any fluid motion in the weld pool, is given by [63]

$$\begin{array}{rcll} \rho\dot{e} + \nabla \cdot \mathbf{h} & = & 0 & \text{for } \mathbf{X} \in V \\ f_\theta^{\partial V} & = & -(\mathbf{k} \cdot \nabla\theta) \cdot \mathbf{N} & \text{for } \mathbf{X} \in \partial V \end{array} \tag{3.7}$$

where $\dot{e}$ is the rate of specific internal energy and h represents the heat flux vectors and $\mathbf{N}$ is the normal to the surface on which the flux, $f^{\partial V_\theta}$, occurs.

The rate of specific internal energy can be written as

$$\dot{e} = C\dot{\theta} + \frac{1}{\rho}\eta_{in}\mathbf{T} : \dot{\mathbf{L}}^{in} \tag{3.8}$$

where C is the specific heat per unit mass for a constant volume and the second term represents the rate of specific inelastic strain energy dissipated. The factor η_{in} is the inelastic heat energy fraction which is less than one as a consequence of the Second Law of Thermodynamics. If we use the heat energy per unit volume $C_v = \rho C$ then we can write the balance of energy as

$$C_v\dot{\theta} + \eta_{in}\mathbf{T} : \dot{\mathbf{L}}^{in} + \nabla \cdot \mathbf{h} = 0 \tag{3.9}$$

We assume that the flow of heat into the body obeys Fourier's law so that

$$\mathbf{h} = -\mathbf{k} \cdot \nabla\theta \tag{3.10}$$

The diagonal tensor of thermal conductivity $\mathbf{k}$ is

$$k_{IJ} = \begin{bmatrix} k_{11} & 0 & 0 \\ 0 & k_{22} & 0 \\ 0 & 0 & k_{33} \end{bmatrix} = \begin{bmatrix} k_x & 0 & 0 \\ 0 & k_y & 0 \\ 0 & 0 & k_z \end{bmatrix} \tag{3.11}$$

where k_x, k_y and k_z are the conductivities in the x, y and z directions, respectively, in the case of anisotropic thermal conductivity. This conductivity tensor is usually considered to be isotropic so that instead we have

$$k_{IJ} = k\ \delta_{IJ} \tag{3.12}$$

where $k = k(\theta, \underline{y})$ is the conductivity, in general, a function of the given temperature for each given phase.

We can thus rewrite Eq. 3.9 as

$$C_v\dot{\theta} - k\delta_{IJ}\theta_{,JI} + \eta_{in}T_{IJ}\dot{L}^{in}_{IJ} = 0 \tag{3.13}$$

Solid phase equilibrium for the volume fractions of metallurgical phases, y_i, is expressed by the following governing equation

$$\begin{aligned} \dot{y_I} + (D^p y_{I\ ,JJ} + \left(f_g D^m \left[\frac{\partial G_{I^\psi}}{\partial \theta}\theta + \frac{\partial G_{I^\phi}}{\partial T_{KL}} T_{KL} \right] \right)_{,JJ} &= 0 \quad , \mathbf{X} \in V \\ \text{with} \qquad (D^p y_{I,J} + f_g D^m G^\psi_{I,J}) N_J &= q^p_I \quad , \mathbf{X} \in \partial V \end{aligned} \tag{3.14}$$

With the assumption that D^p, f_g and D^m are defined for a given temperature, volume fraction of a particular phase and stress state existing at a material point, the gradients of these coefficients are zero. Hence we can write eq.3.14 as

$$\dot{y_I} + D^p y_{I\ ,JJ} + f_g D^m \left(\frac{\partial G^\psi_I}{\partial \theta}\theta + \frac{\partial G^\psi_I}{\partial T_{KL}} T_{KL} \right)_{,JJ} = 0 \tag{3.15}$$

Balance laws for momentum, internal energy and volume phase fraction transformation can be expressed in functional forms and then approximated by the Galerkin type Finite Element Method. A formulation of the functional forms of the balance laws following [36], [65] follows.

To formulate the weak solution to the CTMM problem we first characterize two classes of functions: the trial solutions $\mathcal{U}$ and the weighting functions $\mathcal{V}$ (or variations), which are defined by

$$\mathcal{U} = \{u_i, \theta, y_i \mid u_i, \theta, y_i \in H^1\} \tag{3.16}$$

where u_i, θ and y_i fulfills boundary conditions for the thermo-mechanical problem,

$$\mathcal{V} = \{\upsilon_i, \vartheta, \varphi_i\} \mid \ \upsilon_i, \vartheta, \varphi_i \in H^1\} \tag{3.17}$$

where $\upsilon_i, \vartheta, \varphi_i$ are equal zero at the boundary ∂V, and H^1 is the Hilbert space. We next express the balance laws Eqs.(3.6), (3.13), (2.74), as differential operators defined by

$$\begin{aligned}
\Phi(\mathbf{u}, \theta, y_I) &= (T_{JK} x_{i,K})_{,J} + b_I & (3.18)\\
\Psi(\mathbf{u}, \theta, y_I) &= C_v \dot{\theta} - k\theta_{,II} + \eta_{in} T_{IJ} \dot{L}^{in}_{IJ} & (3.19)\\
\Upsilon(\mathbf{u}, \theta, y_I) &= \dot{y}_I + D^p y_{I\,,JJ} + f_g D^m \left(\frac{\partial G^{\psi}_I}{\partial \theta} \theta_{,JJ} + \frac{\partial G^{\psi}_I}{\partial T_{KL}} T_{KL,JJ} \right) & (3.20)
\end{aligned}$$

We apply the Galerkin method to these coupled differential equations. We multiply each equation by the corresponding weighting function and integrate over the volume.

$$\int_{V_0} (T_{JK} x_{i,K})_{,J} \upsilon_I + b_I \upsilon_I \, dV = 0 \tag{3.21}$$

$$\int_{V_0} \left(C_v \dot{\theta} - k\theta_{,II} + \eta_{in} T_{IJ} \dot{L}^{in}_{IJ} \right) \vartheta \, dV = 0 \tag{3.22}$$

$$\int_{V_0} \left[\dot{y}_I + D^p y_{I\,,JJ} + f_g D^m \left(\frac{\partial G^{\psi}_I}{\partial \theta} \theta_{,JJ} + \frac{\partial G^{\psi}_I}{\partial T_{KL}} T_{KL,JJ} \right) \right] \varphi_I \, dV = 0 \tag{3.23}$$

Applying Gauss's divergence theorem we can decompose part of Eq.3.21

$$\int_{V_0} (T_{JK} x_{i,K})_{,J} \upsilon_I = \int_{\partial V_0} \upsilon_I x_{i,K} T_{JK} N_J \, d\mathcal{P} - \int_V x_{i,K} T_{JK} \upsilon_{I,J} \, dV \tag{3.24}$$

For the second Piola-Kirchoff stress the surface tractions are given by

$$T_I = x_{i,K} T_{JK} N_J \tag{3.25}$$

Combining Eq. 3.24 and Eq. 3.25 with 3.21 we obtain

$$\int_{V_0} x_{i,K} T_{JK} \upsilon_{I,J} \, dV = \int_{\partial V_0} T_I \upsilon_I \, d\mathcal{P} + \int_{V_0} b_I \upsilon_I dV \tag{3.26}$$

Noting that $x_i = x_I - u_I$ gives

$$x_{i,K} = (\delta_{IK} - u_{I,K}) \tag{3.27}$$

So that we may rewrite Eq. 3.26 as

$$\int_{V_0}(\delta_{IK}-u_{I,K})T_{JK}\upsilon_{I,J}\,dV=\int_{\partial V_0}T_I\upsilon_I\,d\mathcal{P}+\int_{V_0}b_I\upsilon_I dV \tag{3.28}$$

which simplifies to

$$\int_{V_0}(u_{I,K}T_{JK}-T_{JI})\upsilon_{I,J}\,dV+\int_{\partial V_0}T_I\upsilon_I\,d\mathcal{P}+\int_{V_0}b_I\upsilon_I dV=0 \tag{3.29}$$

We can use Gauss's theorem to decompose the integral with the divergence of temperature in the heat equation (Eq. 3.13)

$$\int_{V_0}k_{IJ}\theta_{,JI}\vartheta dV=\int_{\partial V_0}k_{IJ}\theta_{,J}N_I\,\vartheta d\mathcal{P}-\int_{V_0}k_{IJ}\,\theta_{,J}\,\vartheta_{,I}\,dV \tag{3.30}$$

Which gives

$$\int_{V_0}\left[C_v\dot{\theta}\,\vartheta+k_{IJ}\theta_{,J}\,\vartheta_{,I}+\eta_{in}T_{IJ}\dot{L}^{in}_{IJ}\,\vartheta\right]\,dV+\int_{\partial V_0}f^{\partial V}_{\theta}\,\vartheta d\mathcal{P}=0 \tag{3.31}$$

where

$$\int_{\partial V_0}f^{\partial V}_{\theta}\,\vartheta d\mathcal{P}=-\int_{\partial V_0}k_{IJ}\theta_{,J}\,N_I\vartheta d\mathcal{P} \tag{3.32}$$

includes the heat in-flux from the welding arc as well as heat out-fluxes due to contact conductance, convection and radiation through the external surface of the body and N_I is the surface normal.

We may similarly obtain a BVP from the governing differential equation for metallurgical phase transformations by applying Gauss's theorem

$$\begin{aligned}
&\int_{V_0}\left[D^p y_{I\,,JJ}+f_g D^m\left(\frac{\partial G^{\psi}_I}{\partial\theta}\theta_{,JJ}+\frac{\partial G^{\psi}_I}{\partial T_{KL}}T_{KL,JJ}\right)\right]\varphi_I\,dV=\\
&\int_{\partial V_0}\left[D^p y_{I\,,J}+f_g D^m\left(\frac{\partial G^{\psi}_I}{\partial\theta}\theta_{,J}+\frac{\partial G^{\psi}_I}{\partial T_{KL}}T_{KL,J}\right)\right]\varphi_I N_J\,d\mathcal{P}\\
&-\int_{V_0}\left[D^p y_{I\,,J}+f_g D^m\left(\frac{\partial G^{\psi}_I}{\partial\theta}\theta_{,J}+\frac{\partial G^{\psi}_I}{\partial T_{KL}}T_{KL,J}\right)\right]\varphi_{I,J}\,dV\,dV
\end{aligned} \tag{3.33}$$

This formulation thus formally yields a quantity describing a flux of phase transformation across the surface of the body

$$\int_{\partial V_0}\left[D^p y_{I\,,J}+f_g D^m\left(\frac{\partial G^{\psi}_I}{\partial\theta}\theta_{,J}+\frac{\partial G^{\psi}_I}{\partial T_{KL}}T_{KL,J}\right)\right]\varphi_I N_J\,d\mathcal{P}=\int_{\partial V_0}q^p_I\varphi_I\,d\mathcal{P} \tag{3.34}$$

which usually in CTMM problems, arising from welding processes, will be zero. Usually the driving force in welding problems is a heat source and applied mechanical surface tractions, T_I, will also be zero in the absence of a clamping jig. There are, however, applications in welding for such a flux of metallurgical phase change. The metallurgical phase change as a result of the diffusion of interstial elements from an electrode or shielding gas could be modelled in this way. Hydrogen diffusion producing a metallurgical change susceptible to fracture could for instance be modelled by such a flux.

Eq. 3.23 can thus be written as

$$\int_{V_0} \dot{y}_I \, \varphi_I - \left[D^p y_{I\,,J} + f_g D^m \left(\frac{\partial G_I^\psi}{\partial \theta} \theta_{,J} + \frac{\partial G_I^\psi}{\partial T_{KL}} T_{KL,J} \right) \right] \varphi_{I,J} \, dV + \int_{\partial V_0} q_I^p \varphi_I \, d\mathcal{P} = 0 \tag{3.35}$$

Stationary conditions for functionals Eq.3.29, Eq.3.31 and Eq.3.35 are the following variational equations:

$$\int_{V_0} (u_{I,K} T_{JK} - T_{JI}) \, \delta \upsilon_{I,J} \, dV + \int_{\partial V_0} T_I \delta \upsilon_I \, d\mathcal{P} + \int_{V_0} b_I \delta \upsilon_I dV = 0 \tag{3.36}$$

$$\int_{V_0} \left[C_v \dot{\theta} \, \delta \vartheta + k_{IJ} \theta_{,J} \, \delta \vartheta_{,I} + \eta_{in} T_{IJ} \dot{L}_{IJ}^{in} \, \delta \vartheta \right] \, dV + \int_{\partial V_0} f_\theta^{\partial V} \, \delta \vartheta d\mathcal{P} = 0 \tag{3.37}$$

$$\int_{V_0} \dot{y}_I \, \delta \varphi_I - \left[D^p y_{I\,,J} + f_g D^m \left(\frac{\partial G_I^\psi}{\partial \theta} \theta_{,J} + \frac{\partial G_I^\psi}{\partial T_{KL}} T_{KL,J} \right) \right] \delta \varphi_{I,J} \, dV + \int_{\partial V_0} q_I^p \delta \varphi_I \, d\mathcal{P} = 0 \tag{3.38}$$

3.3 Singularities and Singular Surfaces in the Solution of the State Variables

As shown in Fig. 3.2 it is possible that singularities could occur in the solution of the state variables due to jumps associated with property changes. Such jumps would actually occur at the level of the grain where grain boundaries would lead to singular surfaces. These don't generally lead to observable jumps in the state variables at the macroscopic level at which the solution is sought. Grain boundaries are generally neglected in normal single phase polycrystalline structures as they form part of the average material properties associated with a given material when properties such as the yield stress or Young's modulus are determined.

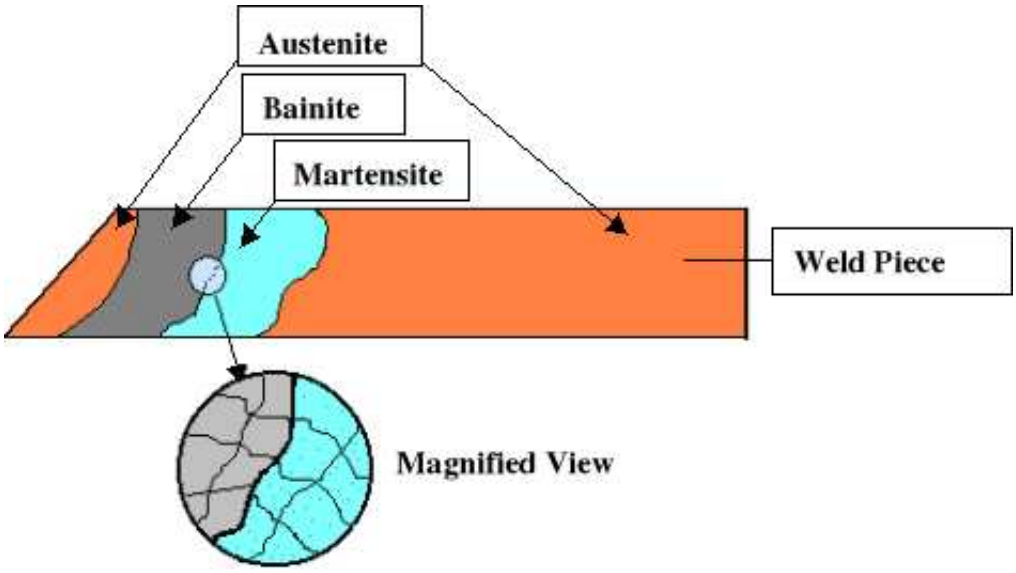

Figure 3.2: Schematic of a typical weld showing how the jumps in solution between grains of different phases can lead to a singular surface in the solution

The situation can be different in the case of a multiphase material as shown if Fig. 3.2 where there is a coincidence of jumps associated with a phase change at the boundaries of zones of dominant phases leading in effect to a singular surface across which the solution is not necessarily continuous. Such a diskontinuity is observable at the macroscopic level in the real structure and can be observed in the numerical solution when two sets of material properties are used to describe a body. This is quite often the case in welding where, even without considering phase changes, two different properties might be ascribed to the filler material and base material.

To be precise in formulating the equilibrium equations then, we have to allow for these singularities. To do this we treat the zonal boundaries, where the dominant phase fraction changes from one type to another, as a singular surface, Γ. We ascribe additional boundary conditions to account for these singular surfaces and take them into account by specifying that the state variables and weighting functions must fulfill these additional boundary conditions when applying the Galerkin method.

To evaluate the derivatives when allowing for singularities we use Gâteaux differentiation. The Gâteaux derivative d_G of a function f, operating over a Banach space, at ϕ in the direction α is defined as

$$d_G(\phi, \alpha) = \lim_{t \to 0} \frac{f(\phi + \alpha t) - f(\phi)}{t} = \frac{d}{dt} f(\phi + \alpha t)|_{t=0} \tag{3.39}$$

We can thus obtain derivatives on singular surfaces, in positive and negative directions normal to the singular surface, using the Gâteux derivative.

Allowing for singular surfaces we can reformulate Eq. 3.6 as

$$\begin{array}{rl} \left(T_{KL}x_{i,L}\right)_{,K} + \ b_i = 0 & \text{for} \quad \mathbf{X} \in V \\ T_{KL}x_{i,L}N_K = T_i & \text{for} \quad \mathbf{X} \in \partial V, \\ T_{KL}x_{i,L}N_K^+ = T_i^+ \ , \ T_{KL}x_{i,L}N_K^- = T_i^- & \text{for} \quad \mathbf{X} \in \Gamma, \end{array} \tag{3.40}$$

Applying Gauss's theorem as before to Eq. 3.21 but using the Gâteux derivative and on $\partial V \cup \Gamma$ instead of just ∂V we obtain instead of Eq. 3.24:

$$\begin{aligned} &\int_{V_0} (T_{JK}x_{i,K})_{,J}\upsilon_I = \int_{\partial V_0} \upsilon_I x_{i,K}T_{JK}N_J \ d\mathcal{P} + \int_\Gamma \upsilon_I x_{i,K}T_{JK}N_J^+ \ d\Gamma \\ &+ \int_\Gamma \upsilon_I x_{i,K}T_{JK}N_J^- \ d\Gamma - \int_V x_{i,K}T_{JK}\upsilon_{I,J} \ dV \end{aligned} \tag{3.41}$$

So that instead of Eq. 3.29 we obtain

$$\begin{aligned} &\int_{V_0} (u_{I,K}T_{JK} - T_{JI})\upsilon_{I,J} \ dV + \int_{\partial V_0} T_I\upsilon_I \ d\mathcal{P} + \int_\Gamma T_I^+\upsilon_I \ d\Gamma \\ &+ \int_\Gamma T_I^-\upsilon_I \ d\Gamma + \int_{V_0} b_I\upsilon_I dV = 0 \end{aligned} \tag{3.42}$$

which we may write as

$$\begin{aligned} &\int_{V_0} (u_{I,K}T_{JK} - T_{JI})\upsilon_{I,J} \ dV + \int_{\partial V_0} T_I\upsilon_I \ d\mathcal{P} \\ &+ \int_\Gamma \langle T_I\rangle\upsilon_I \ d\Gamma + \int_{V_0} b_I\upsilon_I dV = 0 \end{aligned} \tag{3.43}$$

where the $\langle \ldots \rangle$ indicates that the quantity is evaluated in the positive and negative direction to a singular surface.

We may similarly reformulate Eq. 3.8 to account for singular surfaces

$$\begin{array}{rcll} \rho\dot{e} + \nabla \cdot \mathbf{h} & = & 0 & \text{for } \mathbf{X} \in V \\ f_\theta^{\partial V} & = & -(\mathbf{k} \cdot \nabla\theta) \cdot \mathbf{N} & \text{for } \mathbf{X} \in \partial V \\ f_\theta^{+\partial V} = -(\mathbf{k} \cdot \nabla\theta^+) \cdot \mathbf{N}^+ \ , \ f_\theta^{-\partial V} & = & -(\mathbf{k} \cdot \nabla\theta^-) \cdot \mathbf{N}^- & \text{for } \mathbf{X} \in \partial\Gamma \end{array} \tag{3.44}$$

Applying Gauss's theorem as before to Eq. 3.29 but allowing for the diskontinuous temperature field and using Gâteaux derivatives we obtain

$$\begin{aligned} &\int_{V_0} k_{IJ}\theta_{,JI}\vartheta dV = \int_{\partial V_0} k_{IJ}\theta_{,J}N_I \, \vartheta d\mathcal{P} + \int_\Gamma k_{IJ}\theta^+{}_{,J}N_I^+ \, \vartheta d\Gamma \\ &+ \int_\Gamma k_{IJ}\theta^-{}_{,J}N_I^- \, \vartheta d\Gamma - \int_{V_0} k_{IJ} \, \theta_{,J} \, \vartheta_{,I} \, dV \end{aligned} \tag{3.45}$$

So that instead of Eq. 3.31 we obtain

$$\int_{V_0}\left[C_v\dot{\theta}\,\vartheta + k_{IJ}\theta_{,J}\,\vartheta_{,I} + \eta_{in}T_{IJ}\dot{L}^{in}_{IJ}\,\vartheta\right]\,dV + \int_{\partial V_0} f^{\partial V}_{\theta}\,\vartheta d\mathcal{P} + \int_{\Gamma} f^{\Gamma+}_{\theta}\,\vartheta d\Gamma + \int_{\Gamma} f^{\Gamma-}_{\theta}\,\vartheta d\Gamma = 0 \tag{3.46}$$

which we may write as

$$\int_{V_0}\left[C_v\dot{\theta}\,\vartheta + k_{IJ}\theta_{,J}\,\vartheta_{,I} + \eta_{in}T_{IJ}\dot{L}^{in}_{IJ}\,\vartheta\right]\,dV + \int_{\partial V_0} f^{\partial V}_{\theta}\,\vartheta d\mathcal{P} + \int_{\Gamma}\langle f^{\Gamma}_{\theta}\rangle\,\vartheta d\Gamma = 0 \tag{3.47}$$

Finally we can allow for diskontinuities in the equilibrium of the volume fraction of phases by reformulating Eq. 3.14

$$\begin{aligned} \dot{y}_I + D^p y_{I\,,JJ} + f_g D^m\left[\frac{\partial G_{I^{\psi}}}{\partial\theta}\theta + \frac{\partial G_{I^{\phi}}}{\partial T_{KL}}T_{KL}\right]_{,JJ} &= 0 \quad , \mathbf{X}\in V \\ \text{with} \qquad (D^p y_{I,J} + f_g D^m G^{\psi}_{I,J})N_J &= q^p_I \quad , \mathbf{X}\in\partial V \\ (D^p y^+_{I,J} + f_g D^m G^{\psi+}_{I,J})N^+_J = q^{p+}_I\ ,\ (D^p y^-_{I,J} + f_g D^m G^{\psi-}_{I,J})N^-_J &= q^{p-}_I \quad , \mathbf{X}\in\Gamma \end{aligned} \tag{3.48}$$

So that Eq. 3.35 similarly becomes

$$\int_{V_0}\dot{y}_I\,\varphi_I - \left[D^p y_{I\,,J} + f_g D^m\left(\frac{\partial G^{\psi}_I}{\partial\theta}\theta_{,J} + \frac{\partial G^{\psi}_I}{\partial T_{KL}}T_{KL,J}\right)\right]\varphi_{I,J}\,dV + \int_{\partial V_0} q^p_I\varphi_I\,d\mathcal{P} + \int_{\Gamma}\langle q^p_I\rangle\varphi_I\,d\Gamma = 0 \tag{3.49}$$

We can thus arrive at the stationary conditions for the functional forms of the equilibrium equations which include singular surfaces

$$\int_{V_0}(u_{I,K}T_{JK} - T_{JI})\,\delta\upsilon_{I,J}\,dV + \int_{\partial V_0} T_I\delta\upsilon_I\,d\mathcal{P} + \int_{\Gamma}\langle T_I\rangle\delta\upsilon_I\,d\Gamma + \int_{V_0} b_I\delta\upsilon_I dV = 0 \tag{3.50}$$

$$\int_{V_0}\left[C_v\dot{\theta}\,\delta\vartheta + k_{IJ}\theta_{,J}\,\delta\vartheta_{,I} + \eta_{in}T_{IJ}\dot{L}^{in}_{IJ}\,\delta\vartheta\right]\,dV + \int_{\partial V_0} f^{\partial V}_{\theta}\,\delta\vartheta d\mathcal{P} + \int_{\Gamma}\langle f^{\partial V}_{\theta}\rangle\,\delta\vartheta d\Gamma = 0 \tag{3.51}$$

$$\int_{V_0}\dot{y}_I\,\delta\varphi_I - \left[D^p y_{I\,,J} + f_g D^m\left(\frac{\partial G^{\psi}_I}{\partial\theta}\theta_{,J} + \frac{\partial G^{\psi}_I}{\partial T_{KL}}T_{KL,J}\right)\right]\delta\varphi_{I,J}\,dV + \int_{\partial V_0} q^p_I\delta\varphi_I\,d\mathcal{P} + \int_{\Gamma}\langle q^p_I\rangle\delta\varphi_I\,d\Gamma = 0 \tag{3.52}$$

3.4 Stress-Strain Constitutive Equations and Tangent Moduli

Deformations of a dispersed particle, i.e. microregion V^{mic}, of an alloy with multiphase internal structure occur due to phase transformations driven by variations of temperature and stress, external thermal and mechanical loadings and internal energy sources. A microregion deformation is separated into reversible and permanent parts, and therefore appropriate elastic, thermal and plastic components of the Green finite strain rate tensor are considered in the total strain rate evaluation. The total strain rate $\dot{\mathbf{L}}$ can be divided into five terms

$$\dot{\mathbf{L}} = \dot{\mathbf{L}}^{el} + \dot{\mathbf{L}}^{th} + \dot{\mathbf{L}}^{tr} + \dot{\mathbf{E}}^{pl} + \dot{\mathbf{E}}^{trip} \tag{3.53}$$

with

$\dot{\mathbf{L}}^{el}$	plastic strain rate
$\dot{\mathbf{L}}^{th}$	thermal strain rate
$\dot{\mathbf{L}}^{tr}$	transformation strain rate
$\dot{\mathbf{E}}^{pl}$	deviator of plastic strain rate
$\dot{\mathbf{E}}^{trip}$	deviator of plastic strain rate induced by phase transformation

The acronym ^{trip} is formed from the initial letters of the name: TRansformation Induced Plasticity. The strain rate $\dot{\mathbf{L}}$ can be also split into a spherical and deviatoric part

$$\dot{\mathbf{L}} = \tfrac{1}{3}\,\mathrm{tr}\dot{\mathbf{L}}\,\mathbf{1} + \dot{\mathbf{E}} \tag{3.54}$$

which are defined in terms of the second-order tensor components

$$\begin{aligned} \mathrm{tr}\dot{\mathbf{L}} &= \dot{L}_{KK} = \left(\dot{L}^{el}_{KK} + \dot{L}^{th}_{KK} + \dot{L}^{tr}_{KK}\right), \\ \dot{E}_{IJ} &= \dot{L}_{IJ} - \tfrac{1}{3}\delta_{IJ}\,\mathrm{tr}\dot{\mathbf{L}} = \dot{E}^{pl}_{IJ} + \dot{E}^{trip}_{IJ} + \dot{E}^{el}_{IJ}. \end{aligned} \tag{3.55}$$

3.4.1 Elastic Strain and Thermal Dilatation

The spherical part of elastic strain rate $\mathrm{tr}\dot{\mathbf{L}}^{el}$ and the deviator of elastic strain rate $\dot{\mathbf{E}}^{el}$ are related to stress rate $\dot{\mathbf{T}}$ by Hooke's law

$$\begin{aligned} \mathrm{tr}\dot{\mathbf{T}} &= \kappa\Big(\,\mathrm{tr}\dot{\mathbf{L}} - \dot{L}^{th}_{KK} - \dot{L}^{tr}_{KK}\Big) + \tfrac{\dot{\kappa}}{\kappa}\,\mathrm{tr}\mathbf{T}, \\ \dot{E}^{el}_{IJ} &\equiv \dot{E}_{IJ} - \dot{E}^{pl}_{IJ} - \dot{E}^{trip}_{IJ} = \tfrac{1}{\mu}\Big(\dot{S}_{IJ} - \tfrac{\dot{\mu}}{\mu}S_{IJ}\Big), \end{aligned} \tag{3.56}$$

with the bulk modulus $\langle\kappa\rangle$ and the shear modulus $\langle\mu\rangle$ defined by

$$\langle\kappa\rangle = \frac{\langle E(\theta)\rangle}{1-2\langle\nu(\theta)\rangle}; \quad \langle\mu\rangle = \frac{\langle E(\theta)\rangle}{2\left(1+\langle\nu(\theta)\rangle\right)}, \tag{3.57}$$

where the Young's modulus $\langle E\rangle$ and the Poisson's ratio $\langle\nu\rangle$ are averaged accordingly to the linear mixture law

$$\langle E(\theta)\rangle = E_i(\theta)y_i; \quad \langle\nu(\theta)\rangle = \nu_i(\theta)y_i. \tag{3.58}$$

The spherical part of thermal strain rate $\mathrm{tr}\dot{\mathbf{L}}^{th} = \dot{L}^{th}_{KK}$ represents the thermal expansion of different phases and at inhomogeneous microregion is defined by

$$\mathrm{tr}\dot{\mathbf{L}}^{th} = \frac{d}{dt}\left(y_i\int_0^{\theta(t)} {}_i\alpha^{dil}_{JK}(\vartheta)\delta_{KJ}d\vartheta\right) = \dot{y}_i\int_0^{\theta(t)} {}_i\alpha^{dil}_{JK}(\vartheta)\delta_{KJ}d\vartheta + \frac{1}{3}\,{}_i\alpha^{dil}_{KK}\;y_i\,\dot{\theta} \tag{3.59}$$

with the diagonal tensor ${}_i\alpha^{dil}_{JK}(\theta)$ representing the temperature dependent thermal expansion coefficients of phase constituent i.

The transformation strain rate $\dot{\mathbf{L}}^{tr}$ is associated with the expansion generated by the change of parent phase density, ie. austenite density ρ_{aus}, into the daughter phase density $\rho_i,\ i = 2, ..., 6$. The spherical part of this strain rate is evaluated by

$$\mathrm{tr}\dot{\mathbf{L}}^{tr} = \alpha^{tra}_i\dot{y}_i \tag{3.60}$$

with the transformation expansion coefficient α^{tra}_i defined by

$$\alpha^{tra}_i = \frac{\rho^{0^\circ C}_{aus} - \rho_i}{\rho^{0^\circ C}_{aus}} \tag{3.61}$$

where austenite density ρ_{aus} is taken at temperature $0°C$.

3.4.2 Inelastic Strain Decomposition

Classical Plasticity

The plastic strain rates $\dot{\mathbf{E}}^{pl}$ are evaluated using the Huber-Mises yield condition and the associated flow rule. The yield surface with the isotropic and kinematic hardening effects is defined by

$$f(S_{KL}) = \phi(\mathbf{\Sigma}) - \langle\kappa\rangle(W^{pl}, \theta); \tag{3.62}$$

where $\mathbf{\Sigma}(\mathbf{S})$ is the effective stress deviator defined later in this chapter, and the plastic work is given by

$$W^{pl} = \int S_{IJ}\, \dot{E}^{pl}_{IJ}\, dt, \tag{3.63}$$

with the hardening function κ. As the function $f(S_{IJ})$ is a potential for strain and a plastic strain rate is normal to the yield surface, $f(S_{IJ}) = 0$, the following flow law can be written:

$$\dot{E}^{pl}_{IJ} = \Lambda_{IJ} = \dot{\Lambda}\frac{\partial f}{\partial S_{IJ}}, \tag{3.64}$$

That can be also expressed in incremental form

$$\Delta E^{pl}_{IJ} = \bar{\Lambda}\frac{\partial f}{\partial S_{IJ}}, \tag{3.65}$$

where $\bar{\Lambda}$ is the plastic function related to stress, strain, strain rate, temperature, as well as phase fractions, and it is, as yet, an unknown proportionality factor or plastic multiplier. The plastic strain increment fulfills the following conditions for unloading of the generalized particle:

$$\Delta E^{pl}_{IJ} = 0 \begin{cases} f(S_{IJ}) < 0 \\ f(S_{IJ}) = 0 \quad \text{and} \quad \Delta E_{IJ} : S_{IJ} < 0 \end{cases} \tag{3.66}$$

Transformation Plasticity

The multiphase alloy, which is subjected to both internal stress and external loading, undergoes plastic deformations for a lower applied stress than the yield stress. This can happen due to the superposition of external and internal stresses. Internal stresses are generated mainly during phase transformations because of the variation of fraction specific volumes. The plastic yielding occurs in the direction of the applied stress.

The constitutive equation for a transformation plasticity is based on the Levy-Mises perfectly plastic equation, and has been proposed by Greenwood and Johnson [26] in the following form:

$$\dot{E}^{trip} = \frac{5}{6}\frac{\mathbf{T}_{ext}}{Y}\frac{\mathrm{tr}\dot{\mathbf{E}}}{J}, \tag{3.67}$$

where $\mathbf{T}_{ext}$ is the applied external stress, Y is the yield stress of the weaker phase of two phases: the daughter and parent. The constitutive equation for

the transformation induced plasticity shown in [73] can be obtained assuming $J \approx 1$ and $\mathrm{tr}\dot{\mathbf{E}} \approx \mathrm{tr}\dot{\mathbf{E}}_i^{tr}$

$$\dot{\mathbf{E}}^{trip} = \frac{5}{2}\frac{tr\dot{\mathbf{E}}_i^{tr}}{Y}\mathbf{T}_{ext}. \tag{3.68}$$

where $tr\dot{\mathbf{E}}_i^{tr}$ is the trace of the transformation strain rate for phase i. The modification of this relation, presented in [15], can be expressed by

$$\dot{E}_{IJ}^{trip} = \frac{3}{2}\frac{\dot{E}_{eq}^{trip}}{S^{eq}}\Sigma_{IJ}, \tag{3.69}$$

where the equivalent transformation induced plastic strain rate is defined by

$$\dot{E}_{eq}^{trip} = \left(\tfrac{2}{3}\dot{E}_{IJ}^{trip}\dot{E}_{IJ}^{trip}\right)^{\frac{1}{2}}. \tag{3.70}$$

Assuming that the softer phase is rigid-ideal plastic, the constitutive equation for the transformation induced plastic strain rate can be expressed in the form:

$$\dot{E}_{IJ}^{trip} = \sum_{i}^{5} K\,(1-y_i)\,\dot{y}_i\,\Sigma_{IJ}, \tag{3.71}$$

which relates explicitly a portion of plastic strain rate with the phase fraction y_i and its rate $\dot{y}_i$.

This has been experimentally verified in [18] for steel with temperature $M_s = 275C$, the material constant $K = 1.5 \times 10^{-10}\left[\frac{m^2}{N}\right]$, and the austenite yield limit equal to $170\left[\frac{MN}{m^2}\right]$.

In the formulation of the TMM problem the volume phase fractions are also state variables and they are stored in a column vector, $\underline{y}$, with the position in the vector determined by a type of phase evolution. Eq. (3.71) can be written in the vector form

$$\dot{\mathbf{E}}^{trip} = K(\underline{1} - \underline{y}) : \underline{\dot{y}}\ \boldsymbol{\Sigma} \tag{3.72}$$

which is required for a consistent mathematical approach to the solution of TMM problem by FEM. The unit vector $\underline{1} = [1, 1, ..., 1]^{\mathrm{T}}$ contains the same number of entries as the number of considered phase transformations.

The trace of strain increment related to transformation plasticity is expressed by

$$\mathrm{tr}\Delta\mathbf{L}^{trip} = \underline{\alpha} : \Delta\underline{y}. \tag{3.73}$$

Tangent Moduli and the Solution Algorithm for Determining the Plastic Strain Rate Multiplier Λ

The algorithmic or consistent tangent moduli is used in forming the finite element stiffness matrices $\mathbf{K}_{uu}, \mathbf{K}_{u\theta}, \mathbf{K}_{\theta u}$ to ensure quadratic convergence of the global Newton-Raphson solution scheme. These matrices arise from the algorithm for the time integration of the plastic strain rate.

A yield criterion for assessment of plastic flow is expressed by

$$f(\mathbf{S}, H_\alpha, K_\alpha) = \|\mathbf{\Sigma}\| - \sqrt{\tfrac{2}{3}} K_\alpha = 0 \tag{3.74}$$

where two hardening effects are represented by isotropic, K_α, and kinematic, H_α, hardening parameters. These parameters are related to equivalent plastic strain $\bar{E}^{pl} = \sqrt{\frac{2}{3}}\|\mathbf{E}^{pl}\|$, equivalent strain rate $\dot{E}^{eq} = \frac{1}{\Delta t}(\frac{2}{3}\Delta\mathbf{E} : \Delta\mathbf{E})^{1/2}$, and temperature θ, that symbolically can be written as $K_\alpha = K_\alpha(\bar{E}^{pl}, \dot{E}^{eq}, \theta)$ and $H_\alpha = H_\alpha(\bar{E}^{pl}, \dot{E}^{eq}, \theta)$.

The direction of plastic flow for an associative flow rule (J_2) is in the direction of applied force per unit area acting on a surface through the material point undergoing deformation.

If n_i^ϕ is a unit vector in the direction of applied surface tractions then we restrict the solutions of the stress state to ones satisfying

$$\frac{\Sigma_{ij}^{pred}}{\Sigma_{lk}^{pred}\Sigma_{lk}^{pred}} n_j^\phi = \frac{\mathbf{\Sigma}^{pred}}{\|\mathbf{\Sigma}^{pred}\|} \cdot \mathbf{n}^\phi = \frac{\mathbf{\Sigma}}{\|\mathbf{\Sigma}\|} \cdot \mathbf{n}^\phi. \tag{3.75}$$

Which implies that the that the corrected stress state, Σ, is associated with a vector of force per unit area of the same direction as that of the elastic predicted stress but in general with a different magnitude.

The effective stress defined by

$$\mathbf{\Sigma} = \mathbf{S} - \mathbf{Z} \tag{3.76}$$

appears in the yield criterion rather than the usual deviatoric stress $\mathbf{S}$. The back stress $\mathbf{Z}$ is determined incrementally from the expression

$$\mathbf{Z}^{n+1} = \mathbf{Z}^n + \sqrt{\tfrac{2}{3}} \Delta H_\alpha \frac{\mathbf{\Sigma}}{\|\mathbf{\Sigma}\|}. \tag{3.77}$$

A predictor-corrector method is used to determine the unknown value of the plastic strain increment $\bar{\Lambda} = \Delta t \dot{\Lambda}$. This increment is determined at time

step $n+1$ by using the backward Euler implicit method. Assuming that the current increment is purely elastic, the starting values of the variables are set up and hence $\dot{\Lambda} = 0$. These starting values are known as the elastic predicted ones:

$$\mathbf{S}^{pred} = \mathbf{S}_n + 2\langle\mu\rangle\Delta\mathbf{E}^{pred} \quad , \quad \mathbf{\Sigma}^{pred} = \mathbf{S}^{pred} - \mathbf{Z}_n \tag{3.78}$$

where the deviatoric part of the strain increment is used without accounting for the thermal and transformation plastic strains, and given by

$$\Delta\mathbf{E}^{pred} = \hat{\mathbf{J}}_{dev} : \left[\Delta\mathbf{L} - \langle\alpha^{thm}\rangle\mathbf{1}\Delta\theta - \tfrac{1}{3}\,\mathrm{tr}\Delta\mathbf{L}^{tp}\mathbf{1}\right] \tag{3.79}$$

The fourth order tensor $\hat{\mathbf{J}}_{dev}$ is an operator converting a second order tensor to its deviator and is defined by $\hat{\mathbf{J}}_{dev} = \hat{\mathbf{J}} - \frac{1}{3}\mathbf{1}\otimes\mathbf{1}$, where $\hat{\mathbf{J}}$ and $\mathbf{1}$ are the fourth and second order unit tensors, respectively.

The formula for the effective stress calculation is determined from Eq.(3.76) and the additive decomposition of strain rates expressed by Eq.(3.53), and can be written as

$$\mathbf{\Sigma} = \mathbf{\Sigma}^{pred} - 2\langle\mu\rangle\Delta t\left[\dot{\mathbf{E}}^{pl} + \dot{\mathbf{E}}^{trip}\right] - \sqrt{\tfrac{2}{3}}\Delta H_\alpha\frac{\mathbf{\Sigma}}{\|\mathbf{\Sigma}\|} \tag{3.80}$$

Substituting this into Eq.(3.74) leads to

$$\left\|\mathbf{\Sigma}^{pred} - 2\langle\mu\rangle\Delta t\dot{\mathbf{E}}^{trip} - (\sqrt{\tfrac{2}{3}}\Delta H_\alpha + 2\langle\mu\rangle\bar{\Lambda})\frac{\mathbf{\Sigma}}{\|\mathbf{\Sigma}\|}\right\| - \sqrt{\tfrac{2}{3}}K_\alpha \leq 0. \tag{3.81}$$

The inequality condition is satisfied when the increment of strain is purely elastic, and the equality must hold for a plastic strain increment.

The plastic corrector algorithm is the following:

1. calculate the derivative:

$$\frac{\partial f(\bar{\Lambda})}{\partial\bar{\Lambda}} = \tfrac{2}{3}K'_\alpha - \gamma\left[2\langle\mu\rangle + \tfrac{2}{3}H'_\alpha\right] \tag{3.82}$$

where

$$\gamma = \frac{1}{1 + 2\langle\mu\rangle\Delta t E^{trip}_\alpha} \tag{3.83}$$

with the transformation induced plastic strain rate, E^{trip}_α, which will be derived later and shown as Eq.(3.71).

2. update $\bar{\Lambda}$ applying the Newton-Raphson scheme

$$\bar{\Lambda}^{(k+1)} = \bar{\Lambda}^{(k)} - f(\bar{\Lambda}) \left[\frac{\partial f(\bar{\Lambda})}{\partial \bar{\Lambda}} \right]^{-1} \tag{3.84}$$

3. update the plastic strain using the current value of the plastic strain increment

$$\bar{E}^{pl}_{n+1} = \bar{E}^{pl}_{n} + \int_t \sqrt{\tfrac{2}{3}} \|\dot{\mathbf{E}}^{pl}\| dt = \bar{E}^{pl}_{n} + \sqrt{\tfrac{2}{3}} \bar{\Lambda} \tag{3.85}$$

4. update hardening functions: ΔH_α , K_α for the $k+1$ iteration of $\bar{\Lambda}$,

5. check the relation: $f(\bar{\Lambda}) <$ TOL, and terminate the procedure when this condition is fulfilled, otherwise repeat the above sequence of evaluations again.

Stress is calculated either by

$$\mathbf{S}^{(k+1)}_{n+1} = \mathbf{Z}^{(k+1)}_{n+1} + \sqrt{\tfrac{2}{3}} K_\alpha \frac{\boldsymbol{\Sigma}}{\|\boldsymbol{\Sigma}\|}, \tag{3.86}$$

when the strain increment is plastic or

$$\mathbf{S}_{n+1} = \mathbf{S}^{pred} \tag{3.87}$$

when the strain increment is elastic.

The full stress tensor is calculated by adding the deviatoric stress and the spherical part of stress, ie.

$$\mathbf{T}_{n+1} = \mathbf{S}_{n+1} + \tfrac{1}{3} \mathrm{tr}\mathbf{T}^{pred} \mathbf{1}, \tag{3.88}$$

where $\mathbf{T}^{pred}$ is the stress predicted for elastic reaction of an alloy.

The tangent modulus $\frac{\partial \mathbf{T}}{\partial \mathbf{L}}$ at the particular time step $(n+1)$ is defined by

$$\frac{\partial \mathbf{T}}{\partial \mathbf{L}} = \langle \kappa \rangle \mathbf{1} \otimes \mathbf{1} + \left[\frac{\partial \mathbf{Z}}{\partial \mathbf{L}} + \sqrt{\tfrac{2}{3}} \frac{\partial K_\alpha}{\partial \mathbf{L}} \otimes \frac{\boldsymbol{\Sigma}}{\|\boldsymbol{\Sigma}\|} + 2\langle \mu \rangle \frac{\partial \Delta \mathbf{E}^{trip}}{\partial \mathbf{L}} \right]_{n+1} \tag{3.89}$$

where the derivative of the back stress expressed in terms of hardening parameters is

$$\left. \frac{\partial \mathbf{Z}}{\partial \mathbf{L}} \right|_{n+1} = \frac{\boldsymbol{\Sigma}}{\|\boldsymbol{\Sigma}\|} \otimes \left[\tfrac{2}{3} H'_\alpha \hat{\mathbf{J}}_{dev} : \frac{\partial \bar{\Lambda}}{\partial \mathbf{E}} + \sqrt{\tfrac{2}{3}} H^r_\alpha \frac{1}{\Delta t} \frac{\Delta \mathbf{E}}{\Delta E^{eq}} \right]_{n+1} \tag{3.90}$$

and the derivative of the isotropic hardening function is

$$\sqrt{\frac{2}{3}}\left.\frac{\partial K_\alpha}{\partial \mathbf{L}}\right|_{n+1} = \left[\tfrac{2}{3}K'_\alpha \hat{\mathbf{J}}_{dev} : \frac{\partial \bar{\Lambda}}{\partial \mathbf{E}} + \sqrt{\tfrac{2}{3}}K^r_\alpha \frac{1}{\Delta t}\frac{\Delta \mathbf{E}}{\Delta E^{eq}}\right]_{n+1}. \tag{3.91}$$

The derivative of the transformation induced plastic strain increment in Eq.(3.89) can be expressed by

$$\begin{aligned} 2\langle\mu\rangle \left.\frac{\partial \Delta \mathbf{E}^{trip}}{\partial \mathbf{L}}\right|_{n+1} &= \bar{\gamma}\hat{\mathbf{J}}_{dev} : \left[2\langle\mu\rangle \mathbf{1} - 2\langle\mu\rangle \frac{\partial \bar{\Lambda}}{\partial \mathbf{E}}\right. \\ &- \left.\left\{\tfrac{2}{3}H'_\alpha \frac{\partial \bar{\Lambda}}{\partial \mathbf{E}} + \sqrt{\tfrac{2}{3}}H^r_\alpha \frac{1}{\Delta t}\frac{\Delta \mathbf{E}}{\Delta E^{eq}}\right\}\right]_{n+1} \otimes \frac{\mathbf{\Sigma}}{\|\mathbf{\Sigma}\|}, \end{aligned} \tag{3.92}$$

where

$$\bar{\gamma} = \gamma 2\langle\mu\rangle \Delta E^{trip}_\alpha \tag{3.93}$$

The derivative $\frac{\partial \bar{\Lambda}}{\partial \mathbf{E}}$ occurring in the above expression is still unknown and it can be obtained by the implicit differentiation technique applied to the yield condition when assuming that plastic yielding occurs within the increment Δt and $\Lambda \neq 0$, so that

$$\left\| \left[\gamma(\|\mathbf{\Sigma}^{pred}\| - 2\langle\mu\rangle\bar{\Lambda}) - \sqrt{\tfrac{2}{3}}\Delta H_\alpha - \sqrt{\tfrac{2}{3}}K_\alpha\right] \frac{\mathbf{\Sigma}}{\|\mathbf{\Sigma}\|}\right\| = 0 \tag{3.94}$$

since $\frac{\mathbf{\Sigma}}{\|\mathbf{\Sigma}\|} \neq 0$, and thus

$$\gamma\|\mathbf{\Sigma}^{pred}\| - 2\gamma\langle\mu\rangle\bar{\Lambda} - \gamma\sqrt{\tfrac{2}{3}}\Delta H_\alpha - \sqrt{\tfrac{2}{3}}K_\alpha = 0. \tag{3.95}$$

Differentiating this with respect to the deviatoric strain, $\mathbf{E}$, yields an implicit expression for the derivative $\frac{\partial \bar{\Lambda}}{\partial \mathbf{E}}$ in the following form:

$$\begin{aligned} &\gamma\frac{\mathbf{\Sigma}^{pred}}{\|\mathbf{\Sigma}^{pred}\|}2\langle\mu\rangle - 2\gamma\langle\mu\rangle\frac{\partial \bar{\Lambda}}{\partial \mathbf{E}} - \tfrac{2}{3}K'_\alpha\frac{\partial \bar{\Lambda}}{\partial \mathbf{E}} - \sqrt{\tfrac{2}{3}}K^r_\alpha\frac{1}{\Delta t}\frac{\Delta \mathbf{E}}{\Delta E^{eq}} \\ &-\gamma\tfrac{2}{3}H'_\alpha\frac{\partial \bar{\Lambda}}{\partial \mathbf{E}} - \gamma\sqrt{\tfrac{2}{3}}H^r_\alpha\frac{1}{\Delta t}\frac{\Delta \mathbf{E}}{\Delta E^{eq}} = 0 \end{aligned} \tag{3.96}$$

which after rearrangement can be written as

$$\frac{\partial \bar{\Lambda}}{\partial \mathbf{E}}\left[\gamma\langle\mu\rangle + \tfrac{1}{3}(K'_\alpha + \gamma H'_\alpha)\right] = \langle\mu\rangle\gamma\frac{\mathbf{\Sigma}}{\|\mathbf{\Sigma}\|} - \frac{\sqrt{\frac{1}{6}}}{\Delta t}\frac{\Delta \mathbf{E}}{\Delta E^{eq}}\left(K^r_\alpha + \gamma H^r_\alpha\right) \tag{3.97}$$

and finally the required derivative is

$$\frac{\partial \bar{\Lambda}}{\partial \mathbf{E}} = \frac{\gamma\langle\mu\rangle \frac{\mathbf{\Sigma}}{\|\mathbf{\Sigma}\|} - \sqrt{\frac{1}{6}}\frac{1}{\Delta t}\frac{\Delta \mathbf{E}}{\Delta E^{eq}}\left(K_\alpha^r + H_\alpha^r\right)}{\gamma\langle\mu\rangle + \frac{1}{3}(K'_\alpha + \gamma H'_\alpha)} \tag{3.98}$$

Using the derivatives expressed by Eqs. (3.90), (3.91), (3.92) and after grouping scalars multiplying $(\hat{\mathbf{J}}_{dev} : \frac{\mathbf{\Sigma}}{\|\mathbf{\Sigma}\|})$, the final form of the stress-strain tangent modulus can be written as

$$\begin{aligned}
\left.\frac{\partial \mathbf{T}}{\partial \mathbf{L}}\right|_{n+1} &= \langle\kappa\rangle \mathbf{1}\otimes\mathbf{1} + 2\hat{\mathbf{J}}_{dev}\{\bar{\gamma}\langle\mu\rangle\}_{n+1} \\
&+ 2\hat{\mathbf{J}}_{dev}\left[\frac{\gamma\langle\mu\rangle\left(\frac{1}{3}[(1-\bar{\gamma})H'_\alpha + K'_\alpha] - \bar{\gamma}\langle\mu\rangle\right)}{\gamma\langle\mu\rangle + \frac{1}{3}(K'_\alpha + \gamma H'_\alpha)}\right]_{n+1} \\
&+ \frac{\mathbf{\Sigma}}{\|\mathbf{\Sigma}\|}\otimes\left[(1-\gamma)H_\alpha^r \frac{1}{\Delta t}\frac{\Delta \mathbf{E}}{\Delta E^{eq}} + K_\alpha^r \frac{1}{\Delta t}\frac{\Delta \mathbf{E}}{\Delta E^{eq}}\right]_{n+1}.
\end{aligned} \tag{3.99}$$

3.5 FE Approximation of TMM Problem

The parent material and a weldment are polycrystalline bodies represented by finite elements. Each element can be composed of various phases that are evaluated at Gaussian integration points or Gauss points). Such elements are called hybrid finite elements. Hybrid finite element contains various microregions or phases represented at elemental integration points, ie. nodes of Gaussian quadrature at elements. This arrangement in the approximation of material properties is consistent with the micro-mechanical model of the alloy and provides for the transmission of information about the micro-material state to the macro-level of finite element method solution.

The Galerkin type FE technique is used to solve the variational problem where the dispersed particles and a real microstructure is not projected into FE structure but the phase composition of welded material is represented in Gauss points where the FE system is integrated.

The approximation of the fully coupled thermo-mechanical problem is based on Galerkin's type finite element approximation of balance laws combined with finite difference method applied to phase evolution laws.

3.5.1 FE Approximation of Virtual Work Balance

The equation of virtual work Eq(3.36) is solved by the Finite Element Method combined with linearization techniques for Finite Element equations. The

linearizations are applied after incremental decompositions for strain and stress given by

$$ {}^{t+\Delta t}\tilde{\mathbf{L}} = {}^{t}\tilde{\mathbf{L}} + \tilde{\mathbf{L}}^{\Delta} \tag{3.100} $$

$$ {}^{t+\Delta t}\mathbf{T} = {}^{t}\mathbf{T} + \mathbf{T}^{\Delta} \tag{3.101} $$

where ${}^{t+\Delta t}\{\tilde{\mathbf{L}}, \mathbf{T}\}$ and ${}^{t}\{\tilde{\mathbf{L}}, \mathbf{T}\}$ corresponds to the actual and the previous strain-stress state. The increments of strain and stress are $\tilde{\mathbf{L}}^{\Delta}$, $\mathbf{T}^{\Delta}$. The increment of the Green strain $\tilde{\mathbf{L}}^{\Delta}$ is further decomposed into its linear and nonlinear components:

$$ \tilde{\mathbf{L}}^{\Delta} = \tilde{\mathbf{L}} + \tilde{\mathbf{L}}_{\nu} \tag{3.102} $$

where

$$ \begin{aligned} &\tilde{\mathbf{L}} = \tfrac{1}{2}\left[\mathbf{F}^{\mathrm{T}}\nabla(\Delta\mathbf{u}) + \nabla(\Delta\mathbf{u})^{\mathrm{T}}\mathbf{F}\right]; \\ &\tilde{\mathbf{L}}_{\nu} = \tfrac{1}{2}\nabla(\Delta\mathbf{u})^{\mathrm{T}}(\nabla\Delta\mathbf{u}). \end{aligned} \tag{3.103} $$

The finite element equation for virtual work, shown in [4], and [36], for the total Lagrangian formulation at time $(n+1)$ is obtained from Eq.(3.36) and expressed by

$$ \left({}^{t}_{0}\mathbf{K}_{L}(\theta) + {}^{t}_{0}\mathbf{K}_{nL}(\theta)\right)\Delta\mathbf{u}^{(i)} = {}^{t+\Delta t}_{0}\mathbf{R}_{u} - {}^{t+\Delta t}_{0}\mathbf{F}^{(i-1)}_{u} \tag{3.104} $$

where ${}^{t}_{0}\mathbf{K}_{L}(\theta)$ and ${}^{t}_{0}\mathbf{K}_{nL}(\theta)$ is the linear and the nonlinear stiffness matrix that are temperature dependent, $\Delta\mathbf{u}^{(i)}$ is the vector of displacement increment, ${}^{t+\Delta t}_{0}\mathbf{R}_{u}$ is the vector of externally applied nodal point loads, ${}^{t+\Delta t}_{0}\mathbf{F}^{(i-1)}_{u}$ is the vector of nodal point forces equivalent to the internal stresses. This equation is linear in respect of $\Delta\mathbf{u}^{(i)}$ and the matrices in Eq.(3.104) are taken at four levels of solution. These matrices are evaluated at two time steps t and $(t+\Delta t)$, and for two iterations i and $(i-1)$. The linear stiffness matrix is defined by

$$ {}^{t}_{0}\mathbf{K}_{L} = \int_{V_0} {}^{t}_{0}\mathbf{B}^{\mathrm{T}}_{L}\ \mathbf{C}_{TL}\ {}^{t}_{0}\mathbf{B}_{L}\ dV_0 \tag{3.105} $$

where meaning of matrices ${}^{t}_{0}\mathbf{B}_{L}$ and $\mathbf{C}_{TL}$ comes from the following expression:

$$ \left({}^{t}_{0}\mathbf{B}^{\mathrm{T}}_{L}\ \Delta\mathbf{u}^{\mathrm{T}}\right)\mathbf{C}_{TL}\left({}^{t}_{0}\mathbf{B}_{L}\Delta\mathbf{u}\right) = \tilde{\mathbf{L}}^{\mathrm{T}} : \mathbf{C}_{TL} : \tilde{\mathbf{L}}. \tag{3.106} $$

The matrix $\mathbf{C}_{TL}$ is the consistent or algorithmic tangent modulus which has to be defined for each material model as the $\left[\frac{\partial \mathbf{T}}{\partial \mathbf{L}}\right]$ contribution to the global stiffness matrix, and ${}^{t}_{0}\mathbf{B}_{L}$ is the linear strain-displacement matrix. The nonlinear stiffness matrix is defined by

$$ {}^{t}_{0}\mathbf{K}_{nL} = \int_{V_0} {}^{t}_{0}\mathbf{B}^{\mathrm{T}}_{nL}\ \mathbf{S}^{[mx]}\ {}^{t}_{0}\mathbf{B}_{nL}\ dV_0. \tag{3.107} $$

The nonlinear strain-displacement matrix ${}^{t}_{0}\mathbf{B}_{nL}$ comes from the substitution

$$ \left({}^{t}_{0}\mathbf{B}^{\mathrm{T}}_{nL}\ \Delta\mathbf{u}^{\mathrm{T}}\right)\mathbf{S}^{[mx]}\left({}^{t}_{0}\mathbf{B}_{nL}\Delta\mathbf{u}\right) = \mathbf{S} : \tilde{\mathbf{L}}_{\nu}, \tag{3.108} $$

where $\mathbf{S}^{[mx]}$ is the matrix representation of 2nd Piola-Kirchoff stress, ${}^{t}\mathbf{S}$. The linear and nonlinear stiffness matrices are not modified in the iteration process during the step $(t+\Delta t)$. They are updated when the iteration process at $(t+\Delta t)$ is completed. The vector of externally applied nodal point loads is given by

$$ {}^{t+\Delta t}_{0}\mathbf{R}_{u} = \int_{\partial V_0} \mathbf{H}^{\mathrm{T}}_{s}\ {}^{t+\Delta t}\mathbf{T} d\mathcal{P} + \int_{V_0} \mathbf{H}^{\mathrm{T}}{}^{t+\Delta t}\mathbf{b}\ dV_0 \tag{3.109} $$

where $\mathbf{H}_s$ is the surface interpolation matrix, and $\mathbf{H}$ is the volume interpolation matrix. These matrices are formed from the interpolating polynomial during the process of Gaussian integration. The matrix $\mathbf{H}_s$ is evaluated for two of the 3-coordinates at Gauss points and one at the given surface. The given nominal stress vector is ${}^{t+\Delta t}\mathbf{T} = \{T_J\}$, and the vector of body forces is ${}^{t+\Delta t}\mathbf{b} = \{b_J\}$. The vector of nodal point forces equivalent to stresses at time $(t+\Delta t)$ and defined for previous iteration $(i-1)$ is expressed in the form

$$ {}^{t+\Delta t}_{0}\mathbf{F}^{(i-1)}_{u} = \int_{V_0} {}^{t}_{0}\mathbf{B}_{L}\ {}^{t+\Delta t}_{0}\mathbf{T}^{(i-1)}\ dV_0 \tag{3.110} $$

3.5.2 FE Approximation of Internal Energy Balance

The variational equation of internal energy balance Eq.(3.8) is solved by the Galerkin type Finite Element Method. The appropriate finite element equation for the fully coupled thermo-mechanical problem is given by:

$$ \begin{aligned} {}^{t}_{0}\mathbf{C} \quad & {}^{t+\Delta t}_{0}\dot{\theta}^{(i)} + \left({}^{t}_{0}\mathbf{K}^{k} + {}^{t}_{0}\mathbf{K}^{M} + {}^{t}_{0}\mathbf{K}^{r} + {}^{t}_{0}\mathbf{K}^{\rho}\right)\Delta\theta^{(i)} \\ = \quad & {}^{t+\Delta t}_{0}\mathbf{R}_{\theta}{}^{(i-1)} - {}^{t+\Delta t}_{0}\mathbf{R}^{(i-1)}_{\Gamma} - {}^{t+\Delta t}_{0}\mathbf{R}^{(i-1)}_{su} - {}^{t+\Delta t}_{0}\mathbf{R}^{(i-1)}_{\Sigma} \\ - \quad & {}^{t+\Delta t}_{0}\mathbf{F}^{(i-1)}_{neq} - {}^{t+\Delta t}_{0}\mathbf{F}^{\rho}, \end{aligned} \tag{3.111} $$

where ${}^{t}_{0}\mathbf{K}^{k}$ is the stiffness matrix corresponding to conduction, ${}^{t}_{0}\mathbf{K}^{M}$ is the stiffness related to the heat generated by mechanical energy, ${}^{t}_{0}\mathbf{K}^{r}$ is the stiffness resulting from entropy radiation, ${}^{t}_{0}\mathbf{K}^{\rho}$ and ${}^{t+\Delta t}_{0}\mathbf{F}^{\rho}$ are related to the dissipation of inelastic energy ($\mathbf{E}^{pl} : \mathbf{S}$), and ${}^{t+\Delta t}_{0}\mathbf{F}^{(i-1)}_{neq}$ is called the matrix of non-equilibrated heat fluxes generated due to convergence criterion applied in the iteration technique. The R.H.S. vector of nodal thermal loads, which correspond to the thermal boundary conditions, is given by

$$ {}^{t+\Delta t}_{0}\mathbf{R}^{(i-1)}_{\theta} = {}^{t+\Delta t}_{0}\mathbf{R}^{k(i-1)}_{\theta} + {}^{t+\Delta t}_{0}\mathbf{R}^{c(i-1)}_{\theta} + {}^{t+\Delta t}_{0}\mathbf{R}^{r(i-1)}_{\theta} \tag{3.112} $$

where $\mathbf{R}^{k}_{\theta}, \mathbf{R}^{c}_{\theta}, \mathbf{R}^{r}_{\theta}$ are fluxes due to conduction, convection and radiation phenomena on external surfaces of the body. The terms ${}^{t+\Delta t}_{0}\mathbf{R}^{(i-1)}_{\Gamma}$ and ${}^{t+\Delta t}_{0}\mathbf{R}^{(i-1)}_{su}$ are connected with internal heat fluxes generated in the thickest FE region containing the singular surface $\partial\Gamma^{pt}$ or separate microregions, where thermally activated phase transformations proceed. The correspondence of terms appearing in Eq.(3.111) has been summarized in Table(3.1).

The FE Eq.(3.111) can be written in the form consistent with the FE virtual work Eq.(3.104)

$$ \begin{aligned} {}^{t}_{0}\mathbf{C} \quad & {}^{t+\Delta t}_{0}\dot{\theta}^{(i)} + \left({}^{t}_{0}\mathbf{K}^{k} + {}^{t}_{0}\mathbf{K}^{M} + {}^{t}_{0}\mathbf{K}^{r} + {}^{t}_{0}\mathbf{K}^{\rho}\right)\Delta\theta^{(i)} \\ = \quad & {}^{t+\Delta t}_{0}\mathbf{R}_{\theta}{}^{(i-1)} - {}^{t+\Delta t}_{0}\mathbf{F}^{(i-1)}_{\theta}, \end{aligned} \tag{3.113} $$

when substituting the matrix of residual fluxes given by

$$ \begin{aligned} {}^{t+\Delta t}_{0}\mathbf{F}^{(i-1)}_{\theta} &= {}^{t+\Delta t}_{0}\mathbf{R}^{(i-1)}_{\Gamma} + {}^{t+\Delta t}_{0}\mathbf{R}^{(i-1)}_{su} + {}^{t+\Delta t}_{0}\mathbf{R}^{(i-1)}_{\Sigma} \\ &+ {}^{t+\Delta t}_{0}\mathbf{F}^{(i-1)}_{neq} + {}^{t+\Delta t}_{0}\mathbf{F}^{\rho}. \end{aligned} \tag{3.114} $$

3.6 Matrices of FE Phase Evolution Equation

3.6.1 Ferritic and Pearlitic Transformations

The general form of evolution law for ferritic and pearlitic diffusional transformations, that has been proposed in [77], can be written in the following form:

$$ \dot{y}_i = \mathcal{A}_i\left(\mathbf{S}, \theta, y_i, t\right)\dot{\theta} + \mathcal{B}_i\left(\mathbf{S}, \theta, y_i, t\right)\dot{\mathbf{S}} + \mathcal{R}_i\left(\mathbf{S}, \theta, y_i, t\right), \tag{3.115} $$

FE Eq.(3.111)	Energy Eq.(3.8)	Meaning
${}^t_0\mathbf{C}\ {}^{t+\Delta t}_0\dot{\theta}^{(i)}$	$-\int_{V_0} c\dot{\vartheta}\ \delta\vartheta dV$	"heat energy"
${}^t_0\mathbf{K}^k\Delta\theta^{(i)}$	$\int_{V_0} k_{IJ}\theta_{,I}\ \delta\vartheta_{,J} dV$	heat flux
${}^t_0\mathbf{K}^M\Delta\theta^{(i)}$	$\int_{V_0} f^M_\theta\ \delta\vartheta dV$	mechanical energy
${}^t_0\mathbf{K}^r\Delta\theta^{(i)}$	$\int_{V_0} f^r_\theta\ \delta\vartheta dV$	entropy radiation
${}^{t+\Delta t}_0\mathbf{R}^{kcr(i-1)}_\theta$	$\int_{\partial V_0} f^{\partial V}_\theta\ \delta\vartheta d\mathcal{P}$	boundary fluxes
${}^{t+\Delta t}_0\mathbf{R}^{(i-1)}_\Gamma$	$\int_{\partial\Gamma^{pt}} f^{su}_\theta\ \delta\vartheta d\mathcal{P}$	surface energy
${}^{t+\Delta t}_0\mathbf{R}^{(i-1)}_{su}$	$\int_{\partial\Gamma^{pt}} f^{su}_\theta\ \delta\vartheta d\mathcal{P}$	energy jump
${}^{t+\Delta t}_0\mathbf{R}^{(i-1)}_\Sigma$	$\sum_{\mathcal{J}} \mathcal{F}^{\mathcal{J}}_\theta \delta\vartheta\mid_{\mathcal{J}}$	point heat source

Table 3.1: Correspondence of matrices in FE equation for thermo-mechanical problem and integrals in the balance of internal energy.

where $\dot{y}_i$ is the ferrite or pearlite phase fraction, $\mathcal{A}_i$, $\mathcal{B}_i$, and $\mathcal{R}_i$ are material functions, and subscript i assumes one of two values: 2 or 3. The time approximation and linearization leads to the linear expression

$$ {}^{t+\Delta t}\dot{\mathbf{y}}_i = {}^t\mathcal{A}_i\ {}^{t+\Delta t}\dot{\theta} + {}^t\mathcal{B}_i\ {}^{t+\Delta t}_0\dot{\mathbf{S}} + {}^t\mathcal{R}_i. \tag{3.116} $$

The stress rate is obtained from the increment of displacement by using the strain-displacement transformation and the stress-strain tangent modulus. The evolution equation expressed in terms of temperature rate and displacement increment can be written as

$$ {}^{t+\Delta t}\dot{\mathbf{y}}_i = {}^t\mathcal{A}_i\ {}^{t+\Delta t}\dot{\theta} + {}^t\hat{\mathcal{B}}_i\ {}^{t+\Delta t}\dot{\mathbf{u}} + {}^t\hat{\mathcal{R}}_i. \tag{3.117} $$

where particular forms of ${}^t\hat{\mathcal{B}}_i$ and ${}^t\hat{\mathcal{R}}_i$ will be shown after introducing constitutive equations for elastic and inelastic deformations.

The simplest evolution equation for diffusional transformations, without metallurgical-mechanical coupling, is given by

$$ \dot{y}_i = (1-y_i)\left[\frac{db_i}{d\theta}\dot{\theta} + \frac{b_i(\theta)n_i}{t}\right] t^{n_i}, \tag{3.118} $$

which, after time approximation, can be written as the following:

$$ {}^{t+\Delta t}\dot{\mathbf{y}}_i = {}^t\mathcal{A}\ {}^{t+\Delta t}\dot{\theta} + {}^t\mathcal{R}, \tag{3.119} $$

with factors given by

$$ \begin{aligned} {}^t\mathcal{A} &= (1-{}^t\mathbf{y}_i)\,{}^t t^{n_i}\left[\tfrac{db_i}{d\theta}\right]_t, \\ {}^t\mathcal{R} &= (1-{}^t\mathbf{y}_i)\,{}^t t^{n_i-1}\ {}^t b_i\ n_i, \end{aligned} \tag{3.120} $$

where b_i and n_i are empirical parameters related to cooling rate and the nucleation rate, t is time equal to zero at the nucleation period.

3.6.2 Bainitic Transformation

The evolution equation for bainitic transformation, shown in [77], can be written in the following form:

$$\begin{aligned} \dot{y}_4 &= \frac{V^{mic}K_1}{\gamma}\left(1-y_4\right)\left(1-\beta\gamma y_4\right)\exp\left[\langle\Gamma_2\rangle y_4 - \frac{K_2}{R\theta}\left(1-\frac{\langle\Delta G^0_{4_{max}}\rangle}{r}\right)\right] \\ \langle\Gamma_2\rangle &= \frac{K_2\langle\Delta G^0_{4_{max}} - G_N\rangle}{r\ R\ \theta} \end{aligned} \tag{3.121}$$

where V^{mic} is the volume of a microregion, K_1 is the parameter related to austenite grain size, $\gamma = y_\gamma\ y_{4max}$, y_γ is the fraction of residual austenite, β is the auto-catalysis factor, K_2 is a constant, R is the ideal gas constant, $\Delta G^0_{4_{max}}$ is the change of maximum nucleation free energy determined from the free energy diagram, r is the positive constant appearing in approximation of the value G_N that is exceeded by $\Delta G^0_{4_{max}}$ at temperature W_s. Note that this equation does not contain rates of variables controlling bainitic transformation. The time approximation and linearization results in the relationship

$${}^{t+\Delta t}\dot{\mathbf{y}}_4 = \left(1-{}^t\mathbf{y}_4\right)\left(1-A_1\ {}^t\mathbf{y}_4\right)A_2\exp\left[\frac{A_3}{{}^t\theta}\left({}^tG_1\ {}^t\mathbf{y}_4 - {}^tG_2\right)\right] \tag{3.122}$$

where

$$\begin{aligned} A_1 &= \beta\gamma;\ \ A_2 = \frac{V^{mic}K_1}{\gamma};\ \ A_3 = \frac{K_2}{r\ R}; \\ {}^tG_1 &= \left[\langle\Delta G^0_{4_{max}} - G_N\rangle\right]_t; \\ {}^tG_2 &= r - \left[\langle\Delta G^0_{4_{max}}\rangle\right]_t. \end{aligned} \tag{3.123}$$

The general form of Eq.(3.122) can be expressed by

$${}^{t+\Delta t}\dot{\mathbf{y}}_4 = {}^t\mathcal{A}_4\ \exp\left(\frac{{}^t\mathcal{F}}{{}^t\theta}\right), \tag{3.124}$$

where

$$\begin{aligned} {}^t\mathcal{A}_4 &\equiv \left(1-{}^t\mathbf{y}_4\right)\left(1-A_1\ {}^t\mathbf{y}_4\right)A_2; \\ {}^t\mathcal{F} &\equiv A_3\left({}^tG_1\ {}^t\mathbf{y}_4 - {}^tG_2\right). \end{aligned} \tag{3.125}$$

3.6.3 Martensitic Transformation

The general form of evolution equation for martensitic transformation shown in [77] following the proposition [51], can be written as the following kinetic law:

$$\dot{y}_6 = \mathcal{A}_6\left(\mathbf{S}, \theta, y_6, t\right)\dot{\theta} + \mathcal{K}_6\left(\mathbf{S}, \theta, y_6, t\right)\mathbf{E}^*_{cr} : \dot{\mathbf{S}}, \tag{3.126}$$

where $\mathcal{A}_6$ and $\mathcal{K}_6$ are material functions, $\mathbf{E}^*_{cr}$ is a value of the macroscopic transformation strain $\mathbf{E}^*$ when $y_6 = 1$ and stress $\mathbf{S}$ is assumed to be homogeneous in a microregion representing a group of finite elements. This stress is balancing the external stress load. The time approximation and linearization result in the expression

$${}^{t+\Delta t}\dot{\mathbf{y}}_6 = {}^{t}\mathcal{A}_6\ {}^{t+\Delta t}\dot{\theta} + {}^{t}\mathcal{B}_6\ {}^{t+\Delta t}_{0}\dot{\mathbf{S}}, \tag{3.127}$$

with

$${}^{t}\mathcal{B}_6 = {}^{t}\mathcal{K}\ \mathbf{E}^*_{cr}. \tag{3.128}$$

Transformation of stress ${}^{t+\Delta t}_{0}\dot{\mathbf{S}}$ to strain rate $\dot{\mathbf{E}}$ and velocity $\dot{\mathbf{u}}$ leads to the following martensitic growth law

$${}^{t+\Delta t}\dot{\mathbf{y}}_6 = {}^{t}\mathcal{A}_6\ {}^{t+\Delta t}\dot{\theta} + {}^{t}\hat{\mathcal{B}}_6\ {}^{t+\Delta t}\dot{\mathbf{u}} + {}^{t}\hat{\mathcal{R}}_6, \tag{3.129}$$

where ${}^{t}\hat{\mathcal{B}}_6$ and ${}^{t}\hat{\mathcal{R}}_6$ will be derived later using elastic constitutive equations.

The simplest evolution equation for martensitic fraction is given by

$$\dot{y}_6 = \alpha\left(1 - y_6\right)\dot{\theta}, \tag{3.130}$$

which after time approximation can be re-written as the following

$$\begin{aligned} {}^{t+\Delta t}\dot{\mathbf{y}}_6 &= {}^{t}\mathcal{A}_6\ {}^{t+\Delta t}\dot{\theta}, \\ {}^{t}\mathcal{A}_6 &= \alpha\left(1 - {}^{t}\mathbf{y}_6\right), \end{aligned} \tag{3.131}$$

where α is the constant coefficient that for most steels equals $1.1 \times 10^{-2}[K^{-1}]$.

Matrices ${}^{t}\hat{\mathcal{B}}_i$, ${}^{t}\hat{\mathcal{B}}_6$, ${}^{t}\hat{\mathcal{R}}_i$, and ${}^{t}\hat{\mathcal{R}}_6$ in Eqs.(3.117) and (3.129) are derived using elastic constitutive relation Eq.(3.56) expressed in the form:

$${}^{t+\Delta t}_{0}\dot{\mathbf{S}}^{(i)} = 2\mu\left({}^{t+\Delta t}_{0}\dot{\mathbf{E}}^{\Delta(i)} - {}^{t+\Delta t}_{0\ in}\dot{\mathbf{E}}^{\Delta(i-1)}\right) + \frac{\dot{\mu}}{\mu}\ {}^{t}_{0}\mathbf{S}, \tag{3.132}$$

where ${}^{t+\Delta t}_{0\,in}\dot{\mathbf{E}}^{\Delta(i-1)}$ is the inelastic strain rate defined for the previous iteration $(i-1)$.

Substituting the following relation:

$$ {}^{t+\Delta t}_{0}\dot{\mathbf{E}}^{\Delta(i)} = \left({}^{t}_{0}\mathbf{B}_L + {}^{t}_{0}\mathbf{B}^{\mathrm{T}}_{nL}\ {}^{t}_{0}\mathbf{B}_{nL} \right) {}^{t+\Delta t}\dot{\mathbf{u}} \tag{3.133} $$

into Eq.(3.132) results in the equation

$$ {}^{t+\Delta t}_{0}\dot{\mathbf{S}}^{(i)} = \check{\mathcal{B}}\ {}^{t+\Delta t}\dot{\mathbf{u}} - {}^{t+\Delta t}\check{\mathcal{R}} + {}^{t}\check{\mathcal{R}} \tag{3.134} $$

where

$$ \begin{array}{rcl} \check{\mathcal{B}} & = & 2\mu \left({}^{t}_{0}\mathbf{B}_L + {}^{t}_{0}\mathbf{B}^{\mathrm{T}}_{nL}\ {}^{t}_{0}\mathbf{B}_{nL} \right); \\ {}^{t+\Delta t}\check{\mathcal{R}} & = & 2\mu\ {}^{t+\Delta t}_{0\,in}\dot{\mathbf{E}}^{\Delta(i-1)}; \\ {}^{t}\check{\mathcal{R}} & = & \frac{\dot{\mu}}{\mu}\ {}^{t}_{0}\mathbf{S}. \end{array} \tag{3.135} $$

Combining Eq.(3.134) with Eq.(3.116) leads to the form of the evolution law for ferritic-pearlitic transformation

$$ {}^{t+\Delta t}\dot{\mathbf{y}}_i = {}^{t}\mathcal{A}_i\ {}^{t+\Delta t}\dot{\theta} + {}^{t}\mathcal{B}_i\ \check{\mathcal{B}}\ {}^{t+\Delta t}\dot{\mathbf{u}} - {}^{t}\mathcal{B}_i\ {}^{t+\Delta t}\check{\mathcal{R}} + {}^{t}\mathcal{B}_i\ {}^{t}\check{\mathcal{R}} + {}^{t}\mathcal{R}_i. \tag{3.136} $$

Introducing the following symbols:

$$ \begin{array}{rcl} {}^{t}\hat{\mathcal{B}} & = & {}^{t}\mathcal{B}_i\ \check{\mathcal{B}}, \\ {}^{t}\hat{\mathcal{R}}_i & = & {}^{t}\mathcal{B}_i\ {}^{t}\check{\mathcal{R}} + {}^{t}\mathcal{R}_i - {}^{t}\mathcal{B}_i\ {}^{t+\Delta t}\check{\mathcal{R}}, \end{array} \tag{3.137} $$

into Eq.3.136 results in the Eq.(3.117). Substituting Eq.(3.134) in Eq.(3.127) gives

$$ {}^{t+\Delta t}\dot{\mathbf{y}}_6 = {}^{t}\mathcal{A}_6\ {}^{t+\Delta t}\dot{\theta} + {}^{t}\mathcal{B}_6\ \check{\mathcal{B}}\ {}^{t+\Delta t}\dot{\mathbf{u}} + {}^{t}\mathcal{B}_6\ {}^{t}\check{\mathcal{R}} - {}^{t}\mathcal{B}_6\ {}^{t+\Delta t}\check{\mathcal{R}}. \tag{3.138} $$

Denoting

$$ \begin{array}{rcl} {}^{t}\hat{\mathcal{B}}_6 & = & {}^{t}\mathcal{B}_6\ \check{\mathcal{B}}, \\ {}^{t}\hat{\mathcal{R}}_6 & = & {}^{t}\mathcal{B}_6 \left({}^{t}\check{\mathcal{R}} - {}^{t+\Delta t}\check{\mathcal{R}} \right). \end{array} \tag{3.139} $$

results in Eq.(3.129).

3.7 FE Equation for TMM Problem

The assemblage of FE equations for virtual work Eq.(3.104) and internal energy Eq.(3.113) together with appropriate phase evolution law yields the combined global Finite Element equation for thermo-mechano-metallurgical problem. The global FE equation for thermo-mechanical problem is formulated at first, and afterwards the more complex thermo-mechano-metallurgical problem will be presented.

3.7.1 Global FE Equation for TM Problem

The displacement increment $\Delta\mathbf{u}$ and temperature θ are state variables for the coupled thermo-mechanical problem which is defined by Eqs.(3.104) and (3.113). The corresponding global FE equation is expressed as the following:

$$\begin{aligned}
&\begin{bmatrix} \mathbf{0} & \mathbf{0} \\ \mathbf{0} & {}^{t}_{0}\mathbf{C} \end{bmatrix} \begin{bmatrix} {}^{t+\Delta t}\dot{\mathbf{u}} \\ {}^{t+\Delta t}\dot{\theta} \end{bmatrix}^{(i)} + \begin{bmatrix} {}^{t}_{0}\mathbf{K}_{uu} & {}^{t}_{0}\mathbf{K}_{u\theta} \\ {}^{t}_{0}\mathbf{K}_{\theta u} & {}^{t}_{0}\mathbf{K}_{\theta\theta} \end{bmatrix} \begin{bmatrix} \Delta\mathbf{u} \\ \Delta\theta \end{bmatrix}^{(i)} \\
&= \begin{bmatrix} {}^{t+\Delta t}\mathbf{R}_{u} \\ {}^{t+\Delta t}\mathbf{R}_{\theta} \end{bmatrix} - \begin{bmatrix} {}^{t+\Delta t}_{0}\mathbf{F}_{u} \\ {}^{t+\Delta t}_{0}\mathbf{F}_{\theta} \end{bmatrix}^{(i-1)}
\end{aligned} \tag{3.140}$$

where ${}^{t}_{0}\mathbf{K}_{uu}$ is the stiffness corresponding to mechanical effects, ${}^{t}_{0}\mathbf{K}_{u\theta}$ is the matrix which transforms thermal energy into mechanical and matrix ${}^{t}_{0}\mathbf{K}_{\theta u}$ transform mechanical energy into thermal, the thermal stiffness ${}^{t}_{0}\mathbf{K}_{\theta\theta}$ is a sum of ${}^{t}_{0}\mathbf{K}^{k}$, ${}^{t}_{0}\mathbf{K}^{c}$ and ${}^{t}_{0}\mathbf{K}^{r}$. The right hand vectors of Eq.(3.140) are defined by Eqs.(3.109), (3.110), (3.112), (3.114). The stiffness matrices ${}^{t}_{0}\mathbf{K}_{uu}$, ${}^{t}_{0}\mathbf{K}_{\theta\theta}$, ${}^{t}_{0}\mathbf{K}_{u\theta}$ and ${}^{t}_{0}\mathbf{K}_{\theta u}$ are defined by appropriate integrals with kernels expressed by a combination of unknowns $\{\Delta\mathbf{u}, \theta\}$, shape functions, and strain-displacement matrices, as has been shown in [65], [66]. They can be also be viewed from the perspective of the Newton-Raphson solution process as the derivatives of vectors $\mathbf{F}_u$, $\mathbf{F}_\theta$ with respect to the state variable $\Delta\mathbf{u}$ and θ. Hence, they can be also expressed as follows:

$$\begin{aligned}
{}^{t}_{0}\mathbf{K}_{uu} &= {}^{t}_{0}\mathbf{F}_{u,u}; \\
{}^{t}_{0}\mathbf{K}_{\theta\theta} &= {}^{t}_{0}\mathbf{F}_{\theta,\theta}; \\
{}^{t}_{0}\mathbf{K}_{u\theta} &= {}^{t}_{0}\mathbf{F}_{u,\theta}; \\
{}^{t}_{0}\mathbf{K}_{\theta u} &= {}^{t}_{0}\mathbf{F}_{\theta,u},
\end{aligned} \tag{3.141}$$

where ',' indicates differentiation.

The balance of internal energy expressed by Eq(3.113) for the temperature rate approximated by the backward Euler scheme can be written in the form

$$\left\{ \frac{1}{\Delta t} {}^{t}_{0}\mathbf{C} + {}^{t}_{0}\mathbf{K}^{k} + {}^{t}_{0}\mathbf{K}^{c} + {}^{t}_{0}\mathbf{K}^{r} + {}^{t}_{0}\mathbf{K}^{\rho} \right\} \Delta\theta^{(i)} = {}^{t+\Delta t}_{0}\mathbf{R}_{\theta} - {}^{t+\Delta t}_{0}\mathbf{F}_{\theta}^{(i-1)}. \tag{3.142}$$

Substituting this to Eq.(3.140), the global finite element equation for the thermo-mechanical system can be rewritten in a more compact form

$$\begin{bmatrix} {}^{t}_{0}\mathbf{K}_{uu} & {}^{t}_{0}\mathbf{K}_{u\theta} \\ {}^{t}_{0}\mathbf{K}_{\theta u} & \frac{1}{\Delta t}\,{}^{t}_{0}\mathbf{C} + {}^{t}_{0}\mathbf{K}_{\theta\theta} \end{bmatrix} \begin{bmatrix} \Delta\mathbf{u} \\ \Delta\theta \end{bmatrix}^{(i)} = \begin{bmatrix} {}^{t+\Delta t}\mathbf{R}_{u} \\ {}^{t+\Delta t}\mathbf{R}_{\theta} \end{bmatrix} - \begin{bmatrix} {}^{t+\Delta t}_{0}\mathbf{F}_{u} \\ {}^{t+\Delta t}_{0}\mathbf{F}_{\theta} \end{bmatrix}^{(i-1)} \tag{3.143}$$

where matrix ${}^{t}_{0}\mathbf{K}_{\theta\theta}$ is defined by

$${}^{t}_{0}\mathbf{K}_{\theta\theta} = {}^{t}_{0}\mathbf{K}^{k} + {}^{t}_{0}\mathbf{K}^{c} + {}^{t}_{0}\mathbf{K}^{r} + {}^{t}_{0}\mathbf{K}^{\rho}. \tag{3.144}$$

3.7.2 Global FE Equation for Body with Phase Transformations

Combining Eq.(3.140) together with evolution equation for ferritic and pearlitic transformations, the following global FE equation is obtained:

$$\begin{aligned} &\begin{bmatrix} -\mathbf{1} & {}^{t}\hat{\mathcal{B}}_{i} & {}^{t}\mathcal{A}_{i} \\ \mathbf{0} & \mathbf{0} & \mathbf{0} \\ \mathbf{0} & \mathbf{0} & {}^{t}_{0}\mathbf{C} \end{bmatrix} \begin{bmatrix} {}^{t+\Delta t}\dot{\mathbf{y}}_{i} \\ {}^{t+\Delta t}\dot{\mathbf{u}} \\ {}^{t+\Delta t}\dot{\theta} \end{bmatrix}^{(i)} + \begin{bmatrix} \mathbf{0} & \mathbf{0} & \mathbf{0} \\ {}^{t}_{0}\mathbf{K}_{uy} & {}^{t}_{0}\mathbf{K}_{uu} & {}^{t}_{0}\mathbf{K}_{u\theta} \\ {}^{t}_{0}\mathbf{K}_{\theta y} & {}^{t}_{0}\mathbf{K}_{\theta u} & {}^{t}_{0}\mathbf{K}_{\theta\theta} \end{bmatrix} \begin{bmatrix} \Delta\mathbf{y}_{i} \\ \Delta\mathbf{u} \\ \Delta\theta \end{bmatrix}^{(i)} \\ = &\begin{bmatrix} {}^{t+\Delta t}\mathbf{R}_{y_i} \\ {}^{t+\Delta t}\mathbf{R}_{u} \\ {}^{t+\Delta t}\mathbf{R}_{\theta} \end{bmatrix} - \begin{bmatrix} {}^{t+\Delta t}_{0}\mathbf{F}_{y_i} \\ {}^{t+\Delta t}_{0}\mathbf{F}_{u} \\ {}^{t+\Delta t}_{0}\mathbf{F}_{\theta} \end{bmatrix}^{(i-1)} \end{aligned} \tag{3.145}$$

where the vector ${}^{t+\Delta t}\mathbf{R}_{y_i}$ is related to the term $\mathcal{R}_i$ of Eq.(3.116), components of stiffness matrix: ${}^{t}_{0}\mathbf{K}_{uu}$, ${}^{t}_{0}\mathbf{K}_{u\theta}$, ${}^{t}_{0}\mathbf{K}_{\theta u}$, and ${}^{t}_{0}\mathbf{K}_{\theta\theta}$, as well as the RHS vectors: ${}^{t+\Delta t}_{0}\mathbf{F}_{u}{}^{(i-1)}$, ${}^{t+\Delta t}_{0}\mathbf{F}_{\theta}{}^{(i-1)}$, ${}^{t+\Delta t}_{0}\mathbf{R}_{u}$, ${}^{t+\Delta t}_{0}\mathbf{R}_{\theta}$, are the same as in Eq.(3.140), and the subscript i assumes two values: 2 for ferritic, and 3 for pearlitic transformation.

Approximating the fraction rate, velocity, and temperature rate by backward finite differences, the system of FE equations can be written in the following form:

$$\begin{bmatrix} {}^{t}_{0}\mathbf{K}_{yy} & {}^{t}_{0}\mathbf{K}_{yu} & {}^{t}_{0}\mathbf{K}_{y\theta} \\ {}^{t}_{0}\mathbf{K}_{uy} & {}^{t}_{0}\mathbf{K}_{uu} & {}^{t}_{0}\mathbf{K}_{u\theta} \\ {}^{t}_{0}\mathbf{K}_{\theta y} & {}^{t}_{0}\mathbf{K}_{\theta u} & {}^{t}_{0}\hat{\mathbf{K}}_{\theta\theta} \end{bmatrix} \begin{bmatrix} \Delta\mathbf{y}_{i} \\ \Delta\mathbf{u} \\ \Delta\theta \end{bmatrix}^{(i)} = \begin{bmatrix} {}^{t+\Delta t}\mathbf{R}_{y_i} \\ {}^{t+\Delta t}\mathbf{R}_{u} \\ {}^{t+\Delta t}\mathbf{R}_{\theta} \end{bmatrix} - \begin{bmatrix} {}^{t+\Delta t}_{0}\mathbf{F}_{y_i} \\ {}^{t+\Delta t}_{0}\mathbf{F}_{u} \\ {}^{t+\Delta t}_{0}\mathbf{F}_{\theta} \end{bmatrix}^{(i-1)} \tag{3.146}$$

with $\tau = \frac{1}{\Delta t}$, and stiffness matrices defined as such

$$\begin{aligned}
{}^{t}_{0}\mathbf{K}_{yy} &= -\tau\ \mathbf{1};\\
{}^{t}_{0}\mathbf{K}_{yu} &= \tau\ {}^{t}\hat{\mathcal{B}}_{i};\\
{}^{t}_{0}\mathbf{K}_{y\theta} &= \tau\ {}^{t}\mathcal{A}_{i};\\
{}^{t}_{0}\mathbf{K}_{uy} &= {}^{t}_{0}\mathbf{K}_{\Lambda};\\
{}^{t}_{0}\mathbf{K}_{\theta y} &= {}^{t}_{0}\mathbf{K}_{mix};\\
{}^{t}_{0}\hat{\mathbf{K}}_{\theta\theta} &= \tau\ {}^{t}_{0}\mathbf{C} + {}^{t}_{0}\mathbf{K}_{\theta\theta},
\end{aligned} \tag{3.147}$$

where ${}^{t}_{0}\mathbf{K}_{\Lambda}$ is related to the plastic function $\Lambda(\mathbf{S}, \mathbf{E}, \int \dot{\mathbf{E}} dt, \theta, y_i)$ and FE displa-cement-strain matrices $\mathbf{B}_L$, $\mathbf{B}_{nL}$, the stiffness matrix ${}^{t}_{0}\mathbf{K}_{mix}$ depends on the mixture rule used to evaluate material parameters for multiphase body.

The kinetic law for bainitic transformation, expressed by Eq.(37), reveals that this phase growth is not related to temperature rate nor to displacement velocity $\dot{\mathbf{u}}$. Therefore the rate of bainitic phase fraction $\dot{\mathbf{y}}_4^{\phi}$ is not coupled explicitly with the other two state variables, $\Delta\mathbf{u}$, $\Delta\theta$, and the thermo-mechano-metallurgical problem is described by Eq.(37) and Eq.(3.140) or Eq.(3.143).

The thermo-mechano-metallurgical problem with martensitic transformation is described by the global FE Eq.(3.146) taken with matrices

$$\begin{aligned}
{}^{t}_{0}\mathbf{K}_{yu} &= \tau\ {}^{t}\hat{\mathcal{B}}_{6};\\
{}^{t}_{0}\mathbf{K}_{y\theta} &= \tau\ {}^{t}\mathcal{A}_{6},
\end{aligned} \tag{3.148}$$

and R.H.S. vectors evaluated appropriately for this reaction, i.e. ${}^{t+\Delta t}_{0}\mathbf{F}_{y_6}$ and ${}^{t+\Delta t}\mathbf{S}_{y_6}$. These matrices and vectors are derived corresponding to factors of equation shown in Table 4 of Part 1.

3.8 Solution of FE Equations

The nonlinear finite element system of equations given either by Eq.(3.143) or Eq.(3.146) is solved iteratively by the Newton-Raphson scheme. The system Eq.(3.146) can be rewritten in the form

$$[\mathcal{K}]\,[\mathcal{U}] = [\mathcal{R}] - [\mathcal{F}] \tag{3.149}$$

where

$$[\mathcal{K}] = \begin{bmatrix} {}^{t}_{0}\mathbf{K}_{yy} & {}^{t}_{0}\mathbf{K}_{yu} & {}^{t}_{0}\mathbf{K}_{y\theta} \\ {}^{t}_{0}\mathbf{K}_{uy} & {}^{t}_{0}\mathbf{K}_{uu} & {}^{t}_{0}\mathbf{K}_{u\theta} \\ {}^{t}_{0}\mathbf{K}_{\theta y} & {}^{t}_{0}\mathbf{K}_{\theta u} & {}^{t}_{0}\hat{\mathbf{K}}_{\theta\theta} \end{bmatrix}; \tag{3.150}$$

$$[\mathcal{U}] = \begin{bmatrix} \Delta\mathbf{y}_j \\ \Delta\mathbf{u} \\ \Delta\theta \end{bmatrix}^{(i)}; \tag{3.151}$$

$$[\mathcal{F}] = \begin{bmatrix} {}^{t+\Delta t}_{0}\mathbf{F}_y \\ {}^{t+\Delta t}_{0}\mathbf{F}_u \\ {}^{t+\Delta t}_{0}\mathbf{F}_\theta \end{bmatrix}^{(i-1)}; \tag{3.152}$$

$$[\mathcal{R}] = \begin{bmatrix} {}^{t+\Delta t}\mathbf{R}_y \\ {}^{t+\Delta t}\mathbf{R}_u \\ {}^{t+\Delta t}\mathbf{R}_\theta \end{bmatrix}; \tag{3.153}$$

The L.H.S. can be defined as the linear function of $[\mathcal{U}]$

$$f\,[\mathcal{U}] = [\mathcal{K}]\,[\mathcal{U}] \tag{3.154}$$

The Newton-Raphson method provides the approximation $[\mathcal{U}]^{i+1}$ of the root $[\mathcal{U}]^{*}$ of the equation

$$f\,[\mathcal{U}] = 0 \tag{3.155}$$

computed from the approximation $[\mathcal{U}]^{i}$ using the equation

$$[\mathcal{U}]^{i+1} = [\mathcal{U}]^{i} - [\mathcal{K}]^{-1}\left([\mathcal{R}] - [\mathcal{F}]^{i}\right) \tag{3.156}$$

The recombination of the last relation leads to the form

$$[\mathcal{K}]\left([\mathcal{U}]^{i+1} - [\mathcal{U}]^{i}\right) = [\mathcal{F}]^{i} - [\mathcal{R}] \tag{3.157}$$

from where the convergence of the method can be evaluated. The matrix $[\mathcal{U}]^{i+1}$ converges to the solution $[\mathcal{U}]^{*}$ when $\left([\mathcal{U}]^{i+1} - [\mathcal{U}]^{i}\right)$ converges to zero that happens when the vector of nodal thermal and mechanical loads $[\mathcal{R}]$ balances the vector of nodal stress vectors and heat fluxes $[\mathcal{F}]^{i}$ i.e. $[\mathcal{F}]^{i} - [\mathcal{R}] = \mathbf{0}$.

3.9 Temperature-Displacement-Phase Fraction Coupling

The global stiffness matrix for the TMM problem consists of terms which couple each two states of the three variables: temperature, displacement, and phase fractions. Sub-matrices will be derived here subsequently.

3.9.1 Displacement-Temperature Coupling

The finite element matrix $\mathbf{K}_{u\theta}$ coupling the displacement and temperature in Eq.(3.145) is defined in terms of stress derivatives by

$$\mathbf{K}_{u\theta} = \int_{V_0} \mathbf{B}_L^{\mathrm{T}} \mathbf{C}_{T\theta}\, dV_0 \tag{3.158}$$

where the matrix

$$\mathbf{C}_{T\theta} = \left[\begin{array}{cccc} \left(\frac{\partial \mathbf{T}}{\partial \theta}\right)_1 & \left(\frac{\partial \mathbf{T}}{\partial \theta}\right)_2 & \cdots & \left(\frac{\partial \mathbf{T}}{\partial \theta}\right)_N \end{array} \right] \tag{3.159}$$

consists of column vectors $\left(\frac{\partial \mathbf{T}}{\partial \theta}\right)_i$ of the dimension 6×1, and N is the number of nodes in the element.

These column vectors are calculated from the stress-temperature derivatives which are evaluated using the same procedure as for derivation of $\left.\frac{\partial \mathbf{T}}{\partial \mathbf{L}}\right|_{n+1}$.

The stress-temperature derivative is expressed by

$$\begin{aligned} \left.\frac{\partial \mathbf{T}}{\partial \theta}\right|_{n+1} &= \langle\kappa\rangle_{,\theta} \left[\mathrm{tr}\Delta\mathbf{L} - \underline{\alpha}^{tra} : \Delta\underline{y} - \langle\alpha^{thm}\rangle\Delta\theta \right]_{n+1} \mathbf{1} \\ &\quad -\langle\kappa\rangle \left[(\underline{\alpha}^{tra}_{,\theta} : \Delta\underline{y} + \Delta t : \underline{\alpha}^{tra} \left\{ \frac{\partial \underline{\dot{y}}}{\partial \theta} + \frac{\partial \underline{\dot{y}}}{\partial \mathbf{S}} : \frac{\partial \mathbf{S}}{\partial \theta} \right\} \right. \\ &\quad \left. +(\alpha^{thm}_{,\theta}\Delta\theta + \langle\alpha^{thm}\rangle) \right]_{n+1} \mathbf{1} \\ &\quad + \left.\frac{\partial \mathbf{Z}}{\partial \theta}\right|_{n+1} + \left[\sqrt{\tfrac{2}{3}} K_{\alpha,\theta} \frac{\Sigma}{\|\Sigma\|} + 2\langle\mu\rangle\Delta t \dot{\mathbf{E}}^{trip}_{,\theta} \right]_{n+1} \end{aligned} \tag{3.160}$$

where the derivative of the transformation plasticity strain rate is

$$\begin{aligned} \frac{\partial \dot{\mathbf{E}}^{trip}}{\partial \theta} &= K_{,\theta}(\underline{1} - \underline{y}) : \underline{\dot{y}}\boldsymbol{\Sigma} + K(\underline{1} - \underline{y}) : \left\{ \frac{\partial \underline{\dot{y}}}{\partial \theta} + \frac{\partial \underline{\dot{y}}}{\partial \mathbf{S}} : \frac{\partial \mathbf{S}}{\partial \theta} \right\} \boldsymbol{\Sigma} \\ &+ K(\underline{1} - \underline{y}) : \underline{\dot{y}} \frac{\partial \boldsymbol{\Sigma}}{\partial \theta} \end{aligned} \tag{3.161}$$

The other derivatives required for evaluation of $\frac{\partial \mathbf{T}}{\partial \theta}\Big|_{n+1}$ are:

$$\frac{\partial \dot{\underline{y}}}{\partial \theta} + \frac{\partial \dot{\underline{y}}}{\partial \mathbf{S}} : \frac{\partial \mathbf{S}}{\partial \theta} = \frac{\partial \dot{\underline{y}}}{\partial \theta} + \frac{\partial \dot{\underline{y}}}{\partial \mathbf{S}} : \hat{\mathbf{J}}_{dev} : \frac{\partial \mathbf{T}}{\partial \theta} \tag{3.162}$$

$$\frac{\partial \mathbf{\Sigma}}{\partial \theta} = \frac{\partial \mathbf{\Sigma}}{\partial \mathbf{S}} : \frac{\partial \mathbf{S}}{\partial \mathbf{T}} : \frac{\partial \mathbf{T}}{\partial \theta} = \hat{\mathbf{J}}_{dev} : \frac{\partial \mathbf{T}}{\partial \theta}, \tag{3.163}$$

$$\frac{\partial \mathbf{Z}}{\partial \theta}\Big|_{n+1} = \left[\sqrt{\tfrac{2}{3}} \frac{\partial H_\alpha}{\partial \theta} \frac{\mathbf{\Sigma}}{\|\mathbf{\Sigma}\|}\right]_{n+1}. \tag{3.164}$$

Substituting these expressions to Eq.(3.160) and rearranging in respect to $\frac{\partial \mathbf{T}}{\partial \theta}$ gives the following:

$$\begin{aligned}
\frac{\partial \mathbf{T}}{\partial \theta}\Big|_{n+1} &= \Big[\hat{\mathbf{J}} + \langle\kappa\rangle \Delta t \underline{\alpha}^{tra} : \frac{\partial \underline{y}}{\partial \mathbf{S}} \otimes \mathbf{1} : \hat{\mathbf{J}}_{dev} \\
&-2\langle\mu\rangle \Delta t K(\underline{1} - \underline{y}) : \frac{\partial \dot{\underline{y}}}{\partial \mathbf{S}} \otimes \mathbf{\Sigma} : \hat{\mathbf{J}}_{dev} + E_\alpha^{trip} \hat{\mathbf{J}}_{dev}\Big]^{-1}_{n+1} : \\
&\Big\{\langle\kappa\rangle_{,\theta}\Big[\mathrm{tr}\Delta\mathbf{L} - \underline{\alpha}^{tra} : \Delta\underline{y} - \langle\alpha^{thm}\rangle \Delta\theta\Big]\mathbf{1} - \langle\kappa\rangle\Big[(\underline{\alpha}^{tra}_{,\theta} : \Delta t \dot{\underline{y}} \\
&+\Delta t \underline{\alpha}^{tra} : \frac{\partial \dot{\underline{y}}}{\partial \theta} + \Big(\alpha^{thm}_{,\theta} \Delta\theta + \langle\alpha^{thm}\rangle\Big)\Big]\mathbf{1} \\
&+(\sqrt{\tfrac{2}{3}} H_{\alpha,\theta} + \sqrt{\tfrac{2}{3}} K_{\alpha,\theta}) \frac{\mathbf{\Sigma}}{\|\mathbf{\Sigma}\|} + 2\langle\mu\rangle \Delta t \Big[K_{,\theta}(\underline{1} - \underline{y}) : \dot{\underline{y}} \mathbf{\Sigma} \\
&+K(\underline{1} - \underline{y}) : \frac{\partial \dot{\underline{y}}}{\partial \theta} \mathbf{\Sigma} - E_\alpha^{trip} \hat{\mathbf{J}}_{dev} : \sqrt{\tfrac{2}{3}} H_{\alpha,\theta} \frac{\mathbf{\Sigma}}{\|\mathbf{\Sigma}\|}\Big]\Big\}_{n+1}
\end{aligned} \tag{3.165}$$

3.9.2 Coupling Between Temperature and Inelastic Energy Dissipation

The matrix ${}^t_0\mathbf{K}_{\theta\theta}$ appearing in Eqs.(3.143) and (3.145) contains ${}^t_0\mathbf{K}^\rho$ which is the only undefined term in Eq.(3.144).

The heat flux generated by dissipation of the inelastic strain energy contributes to the variation of the body stiffness, so that the corresponding stiffness term has the form:

$$\mathbf{K}^\rho = \int_{V_0} \mathbf{H}^{\mathrm{T}} F^{in}_{\theta\,,\,\theta}\, dV_0. \tag{3.166}$$

and this belongs to the L.H.S of Eq.(3.111). This stiffness contribution is associated with the corresponding R.H.S. vector of Eq. (3.111)

$$\mathbf{F}^\rho = \int_{V_0} \mathbf{H}^{\mathrm{T}} F^{in}_{\theta\,,\,\theta}\, \theta^{(i-1)}\, dV_0 \tag{3.167}$$

where the derivative of the heat flux $F_\theta^{in} = f_\theta\left(\mathbf{T} : \dot{\mathbf{L}}^{in}\right)$ related to the dissipation of inelastic energy is

$$\frac{\partial F_\theta^{in}}{\partial \theta} \equiv F_{\theta,\theta}^{in} = f_\theta \left[\frac{\partial \mathbf{T}}{\partial \theta} : \dot{\mathbf{L}}^{in} + \frac{\partial \dot{\mathbf{L}}^{in}}{\partial \theta} : \mathbf{T}\right], \tag{3.168}$$

where $\mathbf{H}^{\mathrm{T}}$ is the finite element interpolation matrix. The derivative appearing in the second term of Eq.(3.168) is

$$\frac{\partial \dot{\mathbf{L}}^{in}}{\partial \theta} = \frac{1}{\Delta t}\frac{\partial \bar{\Lambda}}{\partial \theta}\frac{\boldsymbol{\Sigma}}{\|\boldsymbol{\Sigma}\|} + \frac{\partial \dot{\mathbf{E}}^{trip}}{\partial \theta} \tag{3.169}$$

where $\frac{\partial \bar{\Lambda}}{\partial \theta}$ can be found by implicit differentiation of the yield function and re-ordering:

$$\begin{aligned}\frac{\partial \bar{\Lambda}}{\partial \theta} = \frac{1}{2\gamma\langle\mu\rangle}\Big[&\gamma_{,\theta}\|\boldsymbol{\Sigma}^*\| + 2\gamma\frac{\partial \boldsymbol{\Sigma}^{pred}}{\partial \theta} : \boldsymbol{\Sigma}^{pred} - 2\bar{\Lambda}(\gamma_{,\theta}\langle\mu\rangle \\ &+\gamma\langle\mu\rangle_{,\theta})\gamma_{,\theta}\sqrt{\tfrac{2}{3}}\Delta H_\alpha - \gamma\sqrt{\tfrac{2}{3}}H_{\alpha\,,\theta} - \sqrt{\tfrac{2}{3}}K_{\alpha\,,\theta}\Big]\end{aligned} \tag{3.170}$$

The other derivatives are defined as the following:

$$\begin{aligned}\gamma_{,\theta} = &-\left[1 + 2\langle\mu\rangle\Delta t K(\underline{1} - \underline{y}) : \underline{\dot{y}}\right]^{-2} 2\Delta t K\left[\langle\mu\rangle_{,\theta}(\underline{1} - \underline{y}) : \underline{\dot{y}}\right. \\ &+ \left.\langle\mu\rangle(\underline{1} - \underline{y}) : \underline{\dot{y}}_{,\theta}\right]\end{aligned} \tag{3.171}$$

$$\begin{aligned}&\frac{\partial \boldsymbol{\Sigma}^{\mathbf{pred}}}{\partial \theta} = 2\langle\mu\rangle_{,\theta}\mathbf{J}_{dev} : \left[\Delta\mathbf{L} - \tfrac{1}{3}\Delta t\underline{\alpha}^{tra} : \underline{\dot{y}}\mathbf{1} - \langle\alpha^{thm}\rangle\Delta\theta\mathbf{1}\right] \\ &-2\langle\mu\rangle\mathbf{J}_{dev} : \left[\left(\langle\alpha^{thm}\rangle_{,\theta}\Delta\theta + \langle\alpha^{thm}\rangle\right) + \tfrac{1}{3}\Delta t\left\{\underline{\alpha}_{,\theta}^{tra} : \underline{\dot{y}} + \underline{\alpha}^{tra} : \underline{\dot{y}}_{,\theta}\right\}\right]\mathbf{1}\end{aligned} \tag{3.172}$$

3.9.3 Temperature-Displacement Coupling

The stiffness matrix related to temperature-displacement coupling is defined by

$$\mathbf{K}_{\theta u} = \int_{V_0} \mathbf{H}^{\mathrm{T}}\frac{\partial F_\theta^{in}}{\partial \mathbf{L}}\mathbf{B}_L \, dV_0, \tag{3.173}$$

where the derivative of the corresponding heat flux generated by inelastic dissipation is

$$\frac{\partial F_\theta^{in}}{\partial \mathbf{L}} = f_\theta \left[\frac{\partial \mathbf{T}}{\partial \mathbf{L}} : \mathbf{L}^{in} + \frac{\partial \dot{\mathbf{L}}^{in}}{\partial \mathbf{L}} : \mathbf{T}\right]. \tag{3.174}$$

The derivative in the second term is derived from

$$\frac{\partial \dot{\mathbf{L}}^{in}}{\partial \mathbf{L}} = \frac{1}{\Delta t}\left[\frac{\partial \bar{\Lambda}}{\partial \mathbf{L}} \otimes \frac{\boldsymbol{\Sigma}}{\|\boldsymbol{\Sigma}\|}\frac{\partial \Delta \mathbf{E}^{trip}}{\partial \mathbf{L}}\right], \tag{3.175}$$

with $\frac{\partial \Lambda}{\partial \mathbf{E}}$ given by Eq.(3.98), and $\frac{\partial \Delta \mathbf{E}^{trip}}{\partial \mathbf{L}}$ determined by Eq.(3.92).

3.9.4 Coupling Between Displacement and Phase Fractions

The finite element stiffness sub-matrix $\mathbf{K}_{uy}$ which couples displacement and phase fractions is defined by

$$\begin{array}{rcl} \mathbf{K}_{uy} & = & \int_{V_0} \mathbf{B}_L^{\mathrm{T}} \mathbf{C}_{Ty}\, dV_0, \\ \mathbf{C}_{Ty} & = & \left[\left(\frac{\partial \mathbf{T}}{\partial \underline{y}}\right)_1 \left(\frac{\partial \mathbf{T}}{\partial \underline{y}}\right)_2 \cdots \left(\frac{\partial \mathbf{T}}{\partial \underline{y}}\right)_N\right]. \end{array} \tag{3.176}$$

The coupling between a phase evolution and the stress requires also the definition of corresponding tangent modulus

$$\begin{aligned} \left.\frac{\partial \mathbf{T}}{\partial \underline{y}}\right|_{n+1} &= \Big[\mathbf{J} + 2\langle\mu\rangle \Delta t E_\alpha^{trip} \mathbf{J}_{dev}\Big]^{-1} : \Big\{\langle \kappa_{,\underline{y}}\rangle \Big[\mathrm{tr}\Delta\mathbf{L} - \Delta t \underline{\alpha}^{tra} : \underline{y} \\ &- \langle \alpha^{thm}\rangle \Delta\theta\Big]\mathbf{1} + \langle\kappa\rangle\Big[-\Delta t(\underline{\alpha}^{tra}_{,\underline{y}} : \dot{\underline{y}} + \alpha^{tra} : \dot{\underline{y}}_{,\underline{y}}) - \langle \alpha^{thm}_{,\underline{y}}\rangle \Delta\theta\Big]\mathbf{1} \\ &+ 2\langle\mu\rangle_{,\underline{y}} \Delta t \mathbf{E}^{trip} + 2\langle\mu\rangle \Delta t \frac{\partial E_\alpha^{trip}}{\partial \underline{y}} \otimes \boldsymbol{\Sigma}\Big\} \end{aligned} \tag{3.177}$$

and

$$\frac{\partial E_\alpha^{trip}}{\partial \underline{y}} = \dot{\underline{y}}_{,\underline{y}} : (\underline{1} - \underline{y}) - \underline{I} : \dot{\underline{y}} \tag{3.178}$$

where the identity matrix for the phase-fraction vector is:

$$\underline{I} = \begin{bmatrix} 1 & 0 & 0 & \dots & 0 \\ 0 & 1 & 0 & \dots & 0 \\ & & \ddots & & \\ 0 & 0 & 0 & \dots & 1 \end{bmatrix}$$

which size depends on the number of considered phases.

3.9.5 Coupling Between Temperature and Phase Fraction

The contribution to the global stiffness matrix arising from the coupling of temperature and phase transformations is defined by

$$\mathbf{K}_{\theta y} = \int_{V_0} \mathbf{H}^{\mathrm{T}} \frac{\partial F_\theta^{in}}{\partial \underline{y}} \, dV_0, \tag{3.179}$$

with the corresponding heat flux derivative expressed by

$$\frac{\partial F_\theta^{in}}{\partial \underline{y}} = f_\theta \Big[\frac{\partial \mathbf{T}}{\partial \underline{y}} : \dot{\mathbf{L}}^{in} + \frac{\partial \dot{\mathbf{L}}^{in}}{\partial \underline{y}} : \mathbf{T} \Big]. \tag{3.180}$$

The derivative in the second term of the R.H.S. is written as

$$\frac{\partial \dot{\mathbf{L}}^{in}}{\partial \underline{y}} = \frac{1}{\Delta t} \frac{\partial \bar{\Lambda}}{\partial \underline{y}} \frac{\mathbf{\Sigma}}{\|\mathbf{\Sigma}\|} + \frac{\partial \dot{\mathbf{E}}^{trip}}{\partial \underline{y}}. \tag{3.181}$$

The derivative $\frac{\partial \bar{\Lambda}}{\partial \underline{y}}$ can be found by implicit differentiation of the consistency condition

$$\begin{aligned} &\gamma_{,\underline{y}} \|\mathbf{\Sigma}^{pred}\| + 2\gamma \frac{\partial \mathbf{\Sigma}^{pred}}{\partial \underline{y}} : \mathbf{\Sigma}^{pred} - 2\bar{\Lambda} \Big[\gamma_{,\underline{y}} \langle \mu \rangle + \gamma \langle \mu \rangle_{,\underline{y}} \Big] \\ &-2\gamma \langle \mu \rangle \frac{\partial \bar{\Lambda}}{\partial \underline{y}} - \gamma_{,\underline{y}} \sqrt{\tfrac{2}{3}} \Delta H_\alpha - \gamma \sqrt{\tfrac{2}{3}} H_{\alpha\,,\underline{y}} - \sqrt{\tfrac{2}{3}} K_{\alpha\,,\underline{y}} = 0, \end{aligned} \tag{3.182}$$

and taking $\frac{\partial \bar{\Lambda}}{\partial \underline{y}}$ to the L.H.S.

$$\begin{aligned} \frac{\partial \bar{\Lambda}}{\partial \underline{y}} = \frac{1}{2\gamma \langle \mu \rangle} \Bigg[&\gamma_{,\underline{y}} \|\mathbf{\Sigma}^{pred}\| + 2\gamma \frac{\partial \mathbf{\Sigma}^{pred}}{\partial \underline{y}} : \mathbf{\Sigma}^{pred} - 2\bar{\Lambda} (\gamma_{,\underline{y}} \langle \mu \rangle + \gamma \langle \mu \rangle_{,\underline{y}}) \\ &-\gamma_{,\underline{y}} \sqrt{\tfrac{2}{3}} \Delta H_\alpha - \gamma \sqrt{\tfrac{2}{3}} H_{\alpha\,,\underline{y}} - \sqrt{\tfrac{2}{3}} K_{\alpha\,,\underline{y}} \Big] \end{aligned} \tag{3.183}$$

The other derivatives in Eq.(3.183) are given by

$$\begin{aligned} \gamma_{,\underline{y}} \;=\; &- \Big[1 + 2\langle \mu \rangle \Delta t K (\underline{1} - \underline{y}) : \underline{\dot{y}} \Big]^{-2} 2\Delta t K \Big[\langle \mu \rangle_{,\underline{y}} (\underline{1} - \underline{y}) : \underline{\dot{y}} \\ &+ \langle \mu \rangle \Big\{ (\underline{1} - \underline{y}) : \underline{\dot{y}}_{,\underline{y}} - \underline{I} : \underline{\dot{y}} \Big\} \Big], \end{aligned} \tag{3.184}$$

$$\frac{\partial \boldsymbol{\Sigma}^{\mathbf{pred}}}{\partial \underline{y}} = 2\langle\mu\rangle_{,\underline{y}}\mathbf{J}_{dev} : \Big[\Delta\mathbf{L} - \frac{1}{3}\Delta t\underline{\alpha}^{tra} : \underline{\dot{y}}\mathbf{1} - \langle\alpha^{thm}\rangle\Delta\theta\mathbf{1}\Big]$$
$$+2\langle\mu\rangle\mathbf{J}_{dev} : \Big[- \Big\{\langle\alpha^{thm}\rangle_{,\underline{y}}\Delta\theta + \langle\alpha^{thm}\rangle\Big\}$$
$$-\frac{1}{3}\Delta t\Big\{\underline{\alpha}^{tra}_{,\underline{y}} : \underline{\dot{y}} + \underline{\alpha}^{tra} : \underline{\dot{y}}_{,\underline{y}}\Big\}\Big]\ \mathbf{1}. \tag{3.185}$$

The derivative in the second term of Eq.(3.181) is expressed by

$$\frac{\partial \dot{\mathbf{E}}^{trip}}{\partial \underline{y}} = K\left[(\underline{1} - \underline{y}) : \underline{\dot{y}}_{,\underline{y}} - \underline{I} : \underline{\dot{y}}\right]\boldsymbol{\Sigma} + K(\underline{1} - \underline{y}) : \underline{\dot{y}} \times$$
$$\left[\left(\hat{\mathbf{J}}_{dev} : \frac{\partial \mathbf{T}}{\partial \underline{y}}\right) - \sqrt{\tfrac{2}{3}}H'_{\alpha}\frac{\partial \bar{\Lambda}}{\partial \underline{y}}\frac{\boldsymbol{\Sigma}}{\|\boldsymbol{\Sigma}\|}\right] \tag{3.186}$$

Chapter 4

Numerical Results Illustrating CTMM Problem

4.1 TMM Benchmark Problem

Results for the theory and the FEM discussed in the first part of this report are illustrated by a benchmark formulated for a fillet welded joint composed of sixteen beads (Table 4.1).

In a benchmark, a high density of FEM mesh is required to model the moving heat source. Backward Euler integration or an implicit method is used to integrate the temperature rate in the transient heat equation. This integration scheme unconditionally stable would become unstable when applied to non-stationary heat source whose motion is described in spatial coordinates. The stability of the transient heat source is further ensured when applying enough Gauss points to define its shape for each time increment. It is also recommended that the element spacing in the longitudinal direction be regular along the welding line. To secure stability of a solution of tran-

Sixteen-beads Benchmark	
Number of beads	16
Dimensions of a plate	100 mm x 75 mm x 20 mm
Symmetry in deposition of beads	NO
Welding technique	MIG
Type of elements	brick elements with eight nodes
Total number of elements	10 304
Total number of nodes	12 360

Table 4.1: Charasteristics of the second benchmark

$F_\theta^{arc} = \frac{\phi\eta VI}{2\pi\delta_{arc}^2}\exp(-r^2/2\delta_{arc}^2)$	
V	voltage
I	current intensity
δ_{arc}	deviation from the standard distribution represents the thermal 'impression' made by the electrode
η	efficiency of the energy transmission via electric arc
ϕ	net fraction of heat input
r	horizontal radial distance from the weld center

Table 4.2: The heat flux of the electric arc

sient thermal problem it is sometimes necessary to use larger time steps or finer mesh. Larger time steps naturally decrease a rate of convergence in the solution of non-linear equations.

Due to the large size of the combined stiffness matrix resulting from the three-dimensional mesh, it is was necessary to use the bi-conjugate gradient iterative method for the solution of this large problem rather than a direct solution method. The bi-conjugate gradient method is used, instead of the conjugate gradient or symmetric iterative method, because the stiffness matrix is unsymmetrical due to the convection type terms that result from the applied thermal boundary conditions.

4.1.1 Initial and Boundary Conditions

Initial Conditions

In order to obtain the reference microstructure, steel plates, parts of welded joint, were normalized at a range of temperatures from 920 C to 600 C during 8 hours following the procedure recommend by the manufacturer of the steel and finally air cooled. The main grain size amounts to approximately 10 μm. In this state the reference microstructure consists of austenite grains (γ-Fe). The initial temperature of welded plates was equal to the environmental temperature.

Heat Source and Thermal Interaction Between Welded Joint and Environment

The heat source produced by an electric arc is assumed to be a normal Gaussian distribution (shown in Fig.4.1) which spreads over several elements and contains several Gauss points in the horizontal plane.

$F_\theta^c = h_c\,(\theta_f - \theta_\infty)$			
$h_c = Nu_f\,\frac{k_f}{l_c}$		$\theta_f = \frac{\theta_\infty + \theta_w}{2}$	
$k_f = (975.603 + 5.71995\,\theta_f)10^{-8}$			
θ_w	temperature of the wall	θ_∞	temperature outside of b.l.
h_c	convection coefficient	k_f	conductivity of b.l.
k_f	units are W/mm	b.l.	boundary layer
l_c	characteristic length		

Table 4.3: Heat flux due to convection

The thermal boundary effects include convection, radiation, and conduction as well as the thermal contact resistance phenomena applied to the base. The radiation and convection heat fluxes from the upper and vertical surfaces of the weld joint are shown as temperature functions in Fig.(4.4) and (4.5).

Convection from the welded piece is given by empirical relations, derived in [35] in terms of non-dimensional constants: Nu_f, Gr_f, Pr_f, Re_f which are the Nusselt, Grashof, Prandtl and Rayleigh numbers evaluated at temperature θ_f.

The heat flux due to convection is defined in Table 4.3.

A specific value of the Nusselt number is related to the Prandtl and the Grashof numbers. The Grashof number depends on both temperature and orientation of the external surface of weld piece. A variation of the Grashof number on the upper surface is shown in Fig.(4.2). The Nusselt numbers for upper and vertical surfaces are given in Table 4.4.

The heat flux due to radiation is defined in Table 4.5.

In a welding benchmark considered here, a base of welded plate is in contact with a workbench which acts as a heat sink and thermal contact relations, shown in [35], are used to estimate the heat flux from the welded piece to the workbench. The corresponding heat flux F_θ^{cc} is defined in Table 4.6.

Mechanical Boundary Conditions

A welded plate rests upon a surface and is fixed only in one point. Such fixing is necessary for the description of a plate dilatation, as it eliminates the effect of a rigid body motion. No effect of friction on the base of welded plates is considered. Following such assumptions it is possible to observe the free dilatation of a welded piece in three directions.

upper surface	
$Nu_f = 0.13(Re_f)^{\frac{1}{3}}$	$Re_f \leq 2 \times 10^8$
$Nu_f = 0.16(Re_f)^{\frac{1}{3}}$	$Re_f > 2 \times 10^8$
$Gr_f = \frac{g\beta\theta_f l_c^3}{\nu^2}$	l_c = area divided by perimeter
vertical surfaces	
$Nu_f = \left[\frac{0.825+0.387(Re_f)^{\frac{1}{6}}}{\left(1+\frac{0.492}{P_f}^{\frac{9}{16}}\right)^{\frac{8}{27}}} \right]^{\frac{1}{2}}$	
$Gr_f = \frac{g\beta\theta_f l_c^3}{\nu^2}$	l_c = vertical height
$Re_f = Gr_f Pr_f$	
$Pr_f = 1.13786\ (\theta_f)^{-0.083107}$	$\theta_f \leq 500$
$Pr_f = 0.651978 + 4.7895 \times 10^{-5}\theta$	$500 < \theta_f \leq 1200$
$Pr_f = 0.705$	$\theta_f > 1200$
$\beta = {\theta_a}^{-1}$	θ_a = absolute temperature of air
$\nu = 8.69754 \times 10^{-4}(\theta_f)^{1.71067}$	ν = viscosity of air

Table 4.4: Expressions for Nusselt numbers for various surfaces and temperatures

$F_\theta^r = h_r(\theta - \theta_{env})$			
$h_r = \sigma_s \epsilon_r(\theta^4 - \theta_{sink}^4)$			
σ_s	Stefan-Bolzman constant	ϵ_r	emmisivity of steel
θ_{sink}	sink temperature	θ_{env}	environmental temperature

Table 4.5: Heat flux due to radiation

$F_\theta^{cc} = h_{cc}(\theta - \theta_c)$			
$h_{cr} = h_{cc}^{-1}$			
h_{cc}	thermal contact conductance	A	contact area
h_{cr}	thermal contact resistance	θ_c	temperature of contact surface

Table 4.6: The heat flux of thermal contact

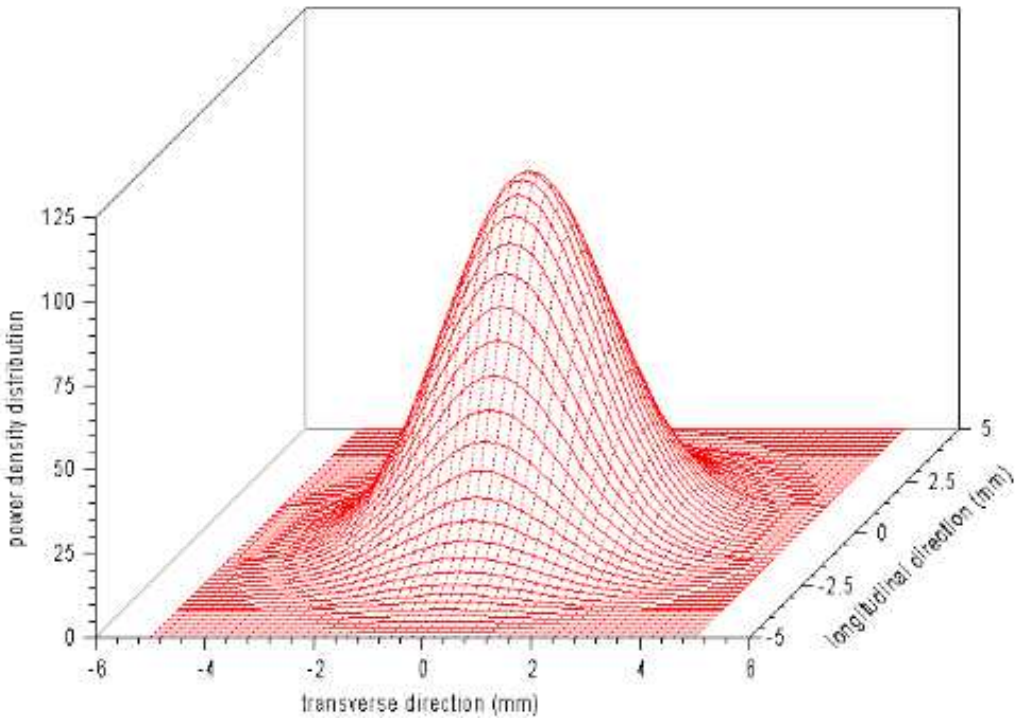

Figure 4.1: The model of the moving welding arc, i.e. surface heat source

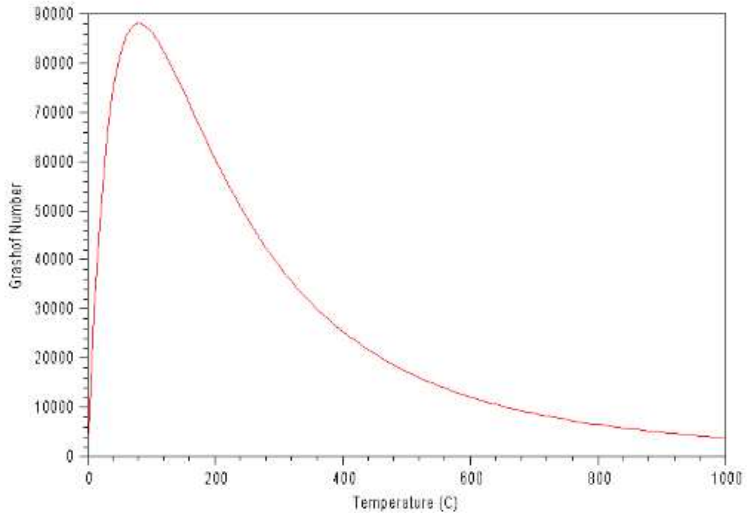

Figure 4.2: The Grashof number on the upper surface

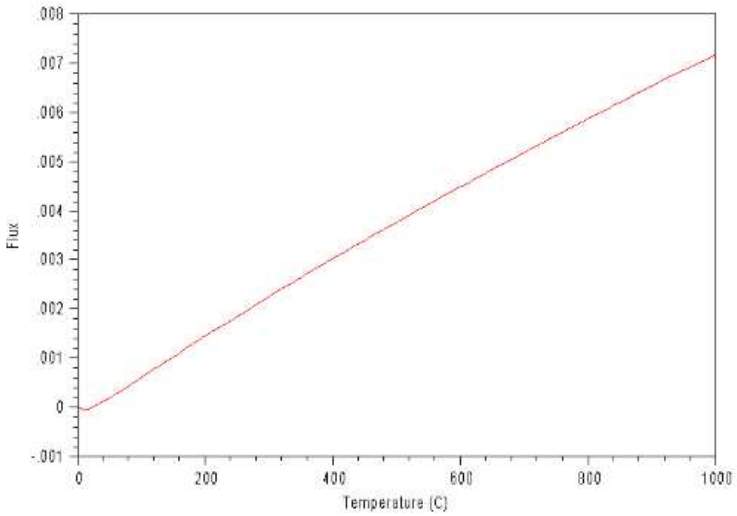

Figure 4.3: Convection flux from the upper surface

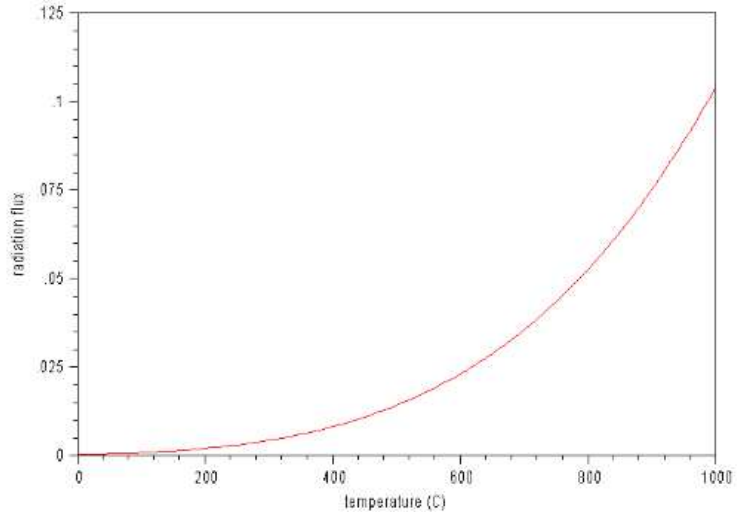

Figure 4.4: Radiation flux

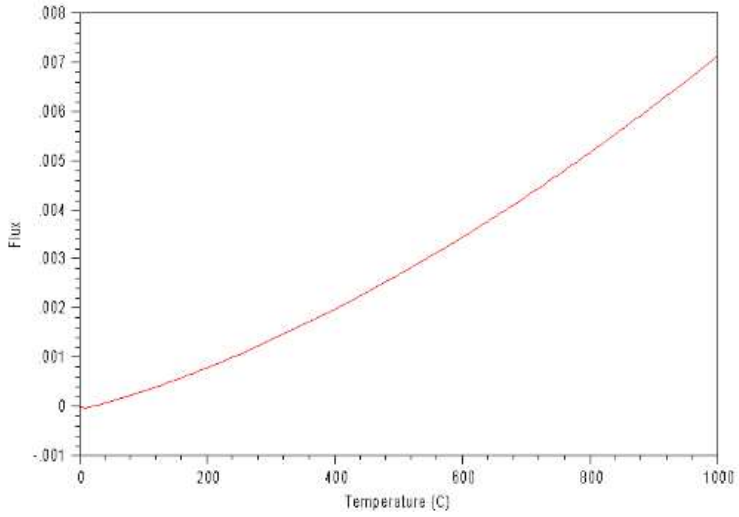

Figure 4.5: Convection flux from the vertical surfaces

4.1.2 Material Data for Simulation of TMM Process

The aim of the simulation is to determine the residual stersses, strains and phase fractions of a welded joint after multi-bead welding. The simulation for the fully coupled TMM process is carried out in one stage. Following other models of TMM processes proposed by Leblond at. al. [43], [44] or by Denis at.al. [16], [15], [17] and known as LSG2M-Nancy model a simulation was carried out in two stages:

- thermo-metallurgical computation performed from an austenitic structure formed after solidification to a structure at 20 C,
- mechanical computation,

Both above mentioned TMM models are implemented in program SYSWELD released by SYSTUS International, ESI Group.

Data required to define the study are:

- geometry,
- thermal and mechanical properties,
- metallurgical transformations,
- heat transfer coefficient

Metallurgical Transformations

The metallurgical transformations are those that occur in the high-temperature construction steel 15 Mo 3, for which the chemical composition is: 0.12-020% C, 0.10-0.35% Si, 0.40-0.90% Mn, $\leq$0.035% P, $\leq$0.030% S, $\leq$0.25% Cr, 0.25-0.35% Mo, $\leq$0.30% Ni, $\leq$0.30% others.

Four phases are considered:

- austenite,
- ferrite,
- bainite,
- martensite.

Thermo-mechanical Properties

Material behaviour is modelled taking the following phenomena into account:

- temperature dependent Young modulus,
- plastic deformation associated with isotropic hardening,
- temperature dependent yield stress defined for each phase,
- temperature deendent strain hardening defined for each phase,
- recovery effect of strain hardening for martensite,
- temperature dependent thermal strain (thermal dilatation) defined for each phase,

The required data are listed in Table 4.7.

Additional Thermo-mechanical Data Available from Tensile Tests

Description of experiments
The testing material was delivered in the form of cold drawing bars of diameter Ø15 mm. Samples of the length 40 mm were cut from the bar. In order to obtain the reference microstructure bar pieces were normalised at 920 C during 0.5 hour and finally air cooled. After such treatment the main grain size amounts to approximately 10 μm and the reference microstructure

Property	Table number
thermal strains	Table 4.8
Young's modulus	Table 4.9
Poisson's ratio	0.3
yield stress	Table 4.10
strain-hardening for phase-α	Table 4.11
strain-hardening for phase-γ	Table 4.12

Table 4.7: Thermo-mechanical data required for simulation of TMM process

Thermal strains					
Temperature	ferrite	pearlite	bainite	martensite	austenite
20	0.00	0.00	0.00	0.00	-0.01104
1250	0.0185	0.0185	0.0185	0.0185	0.0173

Table 4.8: Temperature and phase depenedent thermal starins

	Temperature												
	20	100	200	300	400	500	600	700	800	900	1000	1100	1250
Young's moduls	207	204	200	192	180	163	132	82	52	33	20	11	0.5

Table 4.9: Temperature dependent Young's modulus, GPa

Phases	Temperature											
	20	100	200	300	400	500	600	700	800	900	1100	1250
ferrite	317	295	278	264	250	225	175	95	60	50		
pearlite	320	310	290	280	260	240	180	100	60			
bainite	750	695	655	635	595	533	417	215	75			
martensite	1250	1160	1100	1055	990	890	695	360	100			
austenite		215	200	175	150	120	95	75	60	45	18	1

Table 4.10: Temperature and phase dependent yield stress, MPa

Temperature	Plastic deformations									
	0.0025	0.005	0.0075	0.010	0.020	0.030	0.040	0.050	0.075	0.1
20	1	2	3	5	52	90	117.5	140	185	220
200	1	2	10	20	62	91	114	135	161	180
300	1	6	17	28	75	107	129	145	186	215
400	11	20	30	40	75	93	105	115	135	150
500	15	25	30	38	55	62	65	67.5	73.7	80
600	2.5	5	7.5	10	14	17	17	17	17	17
650	0.125	0.25	0.37	0.5	1	1.5	2	2.5	3.75	5
1250	0.125	0.25	0.37	0.5	1	1.5	2	2.5	3.75	5

Table 4.11: Temperature and phase dependent strain hardenning for phase-α

Temperature	Plastic deformations	
	0.00	0.05
200	0.00	145
500	0.00	145
600	0.00	140
700	0.00	129
800	0.00	95
900	0.00	55
1000	0.00	20
1100	0.00	5
1250	0.00	2.5

Table 4.12: Temperature and phase dependent strain hardenning for phase-γ

is composed of equiaxed ferrite grains α-Fe together with inter-crystalline pearlite lamellae of about 10% volume fraction.

After normalisation twenty cylindrical tensile samples of gauge length of 20 mm and the total length of 40 mm and diameter of 4 mm were machined from annealed pieces. The tensile tests, with one sample for each temperature, were performed on the computer controlled tensile testing machine INSTRON-Type 6025 using appropriate high-temperature three-zone furnace. At temperatures higher than 300 C the argon atmosphere was employed for protection of a sample surface. The transverse velocity was 1 mm/min corresponding to tensile strain rate of $\varepsilon = 8.3 \times 10^{-4} s^{-1}$.

Results of tensile tests
For each sample the relation between a tensile force and elongation was automatically recorded and following that a relation between the true stress and the true strain (logarithmic strain) was evaluated. At the end of each measurement test parameters were evaluated according to the European Tensile Testing Norm EN 10 002.

Thermal Properties

Thermal properties used for the complex thermo-mechano-metallurgical simulation are the thermal conductivity and heat capacity determined for austenite and other phases and shown in Table 4.14.

Temp. C	0.2% Yield Strength MPa	UTS MPa	Fracture Stress MPa	Elongation %	Uniform Strain %	Area Reduction %
20	371.1	489.9	976.9	38.3	20.9	69.9
100	349.5	467.1	980.2	26.1	15.8	69.3
200	303.9	531.1	870.9	19.9	10.1	55.6
300	281.5	509.4	819.5	26.9	14.1	55.9
400	238.3	473.9	835.9	29.1	13.6	70.1
500	225.5	371.5	688.5	27.4	10.5	75.4
600	188.7	236.2	435.6	32.2	7.8	72.8
650	99.2	128.8	174.0	85.0	7.1	71.5
700	75.2	93.7	86.0	66.5	6.2	73.6
725	53.6	73.5	55.3	87.5	9.1	63.8
750	48.3	59.1	48.6	61.2	5.4	55.2
775	44.9	57.0	47.1	46.0	7.9	53.2
800	40.3	50.5	35.8	50.5	7.4	38.8
825	40.2	53.3	57.9	22.2	10.1	31.2
850	42.9	60.8	44.3	29.3	10.8	21.7
875	36.5	53.0	48.1	22.6	10.7	22.2
900	32.9	48.5	38.8	21.0	8.1	20.8
925	31.3	43.6	35.2	18.5	7.1	18.1
950	29.4	39.2	26.1	18.2	5.8	18.1
1000	21.4	28.9	14.3	30.4	9.8	22.6

Table 4.13: Mechanical properties of 15Mo3 steel obtained from tensile tests carried out for the range of temperatures from 20 C to 1000 C

Temperature C	Conductivity W/C		Heat capacity J/mm^3C	
	Austenite	Other	Austenite	Other
20		0.052		470
100		0.049		490
200	0.0175	0.0465	530	525
300	0.01825	0.0435	545	565
400	0.01975	0.041	560	615
500	0.021	0.038	570	680
600	0.0225	0.035	580	770
650		0.033		815
700	0.0235	0.032	590	850
800	0.0245		600	
900	0.026		620	
1000	0.0275		630	
1200	0.030		650	
1400	0.0325		680	

Table 4.14: Thermal conductivity and heat capacity for austenite and other phases as temperature functions

4.2 Results the Benchmark Problem with Sixteen Beads Welding

Volume fractions of bainite, martensite, residual austenite and Von Mises-equivalent stress as well as the temperature distribution and magnified deformed mesh generated on the welded body illustrate results obtained for the second benchmark problem for welding.

The temperature distribution is shown for a deposition of the final bead (the weld cap) in Fig. 4.6 and has the characteristic ellipsoid shape as expected.

The initial austenitic structure transforms to one of bainite, martensite and residual austenite. The bainite volume phase fraction shown in Fig. 4.7 reaches a maximum of 0.79 or 79% of the the volume and is concentrated in the weld bead. The 16-pass weld results in a much larger heat affected zone and, disregarding the initial run on phenomenon, there is a quite broad zone of bainite as a result of the increased size of HAZ. The volume phase fraction results are approximately symmetric for the two half plates even though welding is applied as an off-centred heat source for most of the passes. Martensite forms in bands parallel to the bainite phase as shown in Fig. 4.8 and reaches a maximum of 79%.

The residual Von Mises stress for the 16-pass weld is shown in Fig.4.10. The interaction between concentrations of bainite and martensite and increased stress is again visible although not quite as obvious as in the three-pass weld. Finally the residual deformation magnified 28.4 times the actual deformation is shown in Fig. 4.11. The characteristic bow-shaped bending of the plate is visible. This is due to the heat input initially causing an expansion followed by the contraction of the constrained plastically deformed structure during cooling.

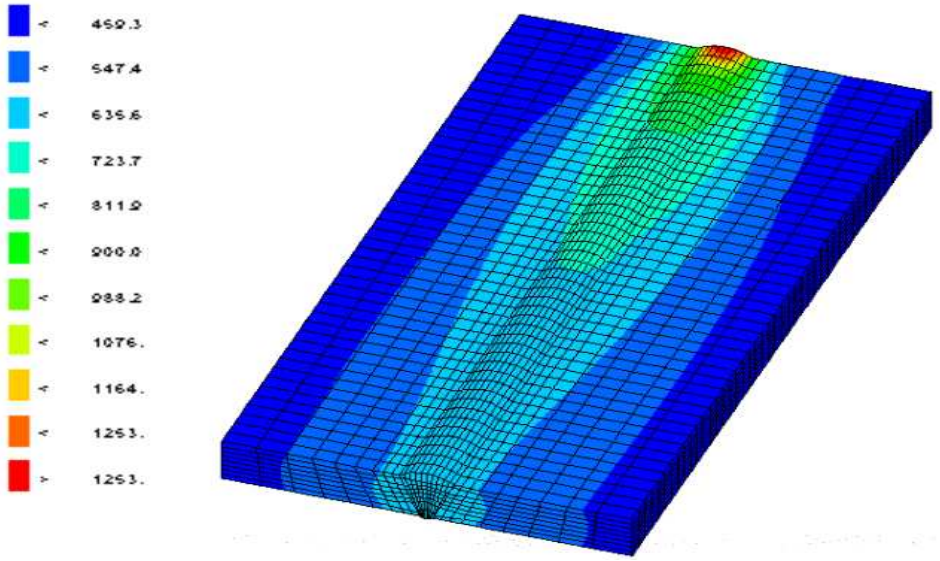

Figure 4.6: The temperature distribution at the end of the 16th pass for the 16-pass weld

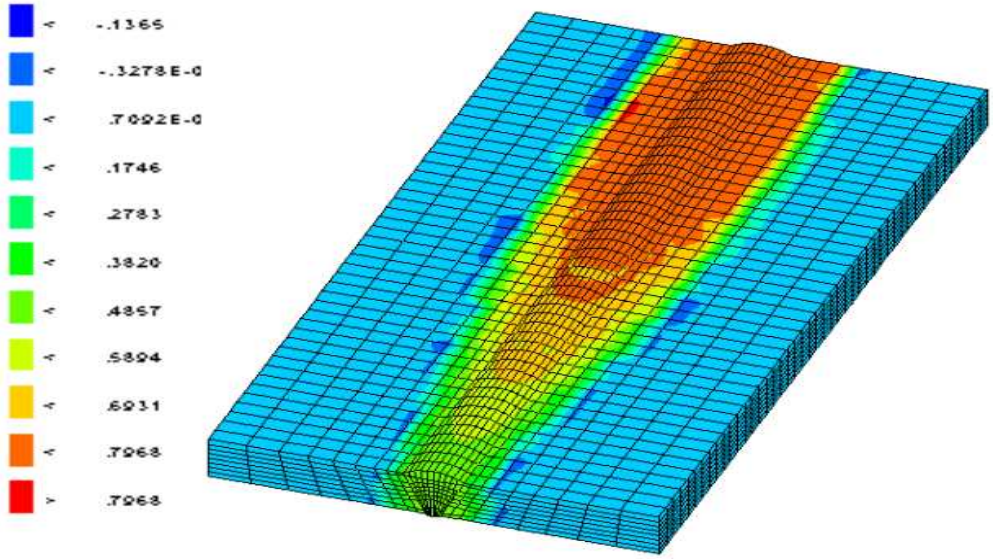

Figure 4.7: The volume fraction of bainite for the 16-pass weld

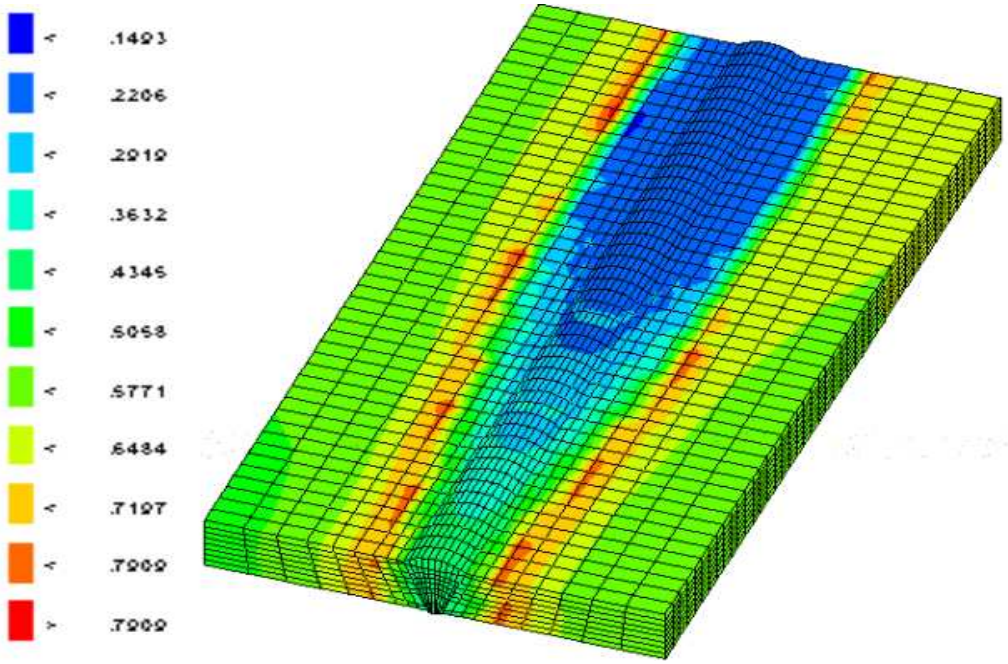

Figure 4.8: The volume fraction of martensite for the 16-pass weld

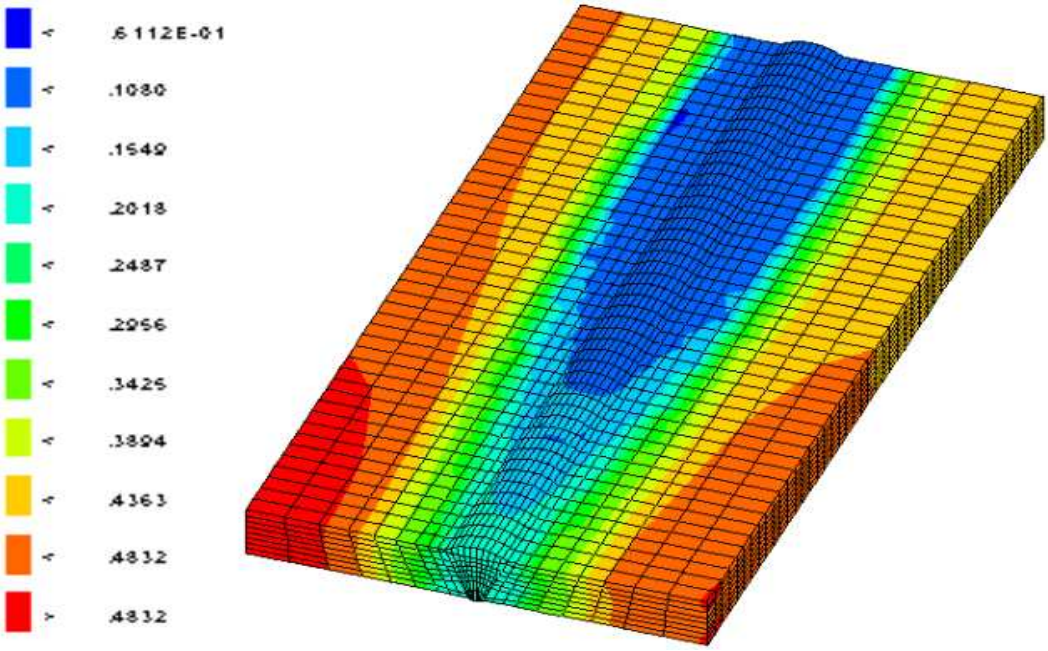

Figure 4.9: The volume fraction of residual austenite for the 16-pass weld

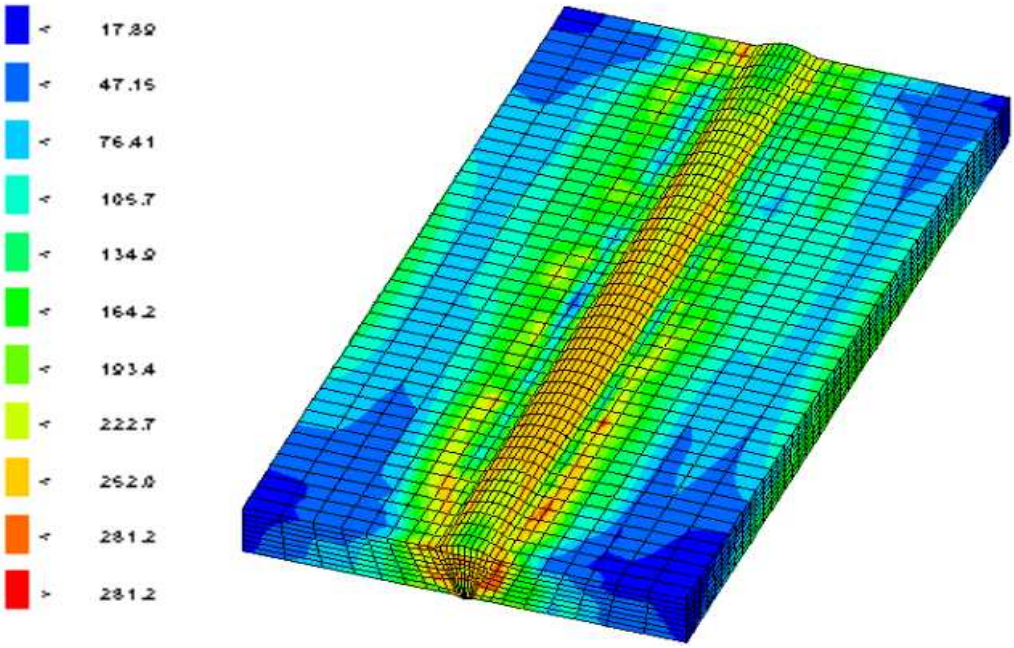

Figure 4.10: The residual Von-Mises equivalent stress for the 16-pass weld

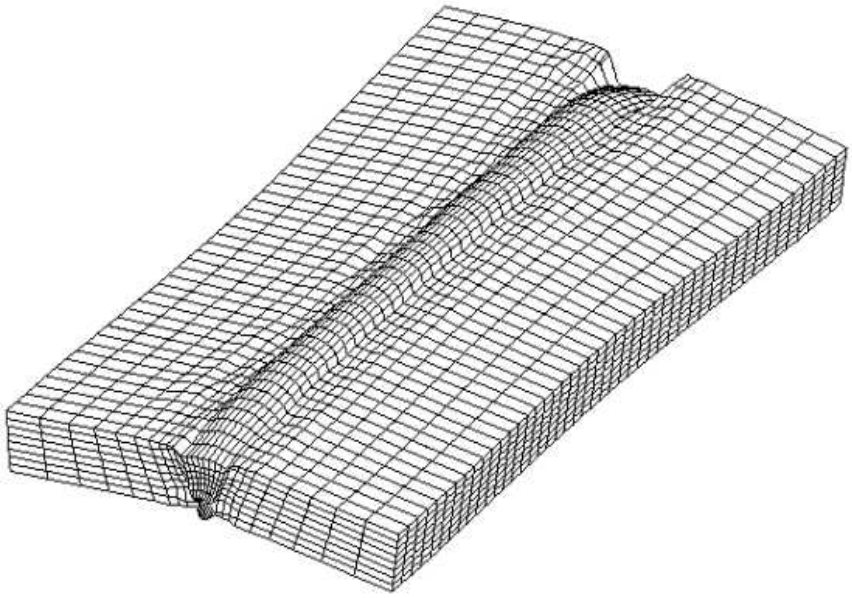

Figure 4.11: The residual deformation in the 16-pass weld magnified 28.4 times actual deformation

Chapter 5

Conclusions

A unified mathematical approach has been applied to several phase growth laws to derive corresponding evolution equations from the basic postulate of proportionality of the new phase increment to the change of a physical quantity controlling the transformation process. Table (5.1) contains a tabulation of basic assumptions for the kinetic laws reviewed. Evolution laws reveal interactions between transformation kinetics and material constitutive variables or phase transformation driving forces. These equations are consistent with the rate type balance laws for conservation of virtual and internal energy. In thermo-mechanical-metallurgical analysis, constitutive variables are defined as a dispersed material particle. Material parameters and physical quantities are averaged according to the phase fraction using a linear mixture rule.

A condensed presentation of the features of nine models is given in Table (5.2) and Table (5.3) which helps in drawing conclusions on the complexity of evolution equations, measurability of model variables, application, and required level of model variables. The simplest evolution laws for diffusional and diffusionless transformations expressed by Eq.(2.23) and Eq.(2.37) respectively, reveal only a relation between $\dot{\mathbf{y}}$ and temperature rate $\dot{\theta}$. Also they provide comparatively easy identification of material and process characteristics. The evolution law deduced in [54] from thermodynamics and statistics for uniaxial loading has been generalized here for the three-dimensional case. This 3-D generalization, expressed by Table(2.6) together with the law derived from thermodynamics, and given by Eq.(2.60) or Eq.(2.63), provides the relation between the rate of martensitic fraction y_5 and rates of strain energy ΔG_{σ}^{mic}, chemical energy $\Delta G_{ch_5}^{mic}$, and temperature θ.

However, they account for different scale effects in a dispersed particle. The strain energy $\mathcal{G}_{\sigma}$ in Table (2.6) is evaluated on the system of habit planes

Model	Proportionality assumption of	
	new phase increment	driving force decrement
JAM Eq.(2.15)	dy_i, $i = 2, 3$	$d\mathcal{G}$; $\dot{\mathcal{G}} = n_i\ b_i\ t^{n_i - 1}$
JAM Eq.(2.21)	dy_i, $i = 2, 3$	$d\mathcal{G}$; $\dot{\mathcal{G}} = n_i\ b_i\ t^{n_i - 1}$
modified JAM Eq.(2.28)	dy_i, $i = 2, 3$	$d\mathcal{G}, d\mathbf{S}, d\theta$
RB Eq.(2.29)	dy_4	$\langle dN_4 \rangle$
KM Eq.(2.36)	dy_5	$d\theta$
extended KM Eq.(2.39)	dy_5	$d\theta, dp$, equivalent stress $d\hat{\mathbf{S}}$
OTC Table 2.6	dy_5	structural defect potency $dN_V(\mathcal{G}_\sigma)$
OFT Eq.(2.47)	dy_5	total Gibbs free energy $\langle d\Delta G_5^{mic} \rangle$

Table 5.1: Basic assumptions for modelling of diffusional and diffusionless transformations. The following abbreviations and symbols are used in the table: JAM: Johnson-Avrami-Mehl, KM: Koistinen-Marburger, OTC: Olson-Tsuzaki-Cohen, OFT: Oberaigner-Fisher-Tanaka, RB: Rees-Bhadeshia.

Model	Level of variables of phase transformation model	
	microscopic	macroscopic
JAM Eq.(2.15)		n_i, b_i, $i = 2, 3$
JAM Eq.(2.21)	$N_i(\theta)$	θ, n_i, $i = 2, 3$
modified JAM Eq.(2.28)		C, n_i, $b_i(\theta)$, J_2', θ, $i = 2, 3$
RB Eq.(2.30)		$\dot{N}_4$
RB Eq.(2.34)		$\Delta G_{4_{max}}, G_N, \theta$, K_1, K_2, β, r, R
KM Eq.(2.36)		θ, α, M_s
extended KM Eq.(2.39)		A, B, α, θ, p, $\hat{S}$
OTC Table 2.6	d_5,A_5^{mic}, ΔG_F^{mic} N_V^0,$\mathcal{G}_\sigma$, $\mathcal{G}_{ch}$,	θ, α, γ_5
OFT Eq.(2.47)	ΔG_{ch}^{mic}	k_F, $tr\mathbf{E}^*$, $\mathbf{E}_{cr}^*$, θ, p, $\dot{\mathbf{T}}$

Table 5.2: Microscopic and macroscopic variables of phase transformation models

Model	complexity of equation	measurability of variables	application
JAM Eq.(2.15)	simple	easy	1- to 3-D
JAM Eq.(2.21)	simple	easy	1- to 3-D
modified JAM Eq.(2.28)	complex	expensive, hard	1- to 3-D
RB Eq.(2.34)	complex	expensive, easy	1- to 3-D
extended KM Eq.(2.36)	simple	expensive, easy	1- to 3-D
KM Eq.(2.39)	simple	easy	1- to 3-D
OTC Table 2.6	complex	generally impossible	specific 1-D
OFT Eq.(2.47)	complex	hard	1- to 3-D

Table 5.3: Evaluation of data acquisition effort, complexity and application of phase transformation model. Symbol: 1-to 3-D means that a transformation model can be applied for one-, two- and three-dimensional problems.

while the mechanical contribution of free energy change $\Delta G_{\sigma}^{mic}(\mathbf{S}, \mathbf{T}_{eq}^{act}, \mathbf{T}_{eq}^{fur})$ in Eq.(2.60) is defined as the value averaged for the entire microregion. This also requires a very small size of a microregion in analysis and can be used only in the case of micromechanics when the body has the diameter of a few grains.

The generalized evolution equation for diffusionless-martensitic transformation is proposed in Eq.(3.126). Coefficients of this equation are identified for three kinetic laws: Eq.(2.37), Table(2.6), and Eq.(2.63). The generalized evolution equation for diffusional transformation is proposed in Eq.(3.115) with coefficients identified for Eq.(2.23) and its modification Eq.(2.28). Constitutive equations for macro-regions are coupled with heat equation and evolution laws by the mixture rule. This technique facilitates transformation of micro-structural state variables: phase fractions, isobaric macro-regional stresses, cooling and nucleation rates, the Gibbs free energy changes, etc. to the level of global state variables for considered body. Constraints for this transformation are the mixture rule and the balance of virtual work for hybrid elements. The microstructure of alloy is approximated by hybrid finite elements. Each element is composed of several grains that contain various phases represented at Gauss points of integration. This hierarchy in approximation of material properties provides a transmission of micro-material state variables to the macro-level of finite element method solution of the welding problem.

We have also presented a form of governing differential equation for metallurgical phase transformation equilibrium in terms volume phase fractions. This governing differential equation combines the transformations due to diffusional and diffusionless mechanisms including the effects of temperature and stress. The Galerkin method is applied to this equation leading to a

boundary value problem for the phase transformation equilibrium which is fully coupled with temperature-displacement equilibrium. This differs from the alternative scheme of producing contributions to the global stiffness matrix directly from the differential equations describing rates of transformation also presented in this work. In addition we have also addressed the issue of singularities or jumps in the solution as a result of changes in the material properties using the concept of singular surfaces in deriving the variational equations with the Galerkin method.

The treatment of the welding simulation problem takes into account the interaction of the three state variables : temperature, displacement and metallurgical volume phase fraction throughout and leads to a consistent formulation using algorithmic tangent moduli for the solution of the non-linear equilibrium equations.

Numerical results were presented showing results which include the effects of metallurgical phase transformations in simulating welding processes. These show agreement with known behaviours of the real structures simulated.

Bibliography

[1] M.F. Ashby, D.R.H. Jones, Engineering Materials 2, (Pergamon Press, Oxford, 1986).

[2] M. Andre, E. Gautier, F. Moreaux, A. Simon and G. Beck, Influence of quenching stresses on the hardenability of steel, *Mat. Sci. Engng.* **55** (1982) 211-217.

[3] S. Atamert and J.E. King, Super Duplex Steels Part 1: Heat affected zone microstructures, *Material Science and Technology* **8** (1992) 896-911.

[4] K-J. Bathe, *Finite Element Procedures in Engineering Analysis* (Prentice-Hall, Englewood Cliffs, 1982).

[5] H.K.D.H. Bhadeshia, Bainite: overall transformation kinetics, *Journal de Physique* **43** (1982) C4-443-448.

[6] H.K.D.H. Bhadeshia and D.V. Edmonds, The bainite transformation in a silicon steel, *Metallurgical Transactions A* **10A** (1979) 895-907.

[7] H.K.D.H. Bhadeshia, The lower bainite transformation and the significance of carbide precipitation, *Acta Metallurgica* **28** (1980) 1103-1114.

[8] H.K.D.H. Bhadeshia and D.V. Edmonds, The mechanism of bainite formation in steels, *Acta Metallurgica* **28** (1980) 1265-1273.

[9] H.K.D.H. Bhadeshia, A rationalization of shear transformations in steels, *Acta Metallurgica* **29** (1981) 1117-1130.

[10] H.K.D.H. Bhadeshia, Bainite: An atom-probe study of the incomplete reaction phenomenon, *Acta Metallurgica* **30** (1982) 775-784.

[11] H.K.D.H. Bhadeshia, Thermodynamic analysis of isothermal transformation diagrams, *Metal Science* **16** (1982) 159-165.

[12] R.E. Cech and D. Turnbull, Heterogeneous nucleation of the martensite transformation, *Journal of Metals, Trans. AIME* **206** (1952) 124-132.

[13] Christensen, N., Davies, V.L., Gjermundsen, K., Distribution of temperatures in arc welding, British Welding Journal, Vol. 12, pp. 54-75, 1965.

[14] M. Cohen and G.B. Olson, Martensitic nucleation and the role of the nucleating defect, in: H. Suzuki at. al., *First JIM Symposium on New Aspects of Martensitic Transformation* (Japan Inst. of Metals, Kobe, Japan, 1976) 93-98.

[15] S. Denis, E. Gautier, A. Simon and G. Beck, Stress-phase-transformation interactions-basic principles, modelling, and calculation of internal stresses, *Materials Science and Technology* **1** (1985) 805-814.

[16] S. Denis, E. Gautier, S. Sjostrom and A. Simon, Influence of stresses on the kinetics of pearlitic transformation during continuous cooling, *Acta Metallurgica* **7** (1987) 1621-1632.

[17] S. Denis, S. Sjostrom and A. Simon, Coupled temperature, stress, phase transformation calculation, model numerical illustration of the internal stresses evolution during cooling of a eutectoid carbon steel cylinder. *Metallurgical Transactions A* **18A** (1987) 1203-1212.

[18] Y. Desalos, J. Giusti and F. Gunsberg, *Deformations et contraintes lors du traitement termique de pieces en acier* (Saint-Germain-en-Laye, Institut de Recherches de la Siderurgie Francaise, RE 902, 1982).

[19] J.D. Eshelby, The determination of the elastic field of an ellipsoidal inclusion, and related problems, *Proc. Roy. Soc. London* **A241** (1957) 376-396.

[20] F.M.B. Fernandes, S. Denis and A. Simon, Mathematical model coupling phase transformation and temperature evolution during quenching of steels, *Materials Science and Technology* **1** (1985) 838-844.

[21] F. Fernandes, S. Denis and A. Simon, Prvsion de l'évolution termique at structurale des acires au cours de leur refroidissement continu, *Mémoires et Etudes Scientifiques Revue de Métallurgie, July-August, 1986.*

[22] F. Fernandes, *Modélisation et calcul de l'évolution de la température et de la microstructure au cours du refroidissement des aciers* (Ph.D. Thesis, INPL, Nancy, 1985).

[23] F.D. Fischer, A micromechanical model for transformation plasticity in steels, *Acta. Metall. Mater.* **38** (1990) 1535-1546.

[24] F.D. Fischer and K. Tanaka, A micromechanical model for the kinetics of martensitic transformation, *Int. J. Solids Structures* **29** (1992) 1723-1728.

[25] M. Fujita and M. Suzuki, The effect of high pressure on the isothermal transformation in high purity Fe-C alloys and commercial steels, *Trans. Iron. Steel Inst. Japan* **14** (1974) 44-53.

[26] G.W. Greenwood and R.M. Johnson, The deformation of metals under small stresses during phase transformations. *Proc. Royal Soc.* **283A** (1965) 403-422.

[27] A.G. Guy, *Introduction to Materials Science* (McGraw-Hill, New York, 1972).

[28] A.M Habraken and M. Bourdouxhe, Coupled thermo- mechanical-metallurgical analysis during the cooling process of steel pieces, *Eur. J. Mech., A/Solids* **11** (1992) 381-402.

[29] E.B. Hawbolt, B. Chau and J.K. Brimacombe, Kinetics of austenite-pearlite transformation in eutectoid carbon steel, *Metallurgical Transactions A* **14A** (1983) 1803-1815.

[30] B. Hildenwall, *Prediction of the residual stress created by during quenching* (Linkoping Studies in Science and Technology, Dissertations 39, 1979).

[31] M. Hillert, Nuclear composition - A factor of interest in nucleation, *Acta Metallurgica* **1** (1953) 764-766.

[32] J.E. Hilliard, Iron-carbon phase diagram: Isobaric sections of the eutectoid region at 35, 50, and 65 Kilobars, *Transactions of the Metallurgical Society of AIME* **227** (1963) 429-438.

[33] T. Hirayama and M. Ogirima, Influence of chemical composition on martensitic transformation in Fe-Cr-Ni Stainless Steel, (in Japanese), *Nippon Kinzoko Gakkaishi* **34** (1970) 507-510.

[34] T. Hirayama and M. Ogirima, Influence of martensitic transformation and chemical composition on mechanical properties of Fe-Cr-Ni Stainless Steel, (in Japanese), *Nippon Kinzoko Gakkaishi* **34** (1970) 511-516.

[35] J.P. Holman, *Heat Transfer* (McGraw-Hill, Singapore, 1989).

[36] T.J.R. Hughes, *The Finite Element Method* (Prentice-Hall, Englewood Cliffs, 1987).

[37] T. Inoue and Z. Wang, Finite element analysis of coupled thermo-inelastic problem with phase transformation, *Proc. Numerical Methods in Industrial Forming Processes* (Swansea, 1982) 391-400.

[38] T. Inoue and Z. Wang, Coupling between stress, temperature, and metallic structures during processes involving phase transformations, *Materials Science and Technology* **1** (1985) 845-850.

[39] A.W. Johnson and F. Mehl, Reaction kinetics in processes of nucleation and growth, *Trans. Metal. Soc. AIME* **135** (1939) 416-458A.

[40] L. Kaufman and M. Hillert, Thermodynamics of martensitic transformations, in: G.B. Olson and W.S. Owen, *Martensite* (ASM International, Materials Park, 1992) 41-58.

[41] D.P. Koistinen and R.E. Marburger, A general equation prescribing the extent of the austenite-martensite transformation in pure iron-carbon alloys and plain carbon steels, *Acta Metallurgica* **7** (1959) 59-60.

[42] S.A. Kulin, M. Cohen and B.L. Averbach, Effect of applied stress on the martensitic transformation, *Trans. AIME, J. Metals.* **4** (1952) 661-668.

[43] J.B. Leblond, G. Mottet, G. Devaux and J.C. Devaux: A theoretical and numerical approach to the plastic behaviour of steels during phase transformations of general relations. Part 1: Derivation of general relations. *Journal of the Mechanics and Physics of Solids* **34** (1986) 395-409.

[44] J.B. Leblond, G. Mottet, G. Devaux and J.C. Devaux: A theoretical and numerical approach to the plastic behaviour of steels during phase transformations of general relations. Part 2: Study of classical plasticity for ideal-plastic phases. *Journal of the Mechanics and Physics of Solids* **34** (1986) 411-432.

[45] P. Lenk, G. Nocke and E. Jansch, Einfluss einer plastischen Verformung des metastabilen Austenits auf das isotherme Umwandlungsverhalten eines ubereutektoiden Stahls in der Perlitstufe, *Neue Hutte* **10** (1970) 598-602.

[46] C.L. Magee, The nucleation of martensite, in: H.I. Aronson, *Phase Transformations* (ASM, 1968) 115-156.

[47] I. Muller, *Thermodynamics* (Pitman Advanced Publishing Program, Boston, 1985).

[48] T.G. Nilan, Morphology and kinetics of austenite decomposition at high pressure, *Trans. Metal. Soc. AIME* **239** (1967) 898-909.

[49] Z. Nishiyama, *Martensitic Transformation* (Academic Press, London, 1978).

[50] G. Nocke, E. Jansch and P. Lenk, Untersuchungen zum Spannungseinfluss auf das isotherme Umwandlungsverhalten des ubereutektoiden Stahls UR38CrMoV21.14, *Neue Hutte* **8** (1976) 468-473.

[51] E.R. Oberaigner, E.D. Fischer and K. Tanaka, A new micromechanical formulation of martensite kinetics driven by temperature and/or stress, *Archive of Appl. Mech.* **63** (1993) 522-533.

[52] Ohji, T., Ohkubo, A. and Nishiguchi, K., Mathematical modelling of molten pool in arc welding, in Karlsson, L., Lindgren, L.E., Johnsson, M., Mechanical Effects of Welding, pp. 207-214, Springer-Verlag, Berlin, Heidelberg, 1992.

[53] G.J. Oliver, *Modelling of welding with various constitutive models for steel* (MSc. Thesis, Department of Applied Mathematics, University of Cape Town, 1994).

[54] G.B. Olson, K. Tsuzaki and M. Cohen, Statistical aspects of martensitic transformation, *Proc. Mat. Res. Soc. Symp.* **57** (1987) 129-148.

[55] E. Pardo and D.C. Weckman, Prediction of weld pool and reinforcement dimensions of GMA welds using a Finite-Element model, *Metallurgical Transactions B* **20B** (1989) 937-946.

[56] J.R. Patel and M. Cohen, Criterion for the action of applied stress in the martensitic transformation, *Acta Metallurgica* **1** (1953) 531-538.

[57] D.A. Porter and K.E. Easterling, *Phase Transformations in Metals and Alloys* (Chapman and Hall, London, 1992).

[58] L.F. Porter and P.C. Rosenthal, Effect of applied tensile stress on phase transformations in steel, *Acta Matallugica* **7** (1959) 504-514.

[59] S.V. Radclife and M. Schatz, The effect of high pressure on the martensitic reaction in iron-carbon alloys, *Acta Metallurgica* **10** (1962) 201-207.

[60] B. Raniecki, Overlay model for determining thermal- hardening stresses in metallic solids, *Mater. Sci. Tech.* **1** (1985) 875-862.

[61] G.I. Rees and H.K.D.H. Bhadeshia, Bainite transformation kinetics, Part1: Modified model, *Materials Science and Technology* **8** (1992) 985-993.

[62] G.I. Rees and H.K.D.H. Bhadeshia, Bainite transformation kinetics, Part2: Non-uniform distribution of carbon, *Materials Sciences and Technology* **8** (1992) 994-996.

[63] A. Romano, Thermomechanics of Phase Transitions in Classical Field Theory, *Series on Advances in Mathematics for Applied Sciences Vol 13* (World Scientific).

[64] J. Ronda and O. Mahrenholtz, Thermal problems of welding, in Karlsson, L., Lindgren, L.E., Johnsson, M., *Mechanical Effects of Welding* (Springer-Verlag, Berlin, Heidelberg, 1992) 75-84.

[65] J. Ronda, O. Mahrenholtz and R. Hamann, Thermomechanical simulation of underwater welding processes *Archive of Applied Mechanics* **62** (1992) 15-27.

[66] J. Ronda, O. Mahrenholtz and R. Hamann, Quality of the TF-3D - A new FEM solver of nonlinear heat transfer problem, *Numerical Heat Transfer, Part B* **22** (1992) 25-48.

[67] J. Ronda, H. Murakawa, G.J. Oliver and Y. Ueda, Thermo-mechano-metallurgical model of welded steel, Part2: Finite element formulation and constitutive equations, *Transactions of JWRI* **24** (1995) 93-113.

[68] E. Scheil, Anlaufzeit der Austenitumwandlung, *Arch. Eisenhuttenwesen* **8** (1934) 565-567.

[69] E. Schmidtmann and H. Hlawiczka, Wirkung einer Thermomechanischen Behandlung auf das Umwandlungsverhalten in der Perlit und in der Martensitstufe, *Arch. Eisenhuttenwesen* **44** (1973) 529-537.

[70] Shinoda, T., Masumoto, I., Prediction of weld geometries for CO_2 butt-welded joints, Mat. Sci. and Tech., Vol. 5, pp. 293-298, 1989.

[71] J.C. Simo and R.L. Taylor, Consistent tangent operators for rate-independent elastoplasticity, *Computer Methods in Applied Mechanics and Engineering* **48** (1985) 101-118.

[72] R. Sinclair and H.A. Mohamed, Lattice imaging study of a martensite-austenite interface, *Acta Metallurgica* **26** (1978) 623-628.

[73] S. Sjostrom, Interactions and constitutive models for calculating quench stresses in steel, *Mater. Sci. Technol.* **1** (1985) 823-829.

[74] Q.P. Sun, K.C. Hwang and S.W. Yu, A micromechanics constitutive model of transformation plasticity with shear and dilatation effect, *J. Mech. Phys. Solids* **39** (1991) 507-524.

[75] K. Tanaka and Y. Sato, A mechanical view of transformation-induced plasticity, *Ingenieur-Archiv* **55** (1985) 147-155.

[76] K. Wilmanski, Thermodynamic foundations of thermoelasticity, in: G. Lebon and P. Perzyna, P. *Recent developments in thermodynamics of solids* (Wien, New York: Springer 1980) 1-92.

[77] Y. Ueda, J. Ronda, H. Murakawa and K. Ikeuchi, Thermo-mechanical-metallurgical model of welded steel. Part I: Evolution equations for internal material structures, *Transaction of JWRI* **24** (1994) 1-19.

[78] M. Umemoto, H. Ohtsuka and I. Tamura, Transformation to pearlite from work-hardening austenite, *Transactions ISIJ* **23** (1983) 775-784.